NTIA Report 14-499

Effects of Radar Interference on LTE Base Station Receiver Performance

Frank H. Sanders
John E. Carroll
Geoffrey A. Sanders
Robert L. Sole

report series

U.S. DEPARTMENT OF COMMERCE • National Telecommunications and Information Administration

NTIA Report 14-499

Effects of Radar Interference on LTE Base Station Receiver Performance

Frank H. Sanders
John E. Carroll
Geoffrey A. Sanders
Robert L. Sole

U.S. DEPARTMENT OF COMMERCE

December 2013
Reissued May 2014

NOTE ON REISSUE

The duty cycles of four radar interference waveforms were misstated in the original version of this report published in December 2013. The error was due to a mistake in the equations on page 8, now corrected, in which a pulse repetition rate (PRR) variable was used instead of a pulse repetition interval (PRI) variable. The waveforms' pulse widths, pulse repetition rates, and chirp bandwidths were correctly reported.

The four waveforms are shown with their corrected duty cycles in the table below. Table 2 and the pertinent figure captions have been corrected in the report body, along with the equations on page 8.

Errata Table 1. Erroneously reported and true duty cycles for four waveforms.

Waveform	Erroneously Reported Duty Cycle (percent)	True Duty Cycle (percent)
Q3N-4	10	0.40
Q3N-7	20	0.20
Q3N-10	30	0.13
Q3N-11	30	13

DISCLAIMER

Certain commercial equipment and materials are identified in this report to specify adequately the technical aspects of the reported results. In no case does such identification imply recommendation or endorsement by the National Telecommunications and Information Administration, nor does it imply that the material or equipment identified is the best available for this purpose.

CONTENTS

FIGURES

TABLES

ABBREVIATIONS/ACRONYMS AND SYMBOLS

BLER	block error rate
CSV	comma separated variable
DC	duty cycle
EIRP	effective isotropic radiated power
FCC	Federal Communications Commission
FDR	frequency dependent rejection
I	interference power
ITS	Institute for Telecommunication Sciences (NTIA)
LNA	low noise amplifier
LTE	Long Term Evolution
MIMO	multiple input multiple output
N	noise power
NPRM	Notice of Proposed Rulemaking
NTIA	National Telecommunications and Information Administration
OOB	out of band
OSM	Office of Spectrum Management
P0N	fixed-frequency carrier wave pulse modulation
PW	pulse width
PRR	pulse repetition rate
Q3N	swept-frequency carrier wave pulse modulation
RF	radiofrequency
RLM	radio link monitoring
S	LTE signal power
TDD	time division duplexing

TDWR Terminal Doppler Weather Radar

UE user equipment

VSG vector signal generator

EXECUTIVE SUMMARY

Recently, the Federal Communications Commission (FCC) issued a Notice of Proposed Rulemaking (NPRM) in FCC Docket 12-354, regarding possible future spectrum sharing between radar and non-radar systems in the band 3550–3650 MHz. This NPRM called for tests and measurements to investigate the compatibility of broadband communications systems and incumbent federal radars operating in that band. In response, personnel from NTIA's Office of Spectrum Management (OSM) and NTIA's Institute for Telecommunication Sciences (ITS) have performed interference-effects tests in which simulated radar signals were injected into a 4G Long Term Evolution (LTE) Time Division Duplexing (TDD) base station receiver that operates in the band 2500–2690 MHz. Since LTE protocols are not frequency-dependent, the results derived from tests on this LTE base station are believed to be equally valid for systems that may in the future operate in the 3550–3650 MHz spectrum range.

The LTE system was of a type used for macro-cell coverage. The NPRM is focused on micro-cell deployment of LTE broadband for possible use in the band 3550–3650 MHz. The authors do not believe that differences in LTE implementation between macro-cell and micro-cell systems would significantly affect the responses of LTE base stations to radar interference, given that the LTE protocols should not depend on the size of cell coverage. Macro and micro LTE base station receivers should only differ in antenna type, height, gain, and orientation. Those differences may affect the level of radar interference coupled into the receiver, but not how it is processed by the receiver's signal processor. These tests have *not* investigated high-power effects such as LTE receiver saturation or front-end overload; the radar interference signal power levels were purposely kept below the LTE receiver's saturation threshold limits as specified by the LTE operator that assisted NTIA in the testing. The LTE operator configured an LTE network for the tests and maintained it in manner similar to an actual deployment during all phases of testing. The testing was done in an RF-shielded subterranean room that was free of any external RF sources that could possibly affect the test results.

Twenty-seven radar interference waveforms were injected into the LTE base station receiver while the receiver communicated with a handset; the tests were performed in a closed-loop test bed under steady-state conditions. Diagnostic software running in the background collected data on the receiver's performance. The desired signal power of the handset signal at the base station receiver was held at a constant level throughout the tests, set to a nominal level by the LTE engineers who assisted the testing. The LTE data throughput, block error rate (BLER), and receiver noise power were measured in one-second intervals and stored for post-test analyses. The nominal data rate was 16 Mbit/s in the absence of interference. Call initiation and hand-off performance were not tested.

Each interference waveform was specified by pulse modulation, pulse width, and pulse repetition rate. Pulse modulation for each waveform was either simple pulsing of a fixed-frequency carrier wave or else swept-frequency for the duration of each pulse (called chirping). The radar waveforms were *not* exact replications of any existing or planned future operational 3.5 GHz radar emissions. By not exactly replicating any operational or possible future radar waveforms,

the authors avoided issues with association, classification, and identification of particular waveforms with individual radar systems. This approach also made the test results applicable to radar interference effects on LTE receivers on a general rather than system-specific basis. The radar interference waveform parameters were carefully tailored to span the entire range of all existing and anticipated future waveforms that do/will occur in the 3.5 GHz spectrum. Two band-limited Gaussian noise waveforms were included as were two waveforms from a test that was previously performed by the European CEPT Electronic Communications Committee (ECC). A waveform that replicated one used by a widely deployed type of weather radar which operates in the band 5600–5650 MHz was also tested.

To perform the tests, the interference waveforms were held at fixed power levels during 30 second intervals of data collection. The injected power for each waveform started at a low level and was increased in discrete steps until reaching a point 7 dB below the LTE receiver saturation level. The impacts of the waveforms on the base station receiver's data throughput rate (handset to base station), BLER and internal noise level were processed to produce graphs showing the impact that each waveform had on the receiver's performance as a function of the receiver's signal over interference-plus-noise (*S/(I+N)*) ratio. Most waveforms produced appreciable effects at *S/(I+N)* levels below 0 dB, and many of the waveforms degraded LTE performance at *S/(I+N)* levels somewhat above 0 dB. As the interference power level was increased, the interference impact gradually increased. Sudden impacts to the data throughput as a function of interference level, the so-called cliffs that often occur in digital communication system performance as error correction reaches its limits and fails, were not observed. Some interference waveforms seemed to have no impact. The measured data show that at times the LTE system mitigated the interference.

Regarding the results for specific waveforms and trends, for the simple pulsed (P0N) waveforms, the ones that caused the most effects or loss of data throughput were P0N2, P0N5, P0N10, and P0N12. All of the P0N waveforms caused some data throughput loss, with the least effects being from P0N4 and P0N6. For the chirped-pulsed (Q3N) waveforms, the two that caused the most data throughput loss were waveforms Q3N1 and Q3N5. Some waveforms caused no loss of data throughput, as in Q3N4, Q3N7, and Q3N10, apparently due to low duty cycles of 0.4, 0.2, and 0.13 percent, respectively. It is beyond the scope of this report to determine *why* those particular waveforms had the most effect, or why others had a minimal effect on the LTE receiver. NTIA welcomes LTE operators to review these data and share their views on these test results.

The authors do not determine the acceptability of radar interference effects on LTE base station performance. The data in this report can be used as a building block in the construction of frequency-and-distance separation curves for radar transmitters and LTE base station receivers, supporting possible future spectrum sharing at 3.5 GHz.

More work is needed in this area to support sharing in the band 3550–3650 MHz. Topics for additional testing could include: these same types of tests with a true micro-cell LTE receiver, an investigation of LTE receiver saturation and gain compressions due to pulsed signals, investigation of pulsed radar interference in an FDD LTE system, and measuring the emissions of more LTE base station transmitters. NTIA is prepared to work with other government agencies and industry to accomplish these goals.

EFFECTS OF RADAR INTERFERENCE ON LTE BASE STATION RECEIVER PERFORMANCE

Frank H. Sanders,[1] John E. Carroll,[1] Geoffrey A. Sanders,[1] Robert L. Sole[2]

In response to proposals to introduce new radio systems into 3550–3650 MHz radio spectrum in the United States, the authors have performed measurements and analysis on effects of interference from a variety of radar waveforms to the performance of a Long Term Evolution (LTE) base station receiver. This work has been prompted by the possibility that LTE base station receivers may eventually share spectrum with radar operations in this spectrum range. The base station receiver that was tested used time division duplex (TDD) modulation. Radar pulse parameters used in this testing spanned the range of both existing and anticipated future radar systems in the 3100–3650 MHz spectrum range. LTE base station receiver data throughput rates, block error rates (BLER), and internal noise levels have been measured as functions of radar pulse parameters and the incident power level of radar pulses in the base station receiver. The authors do not determine the acceptability of radar interference effects on LTE base station performance. Rather, these data are presented for the use of spectrum managers and engineers who can use this information as a building block in the construction of frequency-and-distance separation curves for radar transmitters and LTE base station receivers, supporting possible future spectrum sharing at 3.5 GHz.

Key words: Block error rate (BLER); chirped pulses; Long Term Evolution (LTE); P0N pulses; radar; spectrum sharing; time division duplexing (TDD)

1 INTRODUCTION

Recently, the Federal Communications Commission (FCC) issued a Notice of Proposed Rulemaking (NPRM) [1], regarding possible future spectrum sharing between radar and non-radar systems in radio spectrum near 3.5 GHz. In response to this NPRM, personnel from NTIA's Office of Spectrum Management (OSM) and NTIA's Institute for Telecommunication Sciences (ITS) have performed interference-effects tests in which simulated radar signals were injected into a 4G Long Term Evolution (LTE) Time Division Duplexing (TDD) base station[3] receiver that operates in the band 2500–

[1] The first three authors are with the Institute for Telecommunication Sciences, National Telecommunications and Information Administration (NTIA), U.S. Dept. of Commerce, Boulder, CO 80305.

[2] The author is with the Office of Spectrum Management, NTIA, U.S. Dept. of Commerce, Washington, DC 20230.

[3] The particular model of LTE base station that was used for these tests is not believed to be relevant to the test results; the model's identification will be provided by NTIA/OSM upon specific request.

2690 MHz. Since LTE protocols are not frequency-dependent, the results derived from tests on this LTE base station are believed to be equally valid for systems that may in the future operate in the 3100–3650 MHz spectrum range.

A macro-cell LTE system was used in the NTIA tests described in this report. Although current plans for LTE operations at 3.5 GHz in the United States envision the use of micro-cell LTE systems, as described in [1], the authors do not believe that differences in LTE implementation between macro-cell and micro-cell systems would significantly affect the responses of LTE base stations to radar interference; the differences between the systems are understood to be primarily in base station antenna types, heights, and gains, along with transmitter power levels. Error correction and other signal processing parameters are believed to be the same between the two types of system.[4] Comments and reply comments made to date to [1] seem to support these assumptions.

The tests were performed in June 2013 at a private-sector carrier laboratory in Herndon, Virginia. The effects of radar interference on the base station receiver's data throughput rate, block error rate (BLER), and internal noise level were observed and recorded. Those results, and the measurements that produced them, are described in this report.

The authors do not determine the acceptability of radar interference effects on LTE base station performance. Rather, these data are presented for the use of spectrum managers and engineers who can use this information as a building block in the construction of frequency-and-distance separation curves for radar transmitters and LTE base station receivers, supporting possible future spectrum sharing at 3.5 GHz.

1.1 Interference Coupling Scenario for Possible Future 3.5 GHz Spectrum Sharing

Spectrum at 3.5 GHz is heavily utilized by a variety of radar systems. Many of these radars operate on ships in near-shore (littoral) waters around American coastlines. These radars are used for a variety of purposes and missions including air surveillance and air defense. These radars' transmitted beams scan through 360 degrees of azimuth around their ship platforms, providing detection, surveillance and tracking of air-breathing aerial targets at distances of up to about 180-240 nautical miles (nmi) and of targets outside the Earth's atmosphere at larger distances. These radar beams are scanned over both oceans and littoral shorelines. The air-search radar beam shapes often have cross sections in the shape of a 1/(squared cosecant) function. The lower-edges 3 dB points of the radars' air-search and space-search beams are typically tilted above any given ship's local horizon at an angle of about 0.5 to 1.0 angular degrees. Additional information about 3.5 GHz radar systems is presented in [2].

Traditional (legacy) long range air-search radar waveforms often utilize pulse widths (PWs) that are between 1 and 10 μs long, at pulse repetition rates (PRRs) of between 300 and 1,000 pulses/sec. The transmitted waveform duty cycles (DC, defined as time interval during which waveform power is transmitted divided by total time of the waveform's periodicity) of

[4] To verify the equivalence between micro and macro cell LTE base station performance in the presence of radar interference, NTIA plans to perform a set of tests similar to those described in this report on a micro-cell LTE system in the near future.

such radars are about 0.1 percent. Such radars use tube-type output devices (e.g., magnetrons, klystrons, crossed-field amplifiers) that generate effective isotropic radiated peak power levels (peak EIRP) of 1–10 GW. Newer radars often use solid-state output devices radiating peak EIRPs of 10–100 MW, but at the cost of proportionally longer PWs and higher DCs that can approach 10 percent.[5] The longer PWs of current and future solid state radars require, in turn, that transmitted pulses be frequency-modulated or phase coded to maintain adequate range resolution. The NTIA radar interference waveforms needed to incorporate the characteristics of both legacy and newer radars.

Future LTE systems at 3.5 GHz are expected to operate with handheld user equipment (UE) units that will usually be at or near ground level. The UEs are expected to communicate with LTE base stations that will typically be located at greater heights than the UEs, for example on the sides of buildings or on building rooftops. Because antenna beams for the radar systems of concern are tilted somewhat above local horizons, they should couple more strongly into LTE systems' base station receivers than into the UE receivers. This coupling scenario is shown schematically in Figure 1. This is the scenario that the authors re-created electronically for tests of the effects of radar interference on possible future 3.5 GHz LTE base station receivers.

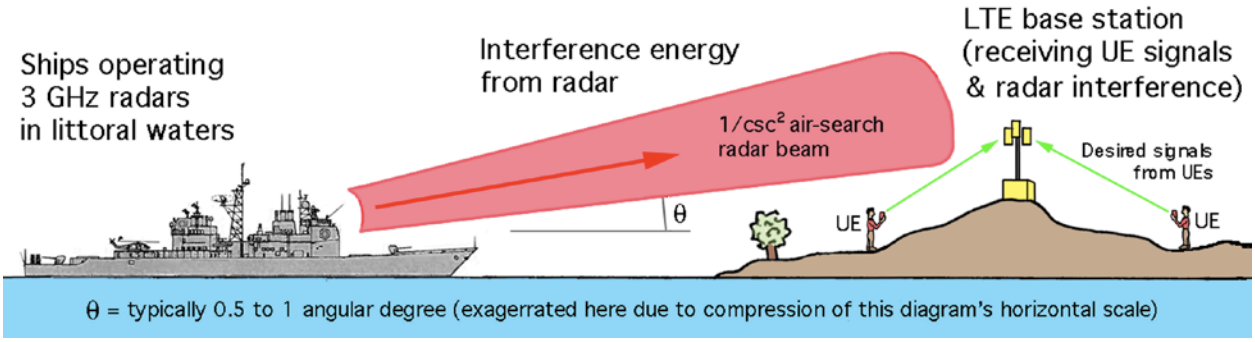

Figure 1. Schematic diagram showing coupling scenario between littoral radar transmitters and possible future 3.5 GHz LTE systems. By geometry, coupling from radar transmitters should occur more into LTE base station receivers than into UEs.

1.2 Implementation of the Interference Scenario in an Interference-Effects Test Bed

The authors assembled a hardware implementation of the coupling scenario of Figure 1 in a test bed. This included an LTE UE, an LTE base station, and a transmitter producing radar interference waveforms. This implementation is shown schematically in Figure 2 and as a more electronically detailed diagram in Figure 3.

Radar interference needed to be injected into the receiver side of the LTE base station along with desired LTE signals originating from an LTE UE. To do this, and to establish and maintain normal LTE communications during the testing, a link had to be established for regular, two-way

[5] Solid-state radars can cause more interference than higher-power tube-transmitter radars because the peak EIRPs of the newer radars is still high enough to exceed interference thresholds for many systems, while their higher DCs of around 10 percent have more impact in the time domain than the 0.1 percent DCs of older radars.

communications between the base station and UE.[6] At the LTE base station receiver input, a radio frequency (RF) combiner was installed to couple radar signals into the receiver along with the desired UE signals. This combiner requirement is shown schematically in Figure 2.

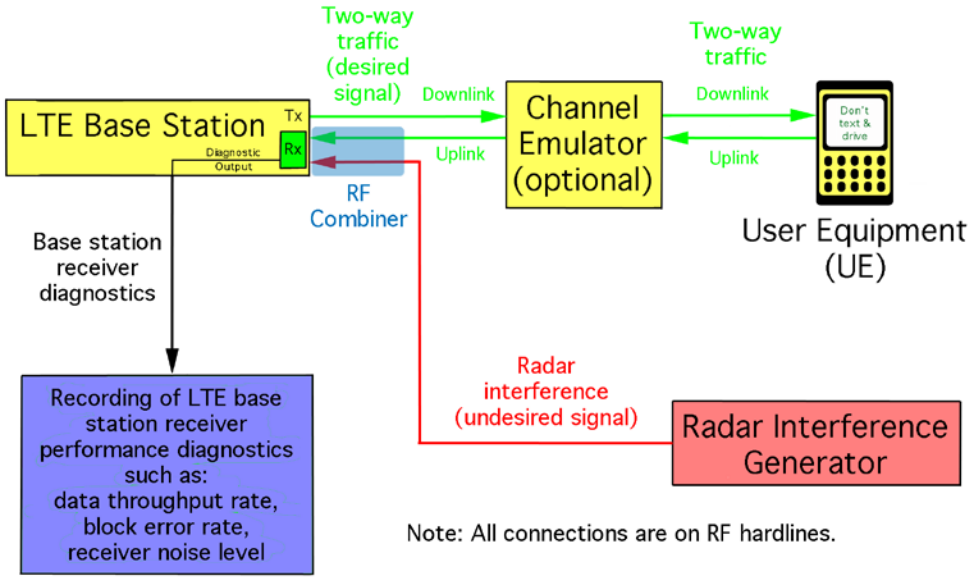

Figure 2. Simple diagram of the test bed for the radar-to-LTE interference scenario of Figure 1.

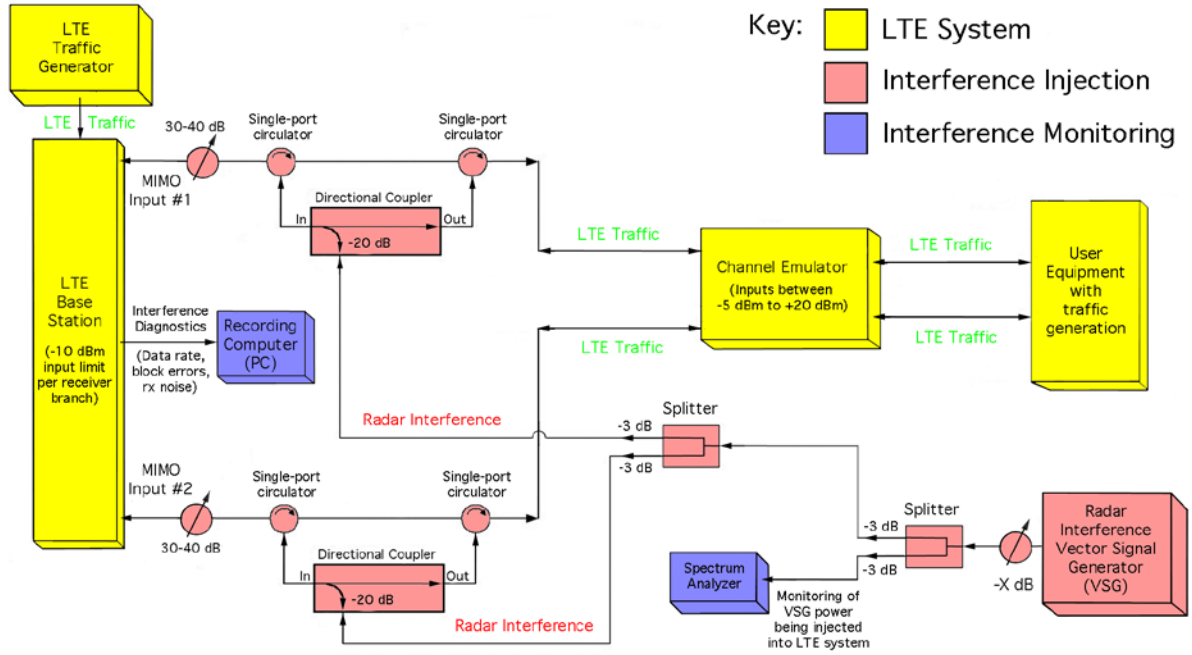

Figure 3. Detailed diagram of the interference-effects test bed of Figure 2.

[6] It is noted that there could be utility in eventually testing an LTE base station with multiple UE inputs.

The effects of interference needed to be determined by observing and recording diagnostic outputs from the LTE base station receiver whilst radar interference was injected. The interference effects were measured as functions of the power levels and waveform modulations of the radar interference. The measured diagnostic parameters were the base station receiver's data throughput rate, BLER, and internal noise level.

All connections within the test-bed were via hard lines; the LTE communication signal and the radar interference were not radiated. Hard lines were used so that the effects of radar interference could be observed without any effects from radio propagation, antenna performance, environmental noise or extraneous signals from other radio systems. While such collateral factors might well affect actual 3.5 GHz spectrum sharing, the purpose of this study was to understand the effects of radar interference alone; a hard line test bed was deemed to be the best approach for observing radar interference effects with a high degree of isolation and acuity. Propagation studies and analysis will eventually be needed to determine the exact power levels that would be coupled from radar transmitters to LTE receivers at actual field locations under a variety of ambient conditions and circumstances, as discussed in [2]. LTE performance degradation that might arise from additional factors associated with radiated signal environments should likewise be studied separately.

Although the basic concept of the radar-to-LTE interference test-bed was reasonably straightforward, as shown in Figure 2, the actual test-bed implementation was somewhat more complicated, as shown in Figure 3. Complications arose principally from the need to run bidirectional communications between the LTE base station and UE while coupling radar interference unidirectionally, into only the base station receiver. To combine bidirectional, desired signal traffic with unidirectional, undesired interference waveforms, the authors assembled the network of RF circulators and directional couplers shown in Figure 3. By installing a circulator at each straight-through path end of a directional coupler and connecting those two circulators to each other and to the UE and the base station (as shown in Figure 3), bidirectional desired traffic was maintained between the LTE base station and UE with a nominal non-interference throughput rate of 16 Mbit/s[7]. The radar interference, meanwhile, was coupled into the two LTE base station MIMO receiver channels via each coupler's -20 dB port and each adjacent circulator, with the UE being effectively isolated from the interference energy.

The authors programmed an Agilent 8267C vector signal generator (VSG) to generate radar interference waveforms and also two Gaussian noise waveforms. The interference waveforms are described in detail in Section 2, below. The VSG output was split between a spectrum analyzer monitor and the LTE base station receiver, and then was split again to feed each of the receiver's MIMO channel inputs, as shown in Figure 3. Appendix A presents the power budget for the radar interference power levels in the LTE test bed system on a component-by-component basis, from the VSG output to the LTE MIMO receiver channel inputs.

[7] The LTE system's communication traffic was generated by a proprietary generator belonging to the carrier. It was the same traffic generator as the carrier uses for LTE system development and performance-verification testing.

2 INTERFERENCE-EFFECTS TESTING PROCEDURES

2.1 LTE Operation During Testing

As shown in Figures 2 and 3, the UE and LTE units operated with traffic generators and communicated via a channel emulator. The UE and an associated channel emulator operated on a pair of MIMO channels. LTE base station receiver performance (data throughput rate, BLER,[8] and noise level) was monitored by third-party software at one-second intervals throughout the testing.[9] These diagnostics were recorded during testing for use in post-measurement analysis. The channel emulator was operated in the carrier's nominal configuration. The emulator's data throughput rate to the base station in the absence of interference was always 16 Mbit/s, as noted above, but further details of the emulator's set-up were not described.

2.2 Radar and Gaussian Noise Interference Waveforms

The interference effects of twenty-seven radar waveforms and two bandwidths of Gaussian noise were tested. Each radar waveform was pulsed and was specified by modulation, PW, and PRR. Radar pulses were modulated as either fixed-frequency carrier waves (designated P0N) or else as swept-frequency carriers (called chirping, designated Q3N).[10] The radar waveforms were *not* exact replications of any existing or planned future operational 3.5 GHz radar emissions. By not exactly replicating any operational or possible future radar waveforms, the authors avoided issues of identification of waveforms with operational radar systems. This approach was also intended to make the test results applicable to radar interference effects on LTE receivers on a generic rather than a system-specific basis. The radar interference waveform parameter space was designed, however, to span the entire range of all existing and possible future radar waveforms that do/may occur in 3.5 GHz spectrum.

Two Gaussian noise waveforms, of 10 MHz and 20 MHz bandwidth, were programmed and used in the testing. The noise testing was intended to provide a sanity check on the results of the radar interference testing. The authors estimated, in advance of the testing, that Gaussian noise testing should verify that the LTE test bed system would yield interference effects even if some or none of radar waveforms were to produce identifiable interference effects.

The technical characteristics of the radar interference waveforms are shown for P0N and Q3N pulse modulations, respectively, in Tables 1 and 2. In these tables, PW is pulse width and PRR is pulse repetition rate. Each entry includes a code printed in red by which each waveform was

---

[8] BLER is used in LTE/4G technology to indicate in-sync and out-of-sync conditions during radio link monitoring (RLM). It is defined as the number of erroneous resource blocks divided by the total number of blocks.

[9] The monitoring software was a proprietary package ordinarily used by the carrier company's laboratory personnel to diagnose the performance of their LTE systems.

[10] P0N and Q3N designations are used to identify these modulations in the *NTIA Manual of Regulations and Procedures for Federal Radio Frequency Management* (the so-called NTIA Red Book), Section 9.8.2. http://www.ntia.doc.gov/page/2011/manual-regulations-and-procedures-federal-radio-frequency-management-redbook

identified in the VSG's on-board program storage; these codes were used in the field-data logs to identify each waveform as testing progressed. The programmed interference waveforms included the 10 MHz and 20 MHz-wide Gaussian noise described above, plus a waveform similar to that of a terminal Doppler weather radar (TDWR) and two waveforms (designated ECC-1 and -2) that were used in similar previous interference testing in Europe [3].

Table 1. P0N (carrier wave) pulsed radar waveform parameters.

Duty Cycle (percent)	PRR = 1000/sec	PRR = 3000/sec	PRR = 10,000/sec
0.1	PW = 1 μs P0N-1	PW = 0.33 μs P0N-2	PW = 0.1 μs P0N-3
1	PW = 10 μs P0N-4	PW = 3.33 μs P0N-5	PW = 1 μs P0N-6
3	PW = 30 μs P0N-7	PW = 10 μs P0N-8	PW = 3 μs P0N-9
10	PW = 100 μs P0N-10	PW = 33.3 μs P0N-11	PW = 10 μs P0N-12

Table 2. Q3N (swept-frequency) pulsed radar waveform parameters, 1 MHz/μs chirp.

Duty Cycle (percent)	Chirped Pulse Group 1		Chirped Pulse Group 2		Chirped Pulse Group 3	
	PW (μs)	PRR (s^{-1})	PW (μs)	PRR (s^{-1})	PW (μs)	PRR (s^{-1})
1	10	1000 Q3N-1	1	10,000 Q3N-2	0.33	30,000 Q3N-3
10	100 → 20	1000 → 200 Q3N-4 (0.4% duty cycle)	10	10,000 Q3N-5	3.3	30,000 Q3N-6
20	200 → 20	1000 → 100 Q3N-7 (0.2% duty cycle)	20	10,000 Q3N-8	6.6	30,000 Q3N-9
30	300 → 20	1000 → 67 Q3N-10 (0.13% duty cycle)	30 → 20	10,000 → 6,667 Q3N-11 (13% duty cycle)	10	30,000 Q3N-12

Table 3. Additional special interference waveforms used in testing.

Duty Cycle (percent)	Waveform Names	PW (μs)	PRR (pulses/sec)
0.4	ECC-1 WFM-1	4	1000
3	ECC-2 WFM-2	100	300
0.05	TDWR P0N-13	1	500

An overall goal of the interference waveform design was to vary interference DC values in an approximately logarithmic progression: 1 percent, 3 percent 10 percent, and so forth. PW and PRR values were adjusted to achieve these duty cycles. For the P0N pulses, setting DC was

straightforward: *DC = (pulse width)/(pulse repetition interval)*. The P0N pulses were tuned to the same frequency as the center frequency of the LTE base station.

For the Q3N (chirped) pulses, the problem was more complicated. While the goal for a DC progression was the same for the chirped pulses as for the P0N pulses, the chirp bandwidth was an additional degree of freedom in the waveform design. The authors dealt with this by holding the chirp frequency-sweeping rate constant at 1 MHz per microsecond. In order to maintain a 1 megahertz/microsecond chirp rate within the 20 MHz LTE receiver bandwidth while also maintaining DC, pulse widths could not be allowed to exceed 20 μs. This adjustment to *PW* required adjustment of pulse repetition interval (PRI) to maintain duty cycle. The relationship is one of proportionality:

$$\frac{\tau'}{PRI'} = \frac{\tau_0}{PRI_0}$$

where τ_0 = full pulse width of a chirped radar pulse, PRI_0 = full pulse repetition interval for chirped radar pulses, τ' = reduced pulse width for testing, and PRI' = reduced pulse repetition interval for testing. Since the reduced pulse widths chirped 20 MHz in 20 μs and were 20 μs long, the adjusted PRI values were computed as:

$$PRI' = \tau' \frac{PRI_0}{\tau_0} = (20\ \mu s) \frac{PRI_0}{\tau_0}$$

These adjustments are shown in Table 2. The chirp direction was always from low to high frequency and the center frequencies were the same as the LTE base station.

2.3 Testing Methodology

The overall concept of the testing methodology was to measure and record the LTE diagnostics of data throughput rate, BLER, and internal receiver noise level for a wide range of interference power levels for every interference waveform listed in Tables 1–3. Interference was quantified in terms of the term *S/(I+N)*, where *S* = the desired signal level from the UE in the base station receiver, *I* = the power level[11] of the interference waveform in the base station receiver, and *N* = the internal, inherent (non-interference) noise power in the base station receiver. Both *S* and *N* were held constant throughout the testing. The interference power level, *I*, was varied during the testing, and interference effects were measured as *I* was varied. Appendix A describes in detail the measurement and quantification of the *S/(I+N)* term in the overall test bed system in general and the LTE receiver in particular. Table 4 shows the values of *S*, *I* and *N* that resulted in the *S/(I+N)* levels shown in the data graphs in this report. The power levels in Table 4 are at the input to the LTE base station receiver.

For each interference waveform, the testing proceeded by first establishing LTE communications between the LTE traffic generators of the base station and the UE in a non-interference state (that is, with the VSG RF output turned off). The base station receiver's diagnostic software outputs

[11] Peak power for radar interference and average power for Gaussian noise interference.

began to record dedicated electronic (comma-separated variable, or CSV format) files for the data throughput rate, BLER, and receiver noise power.

Table 4. Values of *S*, *I* and *N* yielding given *S/(I+N)* levels.

Signal level, *S*, in LTE resource block (dBm/180 kHz)	Interference level, *I*, in LTE resource block (dBm/180 kHz)[12]	LTE receiver inherent noise level, *N*, in LTE resource block (dBm/180 kHz)	*S/(I+N)* in LTE resource block (dB)
-103 (fixed)	-186 (VSG off)	-118 (fixed)	15
-103 (fixed)	-115	-118 (fixed)	10
-103 (fixed)	-108	-118 (fixed)	5
-103 (fixed)	-103	-118 (fixed)	0
-103 (fixed)	-98	-118 (fixed)	-5
-103 (fixed)	-93	-118 (fixed)	-10
-103 (fixed)	-88	-118 (fixed)	-15

All three of these diagnostic parameters were recorded every second throughout every waveform test, in the same manner as if those data were streaming to a continuously running tape or strip-chart recorder. The interference was initially kept off while the base station's diagnostic software recorded interference-free data for at least 30 seconds (and occasionally longer); this initial set of points documented the base station's baseline condition.

Then, with the diagnostics still running and recording, a selected VSG interference waveform was turned on at a low interference power level, *I* (corresponding to $S/(I+N) \approx S/N$). That level was maintained for 30 seconds as the data recording continued. As the LTE base station diagnostics continued to record, the *I* level was gradually increased (causing the *S/(I+N)* level to gradually decrease). The *I* level was stepped upward in fixed increments, usually 4 dB at a time.[13] Each successive interference power level was maintained for 30 seconds as diagnostics recorded. The testing for each interference waveform was terminated when the *I* level reached the upper limit that the carrier company would permit for their equipment.[14]

After the final, maximum interference power level was reached with the corresponding data throughput recorded, the interference was turned off and an additional 30 seconds of data were recorded in a baseline, non-interference condition as the base station receiver recovered. This condition concluded each waveform test.

[12] Interference power level is RMS average detected for Gaussian noise and is peak detected for radar interference waveforms.

[13] A first run of interference testing was performed with a 10 dB interference power stepping increment, but a second series of runs was performed with this increment reduced to 4 dB for radar interference and 2 dB for noise interference. This change was prompted by increasing familiarity of the authors with the performance of the LTE system in the presence of interference, and the authors' examination of the initial set of 10 dB-increment test results. All interference results for all increments were combined to produce the analyzed interference-effects graphs in this report.

[14] This limit was based on the maximum reverse-flow radar power that the operator would allow to reach the channel emulator; that power limit resulted in a minimum *S/(I+N)* level (maximum interference power level) of -7 dB for all testing.

3 INTERFERENCE-EFFECTS TEST RESULTS

3.1 Notes on the Interference-Effects Data Graphs

Figures 4–61 show the effects of radar waveform interference and Gaussian noise interference on LTE base station receiver data throughput rate, BLER, and internal noise. The data-throughput graphs are presented in Figures 4–32, and the BLER graphs are presented in Figures 33–61. The noise data are plotted as green lines on the data-throughput and BLER graphs. On all data graphs, a *decreasing* level of *S/(I+N)* corresponds to an *increasing* level of interference power, *I*.

For each data point on each graph, vertical bars are plotted at 10 percent and 90 percent values for the diagnostic 28 (and occasionally a few more more) samples that were recorded and analyzed at each interference waveform power level. In Figures 4–32, a smoothing spline was used to fit curves through the data points.

The baseline condition of *S/(I+N)* = +15 dB represents a very strong desired signal level for LTE; one source [4] indicates that an *S/(I+N)* of -7 dB is considered a nominal condition for LTE systems in non-interference conditions. The strong baseline signal used in these tests represents a condition that accommodates shadowing for outdoor operation and building penetration losses for indoor operation of LTE.

3.2 Interference-Effects Data Graphs

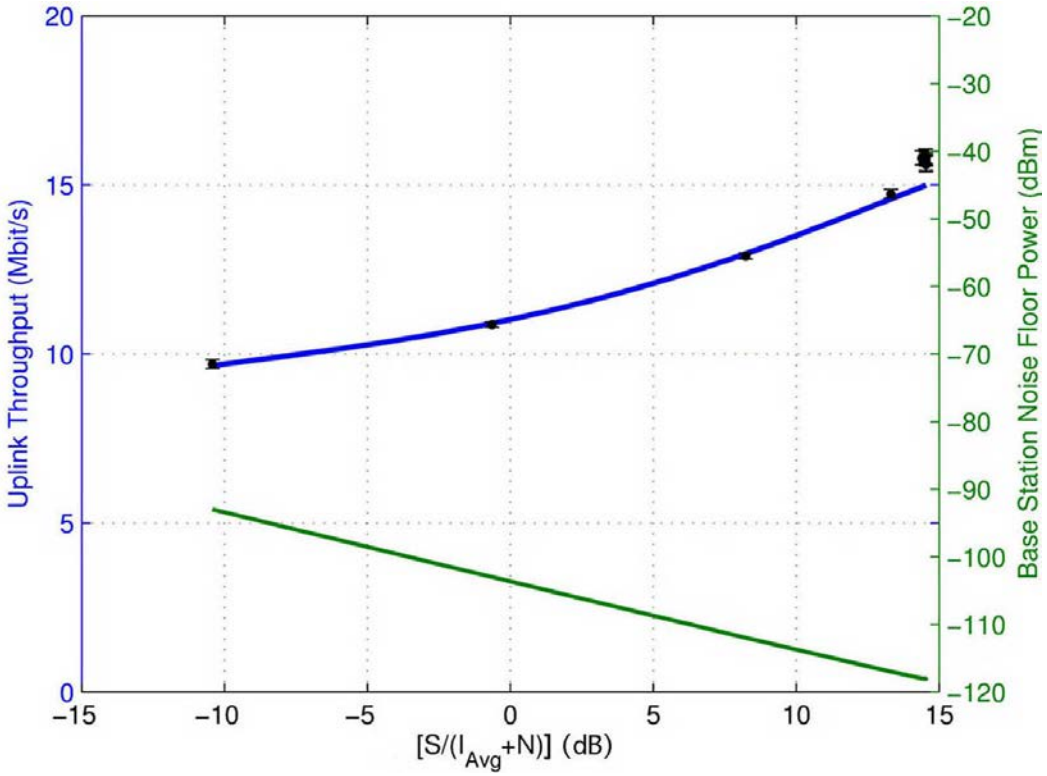

Figure 4. Data throughput for 10 MHz-wide Gaussian noise interference.

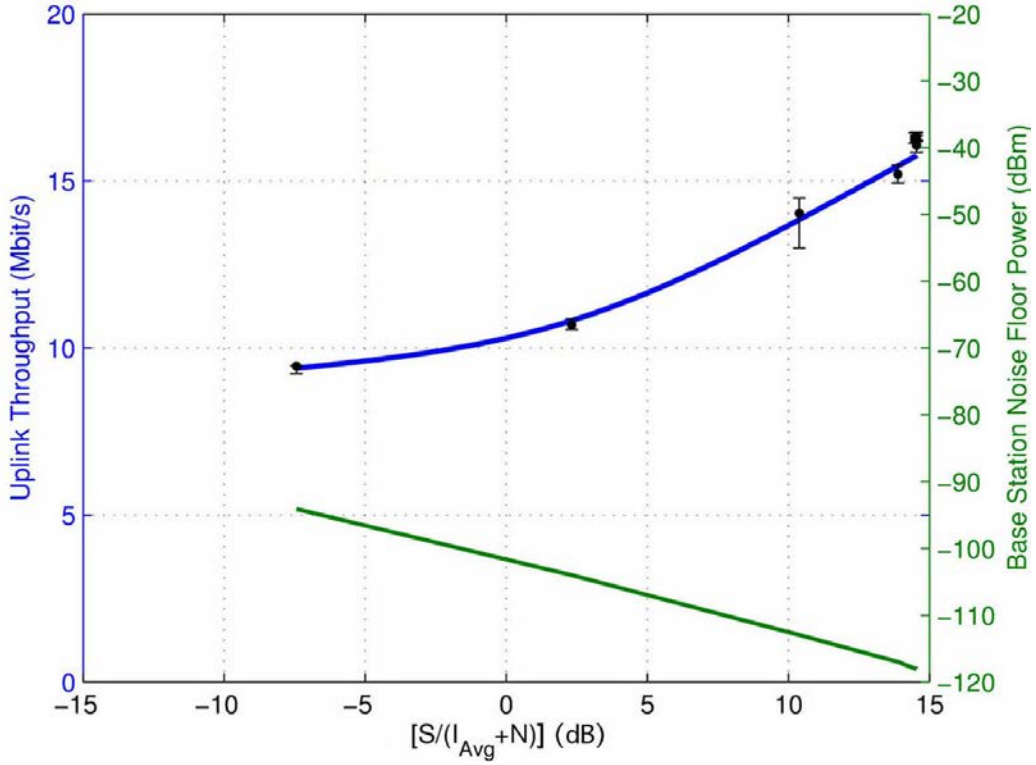

Figure 5. Data throughput for 20 MHz-wide Gaussian noise interference.

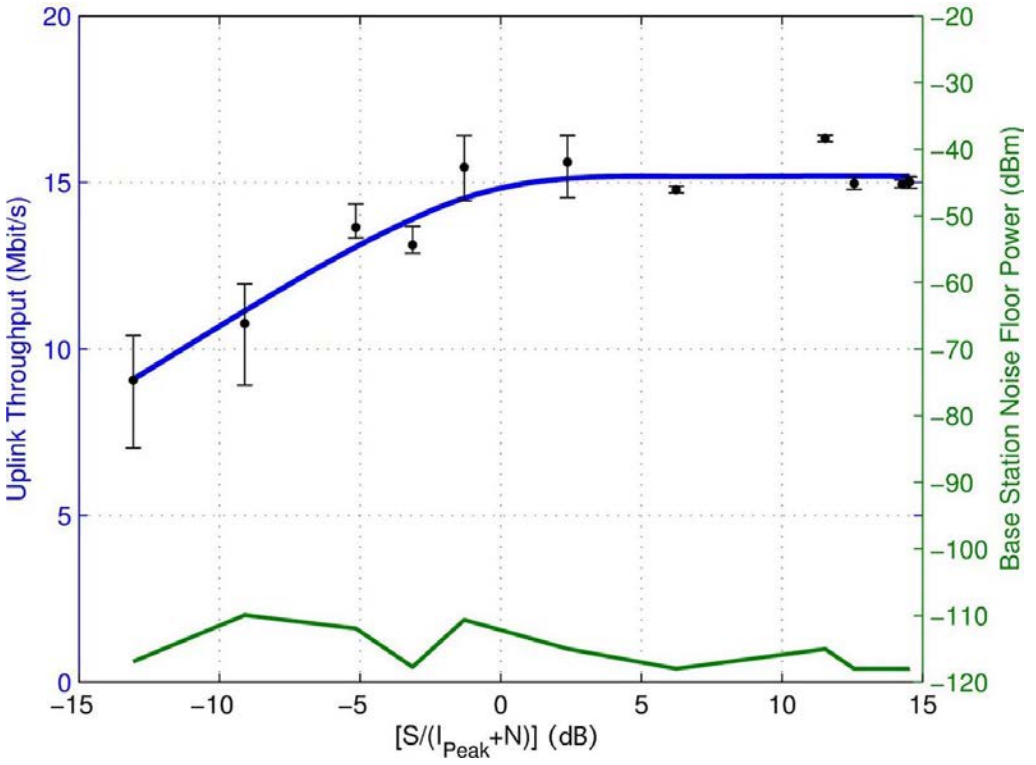

Figure 6. Data throughput for ECC-1/WFM-1 (PW = 4 μs, PRR =1000/sec, DC = 0.4%) interference.

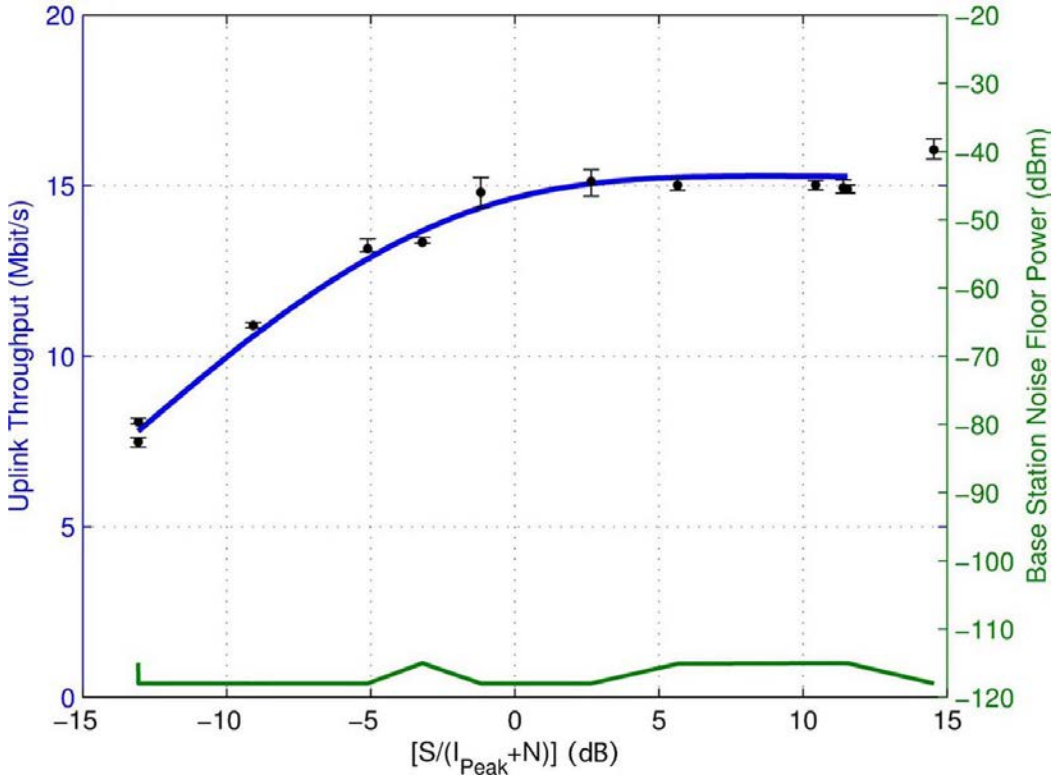

Figure 7. Data throughput for ECC-2/WFM-2 (PW = 100 µs, PRR = 300/sec, DC = 3%) interference.

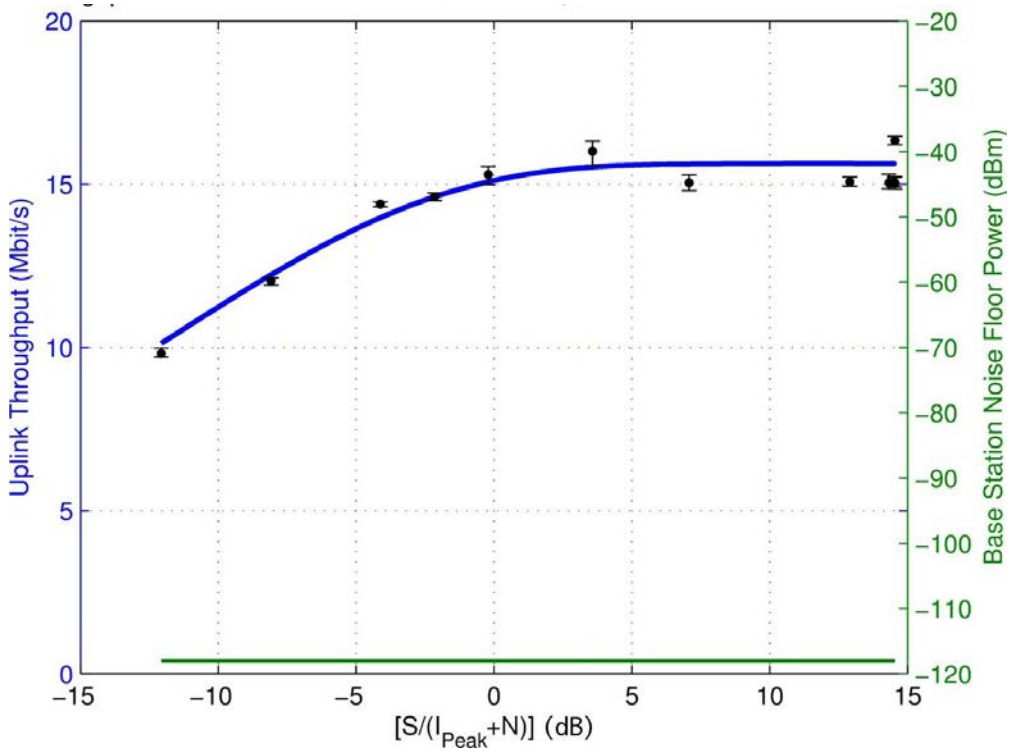

Figure 8. Data throughput for P0N-1 (PW = 1 µs, PRR = 1000/sec, DC = 0.1%) interference.

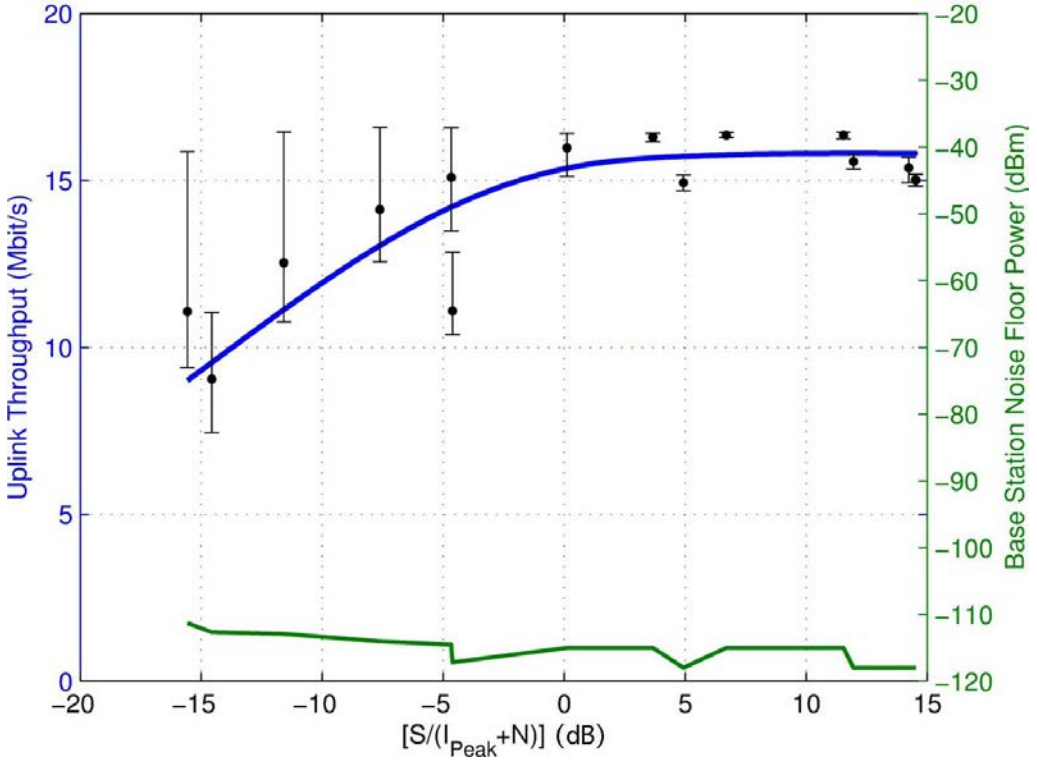

Figure 9. Data throughput for P0N-2 (PW = 0.33 μs, PRR = 3000/sec, DC = 0.1%) interference.

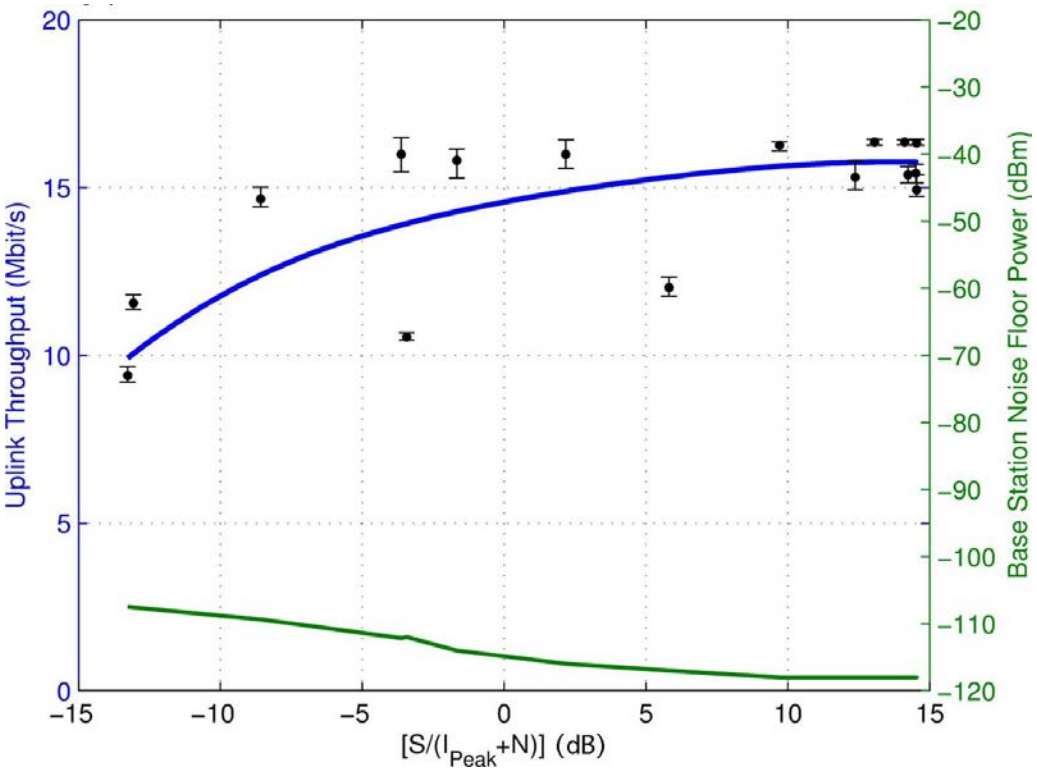

Figure 10. Data throughput for P0N-3 (PW = 0.1 μs, PRR = 10,000/sec, DC = 0.1%) interference.

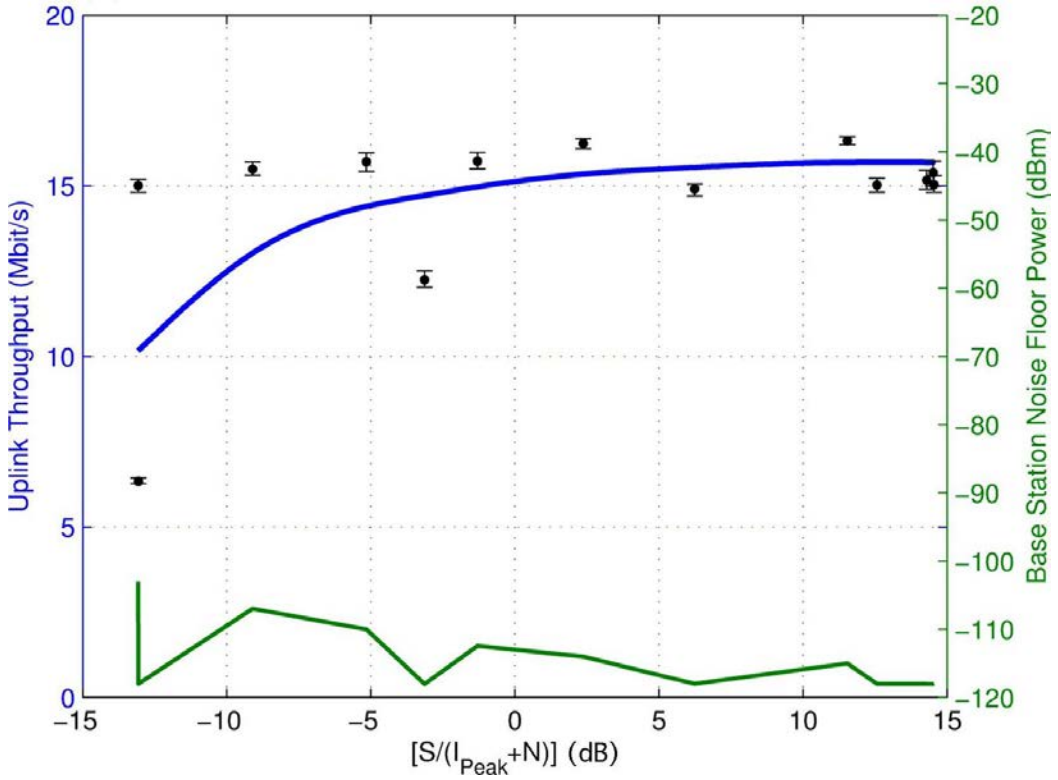

Figure 11. Data throughput for P0N-4 (PW = 10 μs, PRR = 1,000/sec, DC = 1%) interference.

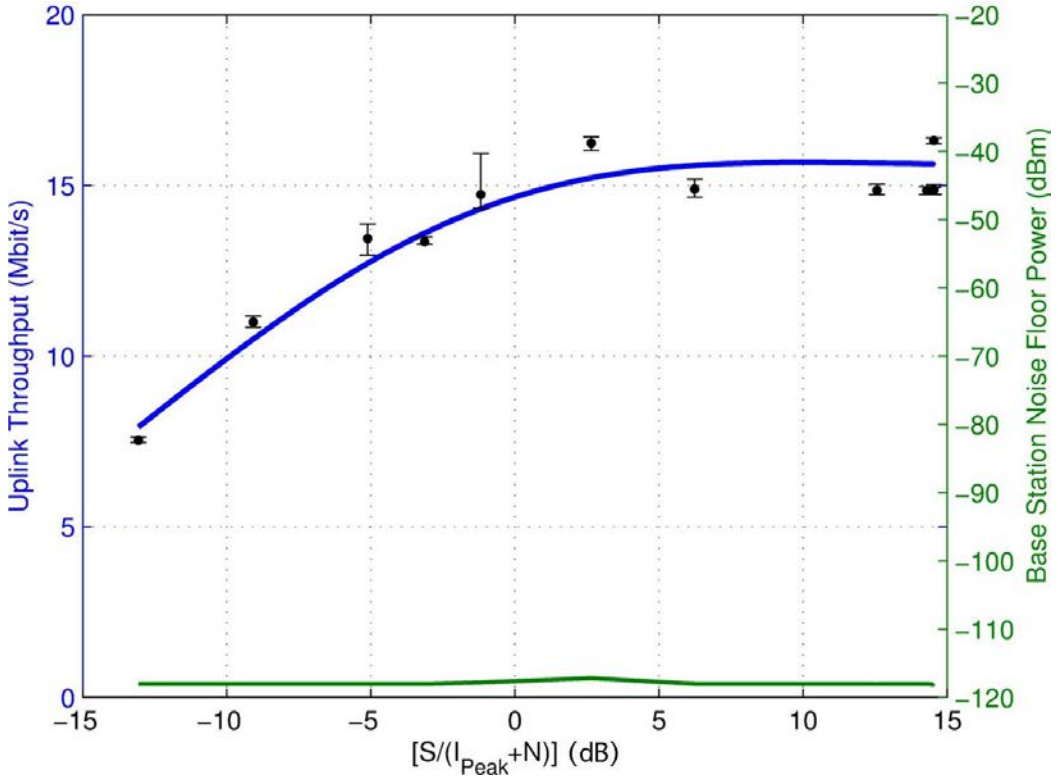

Figure 12. Data throughput for P0N-5 (PW = 3.33 μs, PRR = 3,000/sec, DC = 1%) interference.

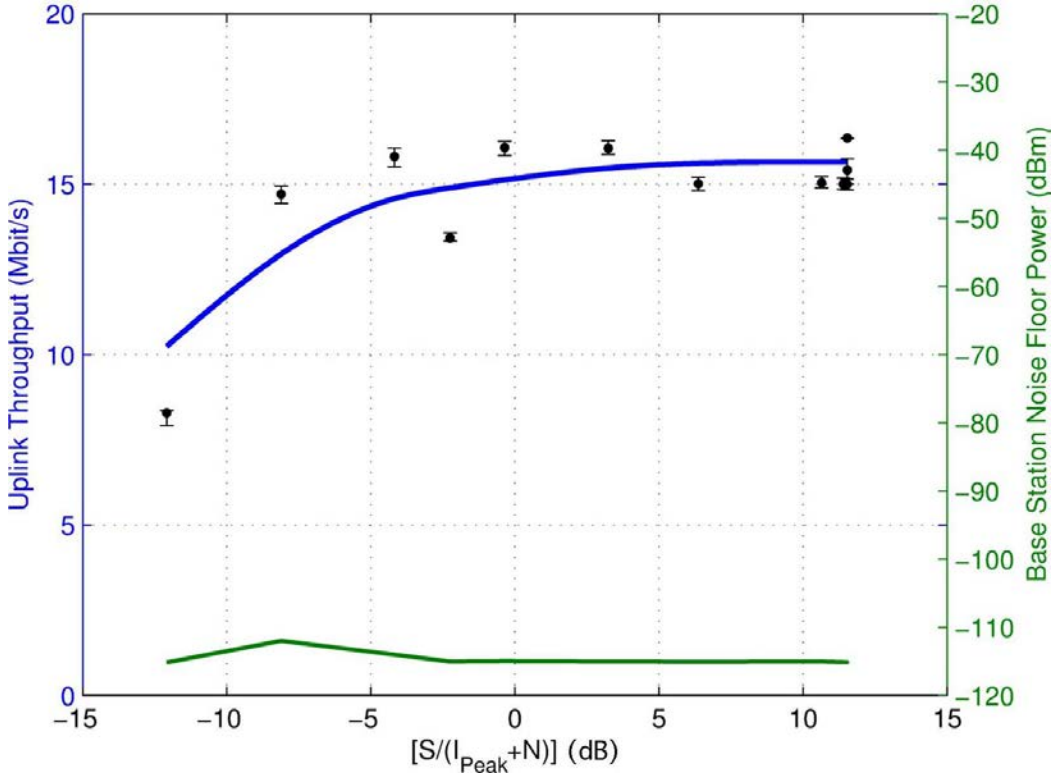

Figure 13. Data throughput for P0N-6 (PW = 1 μs, PRR = 10,000/sec, DC = 1%) interference.

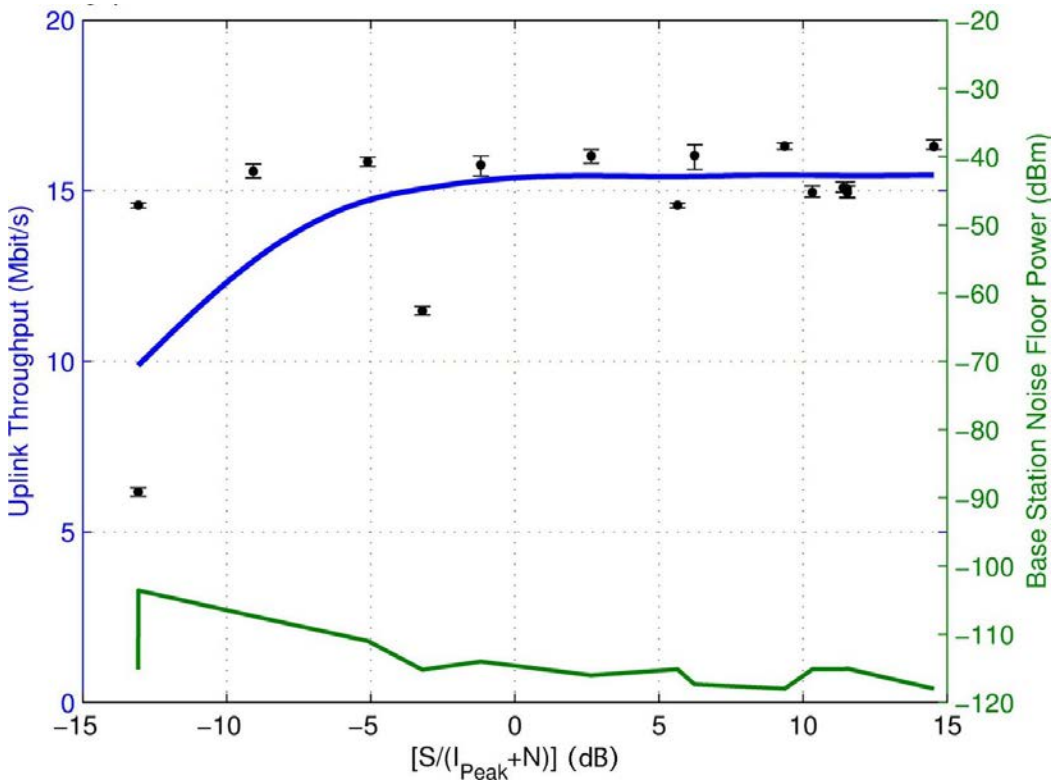

Figure 14. Data throughput for P0N-7 (PW = 30 μs, PRR = 1,000/sec, DC = 3%) interference.

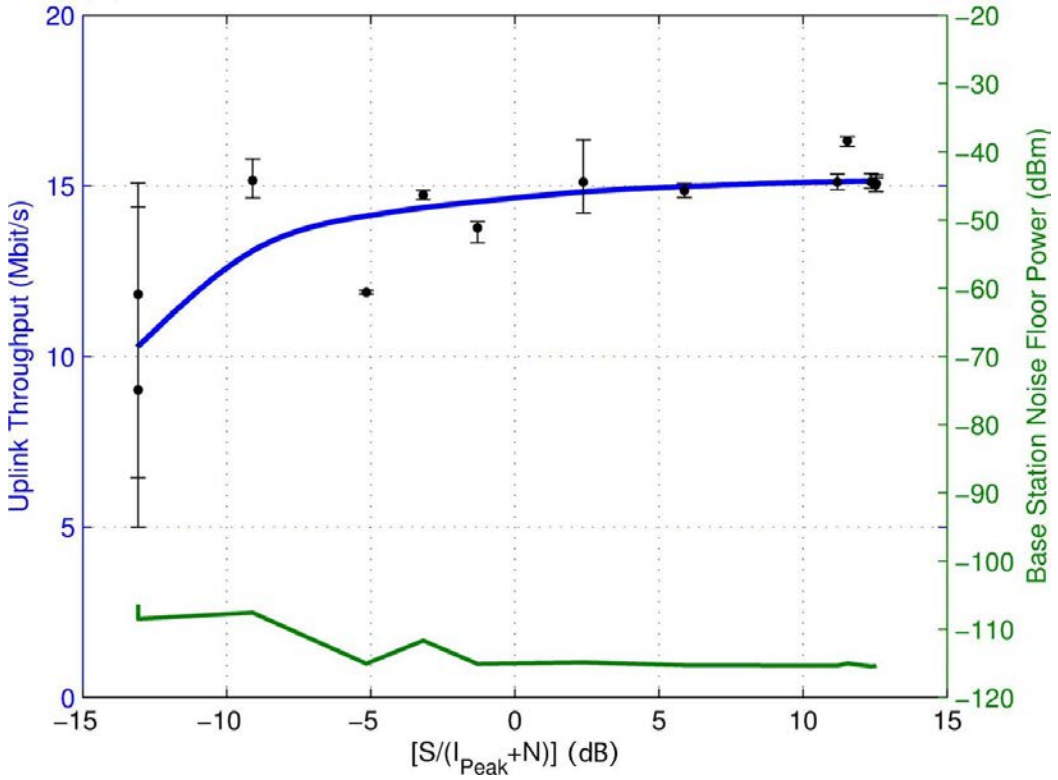

Figure 15. Data throughput for P0N-8 (PW = 10 µs, PRR = 3,000/sec, DC = 3%) interference.

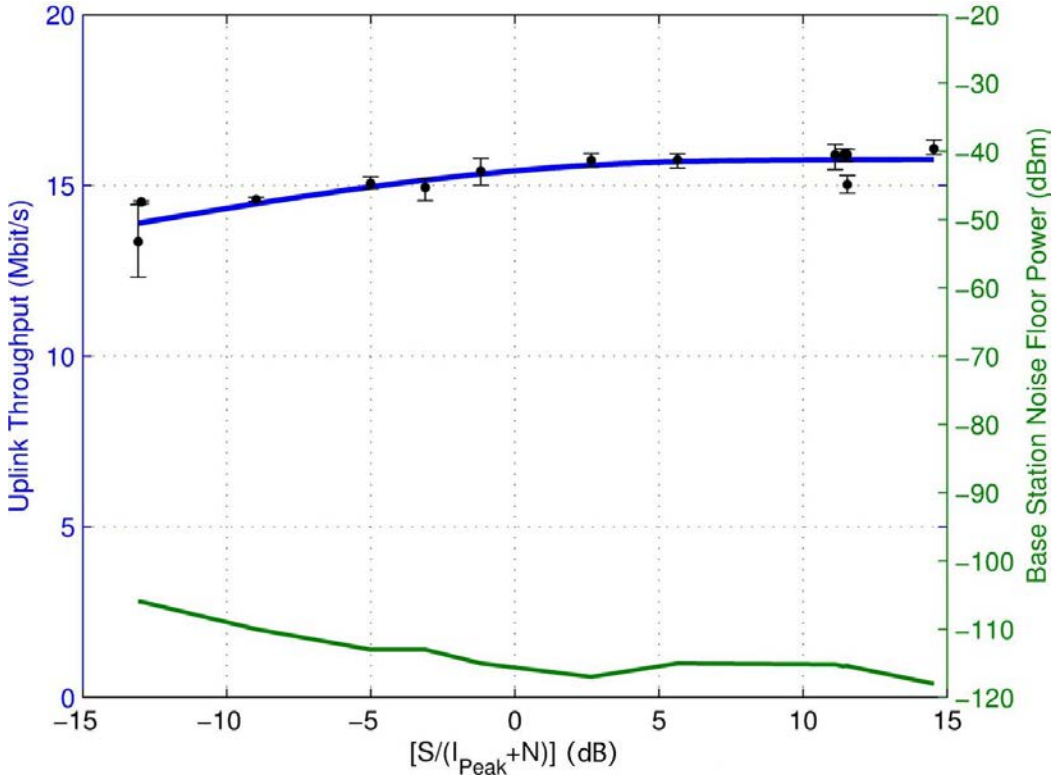

Figure 16. Data throughput for P0N-9 (PW = 3 µs, PRR = 10,000/sec, DC = 3%) interference.

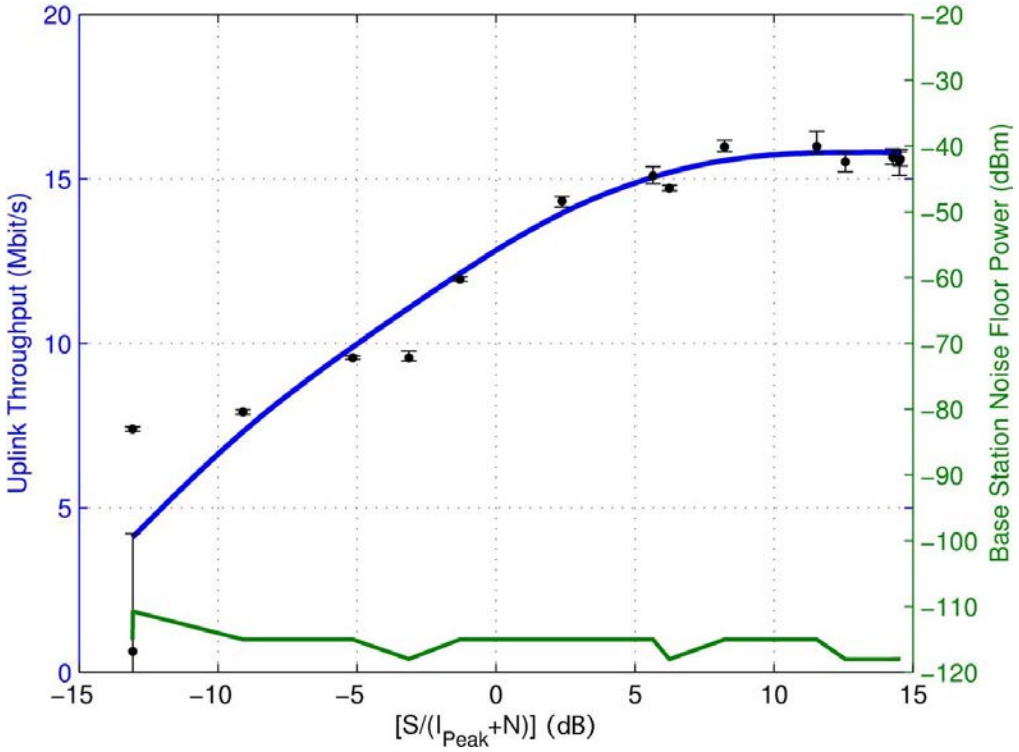

Figure 17. Data throughput for P0N-10 (PW = 100 µs, PRR = 1,000/sec, DC = 10%) interference.

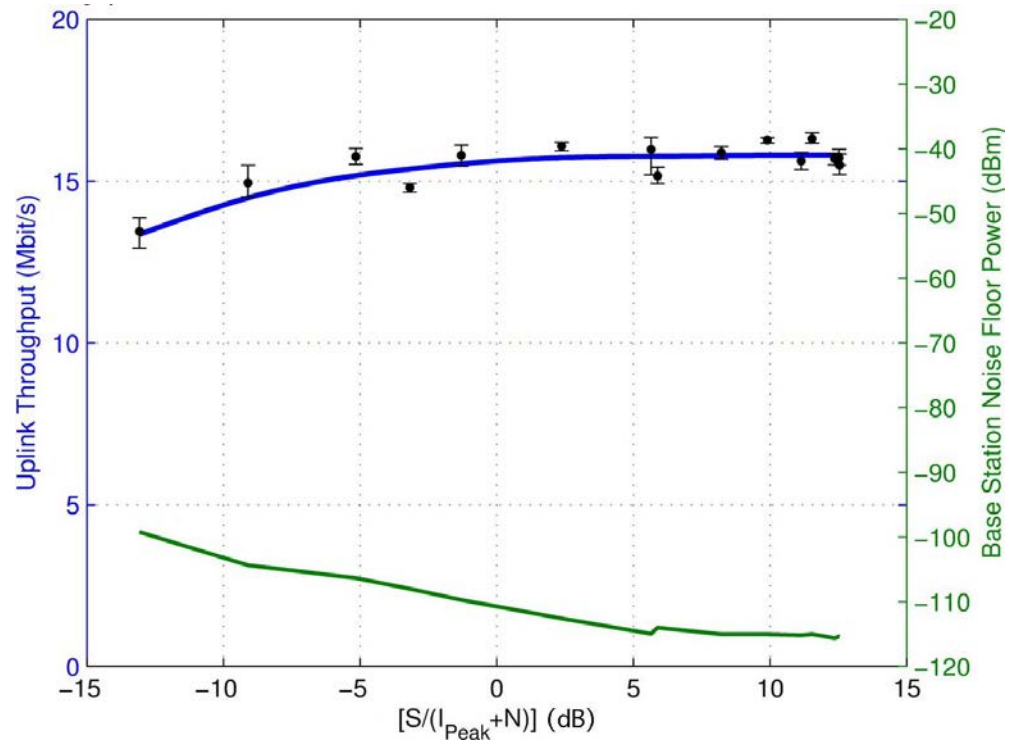

Figure 18. Data throughput for P0N-11 (PW = 33.3 µs, PRR = 3,000/sec, DC = 10%) interference.

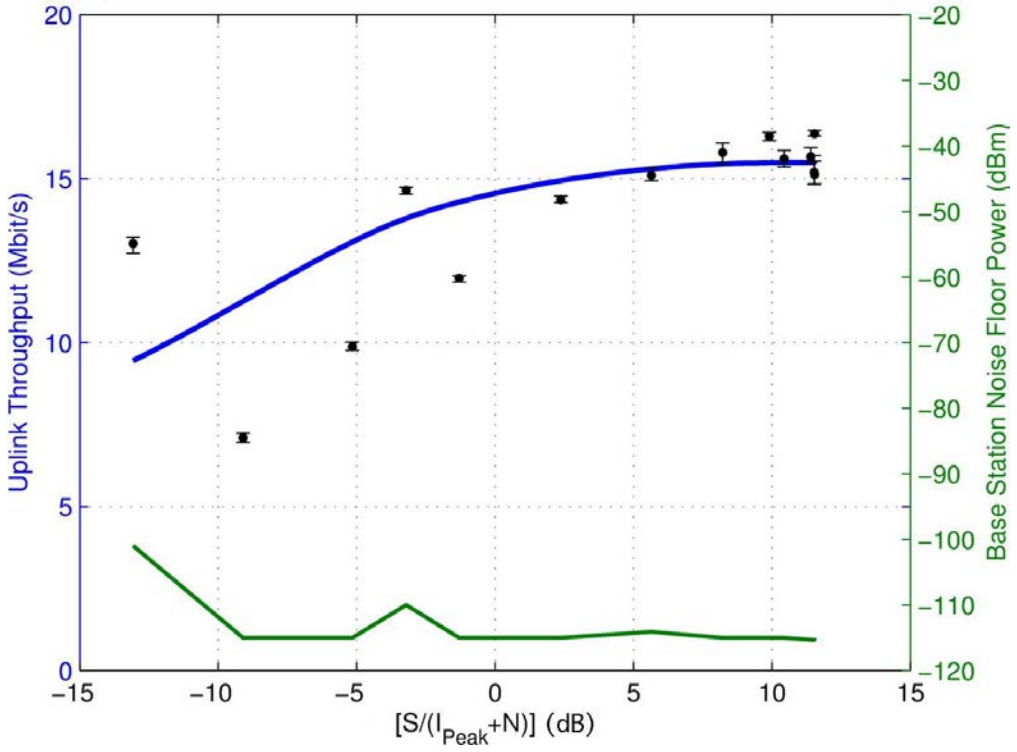

Figure 19. Data throughput for P0N-12 (PW = 10 µs, PRR = 10,000/sec, DC = 10%) interference.

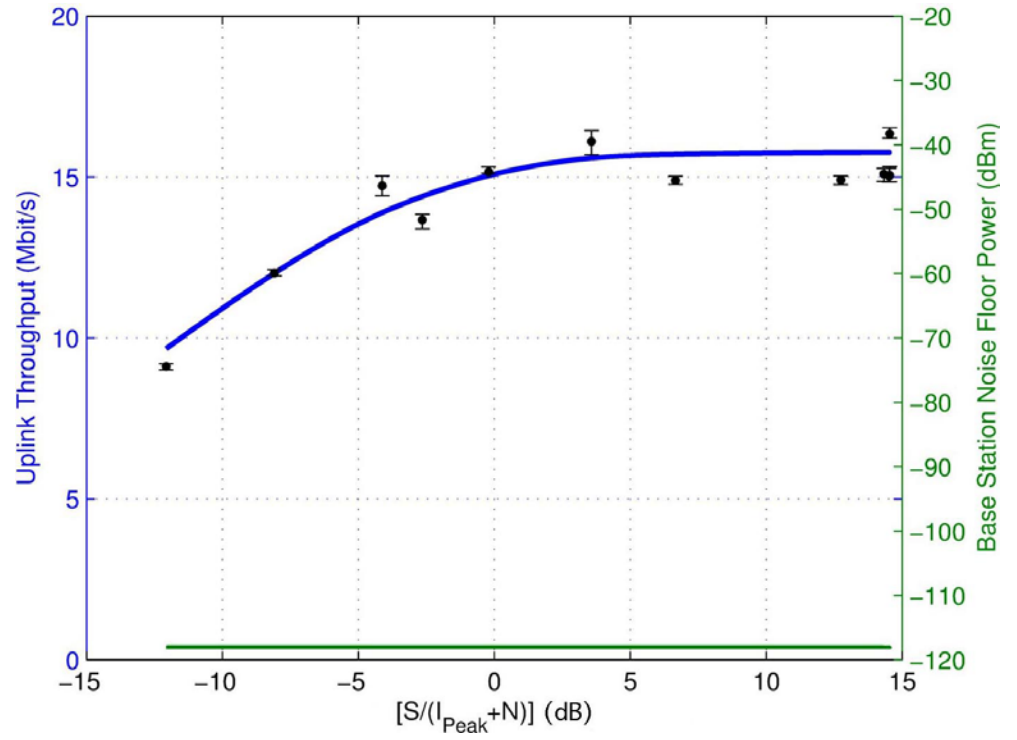

Figure 20. Data throughput for P0N-13/TDWR (PW = 1 µs, PRR = 500/sec, DC = 0.05%) interference.

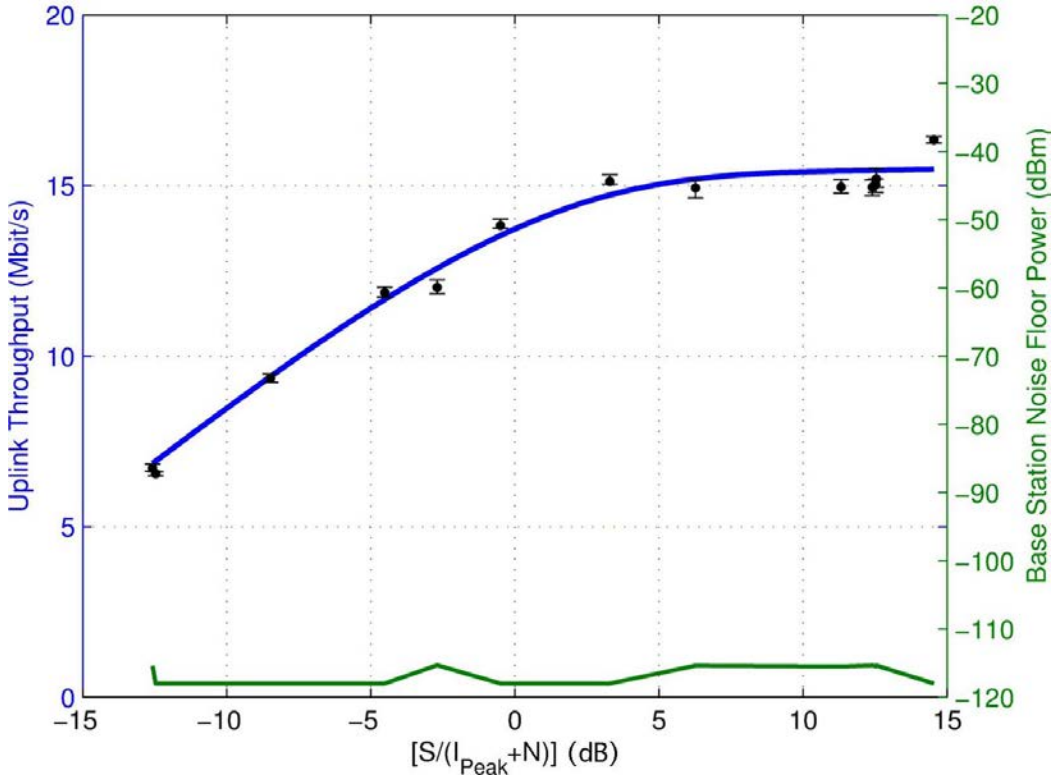

Figure 21. Data throughput for Q3N-1 (PW = 10 µs, PRR = 1,000/sec, DC = 1%) interference.

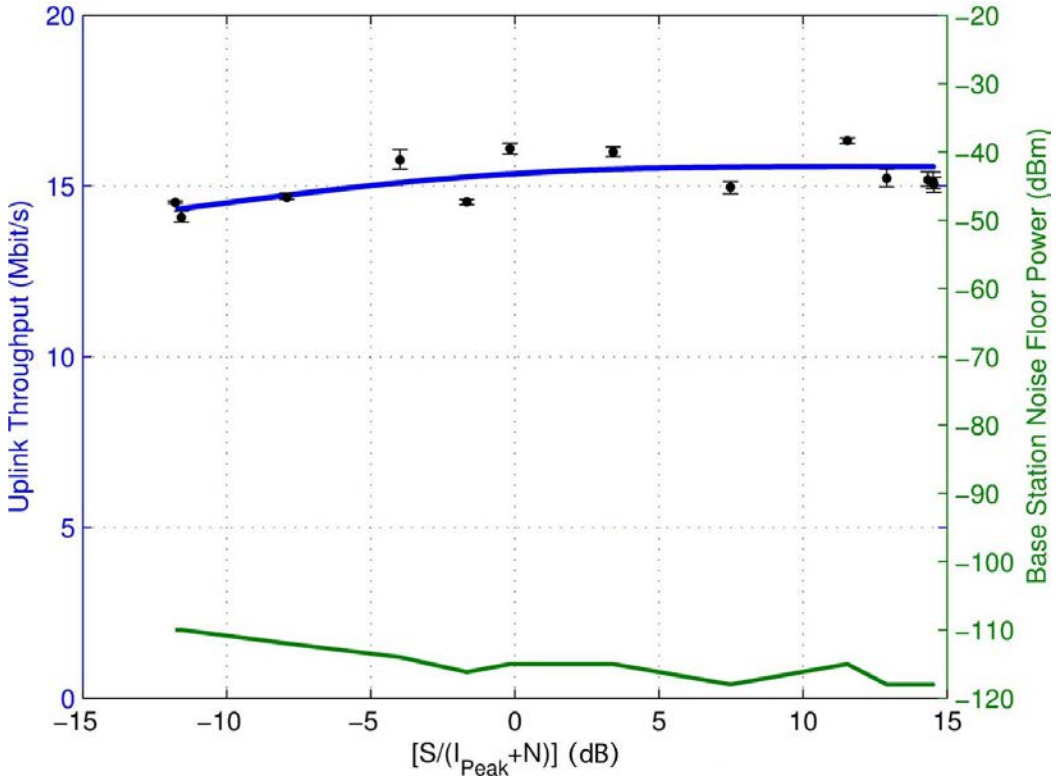

Figure 22. Data throughput for Q3N-2 (PW = 1 µs, PRR = 10,000/sec, DC = 1%) interference.

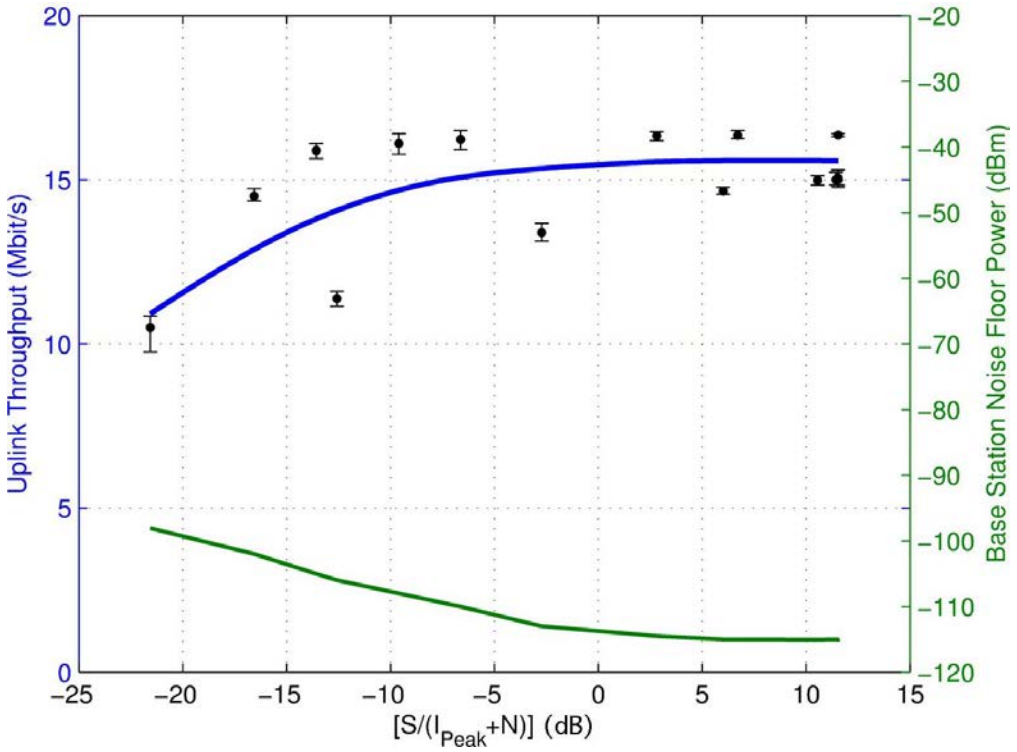

Figure 23. Data throughput for Q3N-3 (PW = 0.33 µs, PRR = 30,000/sec, DC = 1%) interference.

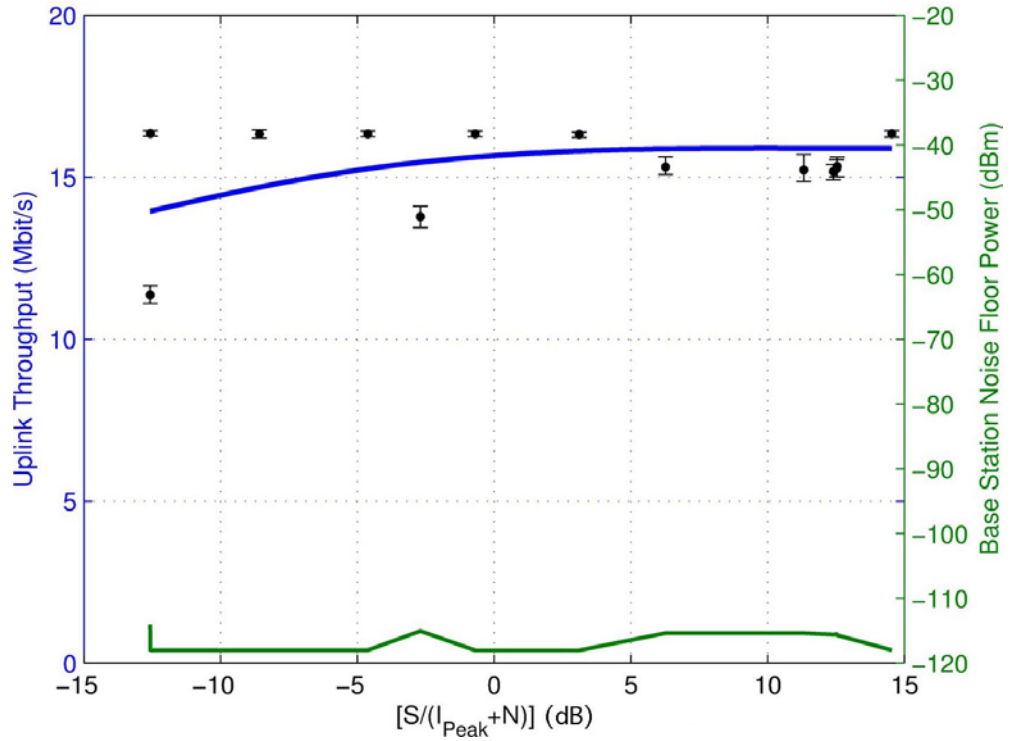

Figure 24. Data throughput for Q3N-4 (PW = 20 µs, PRR = 200/sec (equivalent to PW = 100 µs, PRR = 1,000/sec), DC = 0.4%) interference.

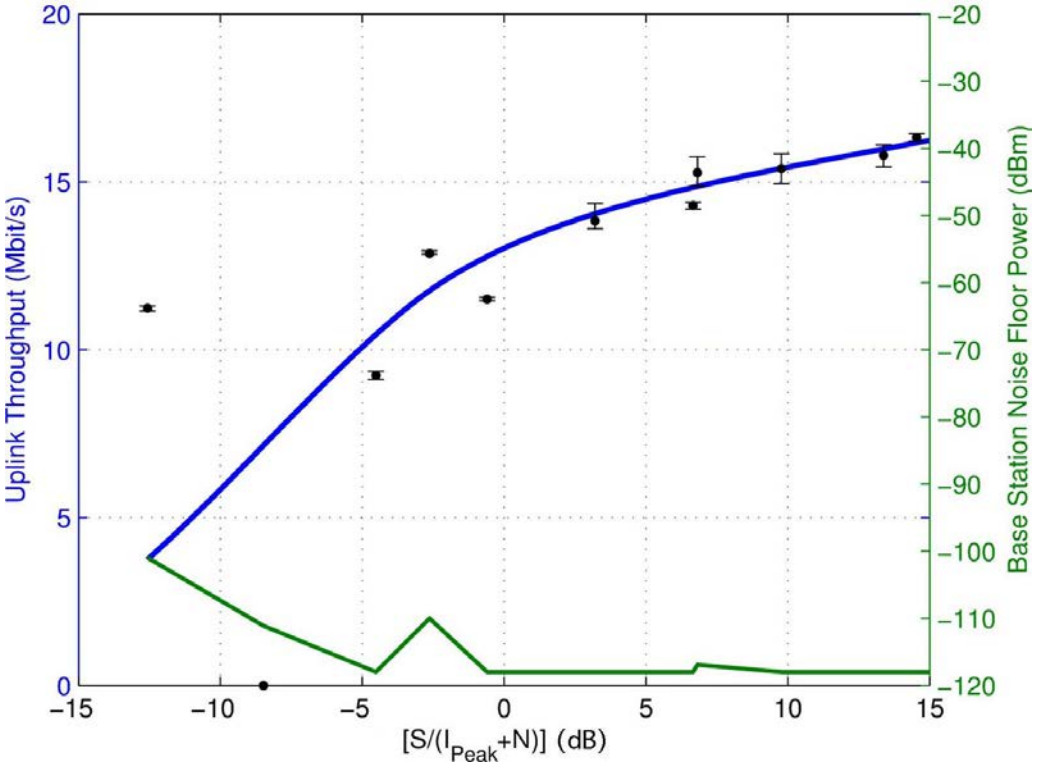

Figure 25. Data throughput for Q3N-5 (PW = 10 µs, PRR = 10,000/sec, DC = 10%) interference.

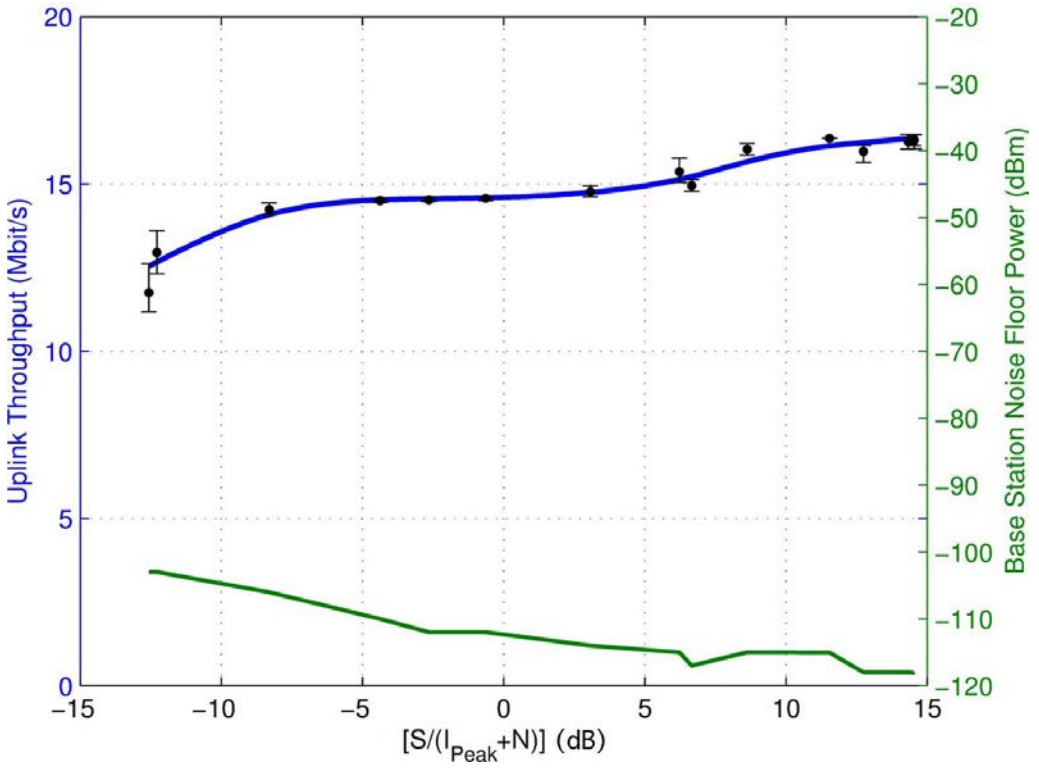

Figure 26. Data throughput for Q3N-6 (PW = 3.3 µs, PRR = 30,000/sec, DC = 10%) interference.

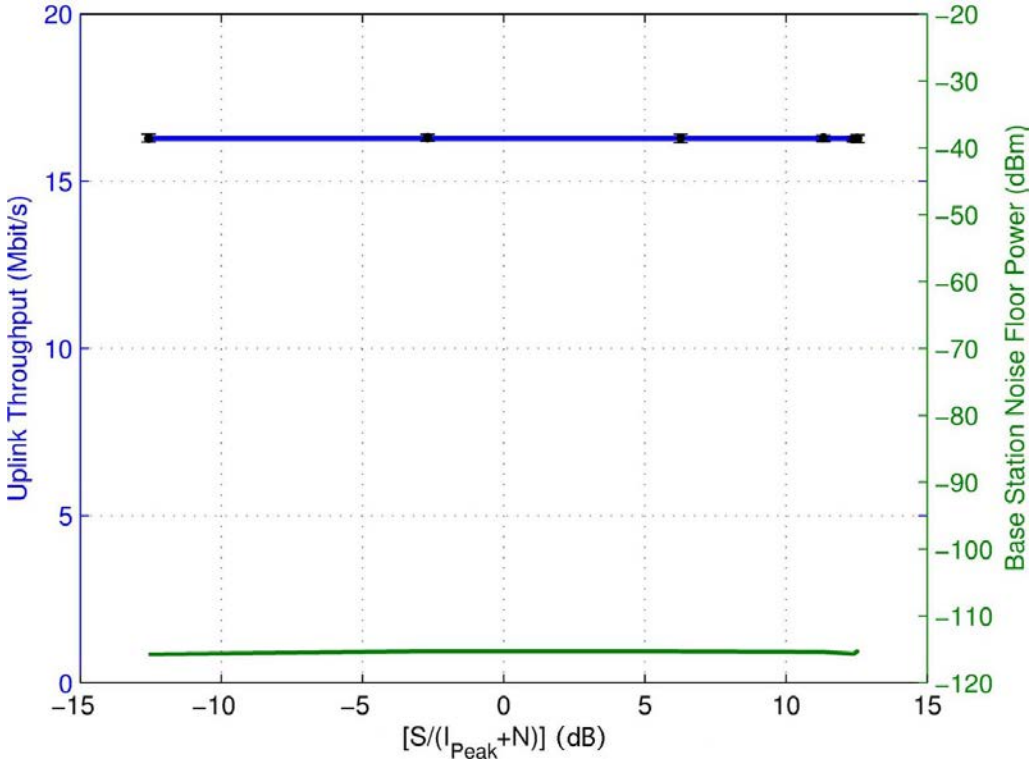

Figure 27. Data throughput for Q3N-7 (PW = 20 µs, PRR = 100/sec (equivalent to PW = 200 µs, PRR = 1,000/sec), DC = 0.2%) interference.

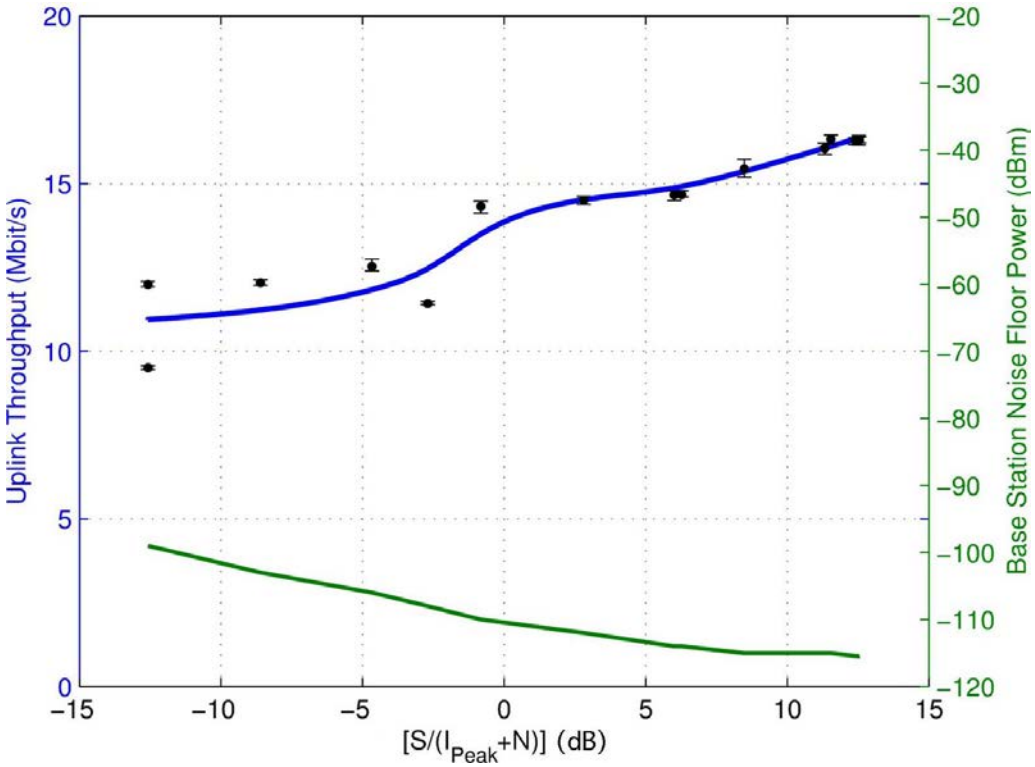

Figure 28. Data throughput for Q3N-8 (PW = 20 µs, PRR = 10,000/sec, DC = 20%) interference.

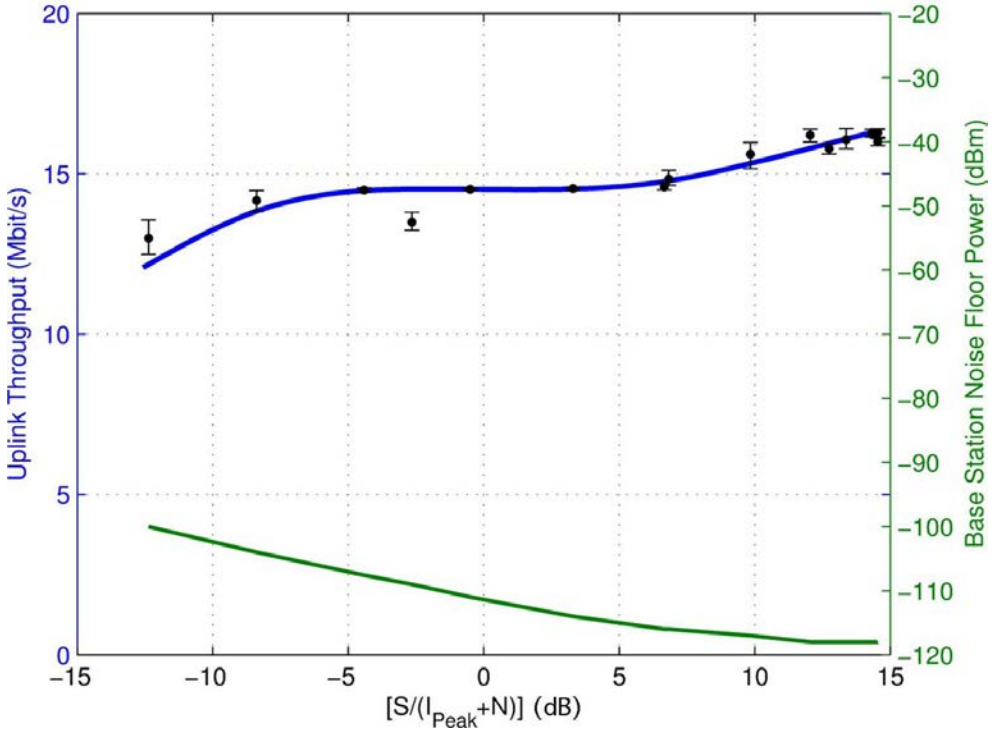

Figure 29. Data throughput for Q3N-9 (PW = 6.6 µs, PRR = 30,000/sec, DC = 20%) interference.

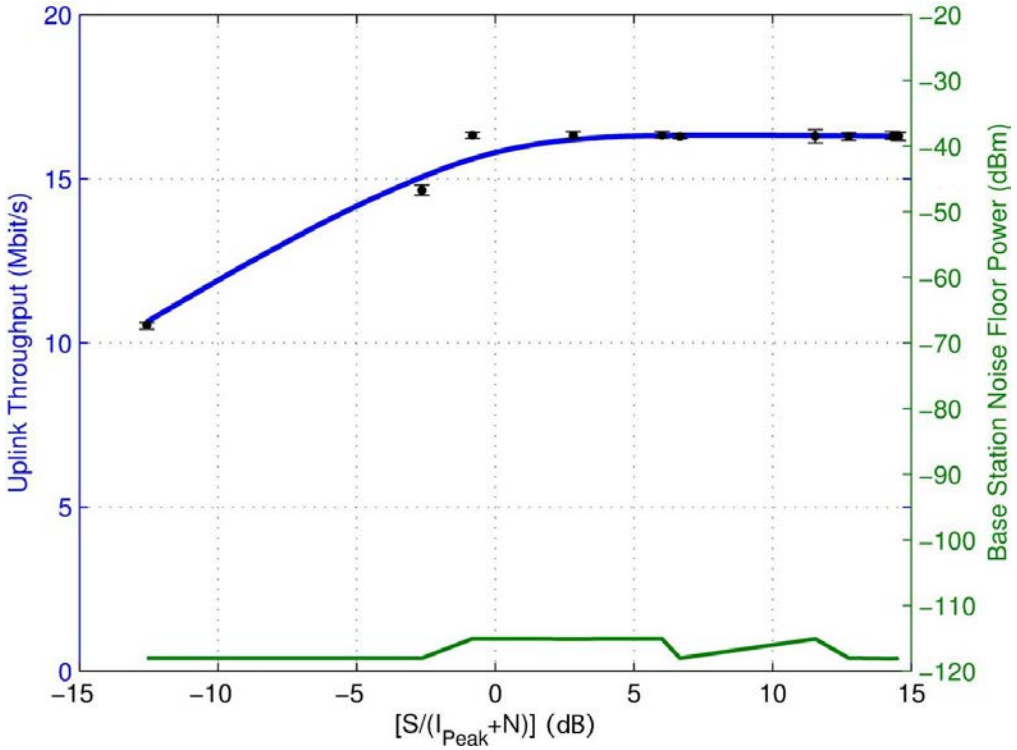

Figure 30. Data throughput for Q3N-10 (PW = 20 µs, PRR = 67/sec (equivalent to PW = 300 µs, PRR = 1,000/sec), DC = 0.13%) interference.

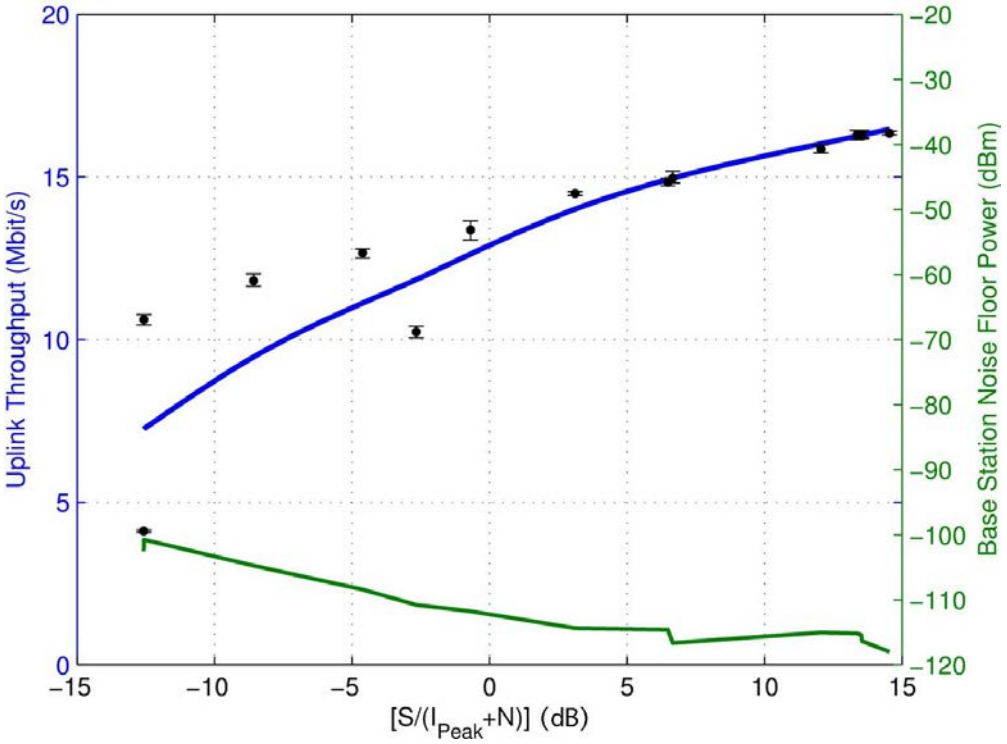

Figure 31. Data throughput for Q3N-11 (PW = 20 µs, PRR = 6,667/sec (equivalent to PW = 30 µs, PRR = 10,000/sec), DC = 13%) interference.

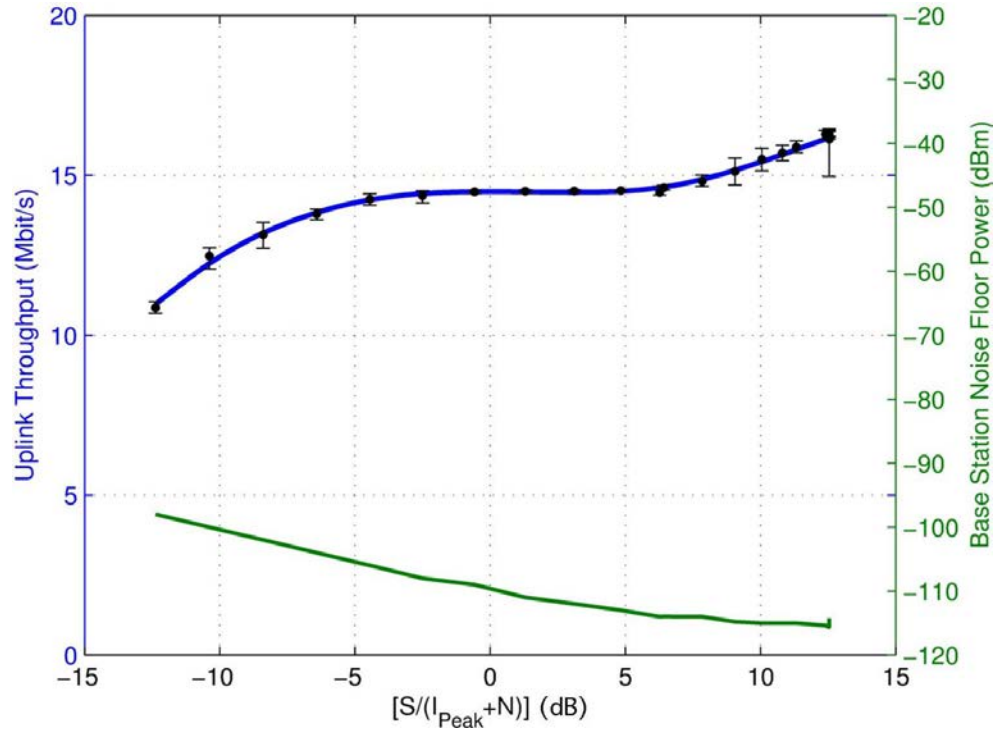

Figure 32. Data throughput for Q3N-12 (PW = 10 µs, PRR = 30,000/sec, DC = 30%) interference.

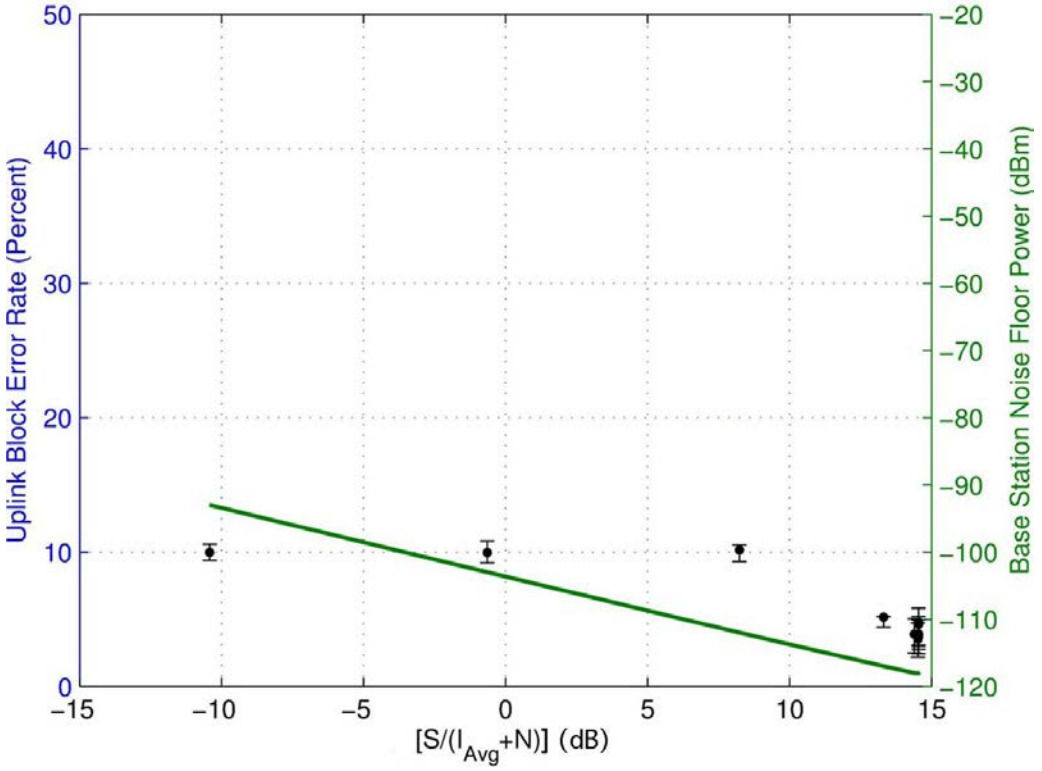

Figure 33. BLER for 10 MHz-wide Gaussian noise interference.

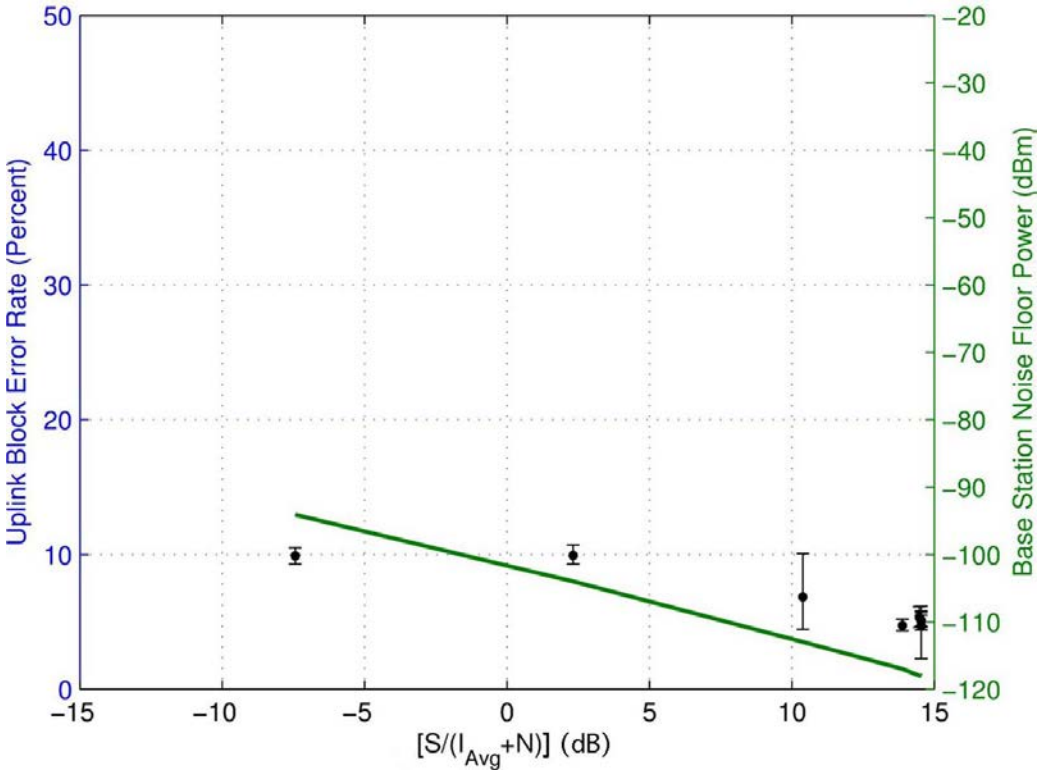

Figure 34. BLER for 20 MHz-wide Gaussian noise interference.

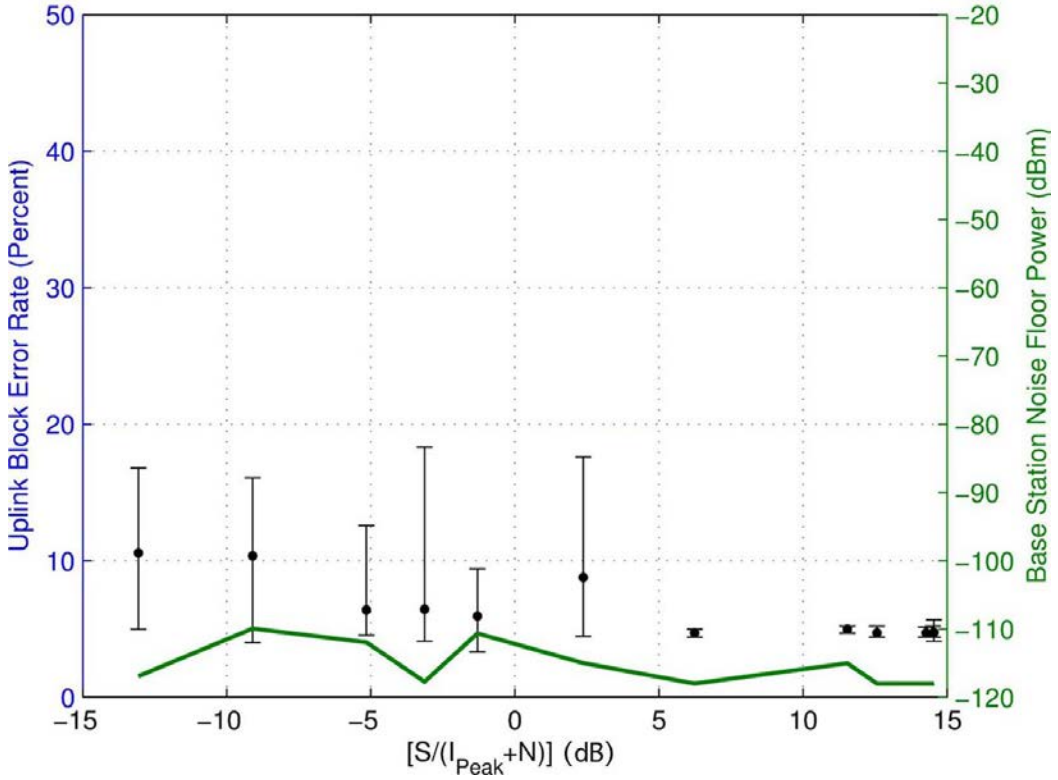

Figure 35. BLER for ECC-1/WFM-1 (PW = 4 µs, PRR =1000/sec, DC = 0.4%) interference.

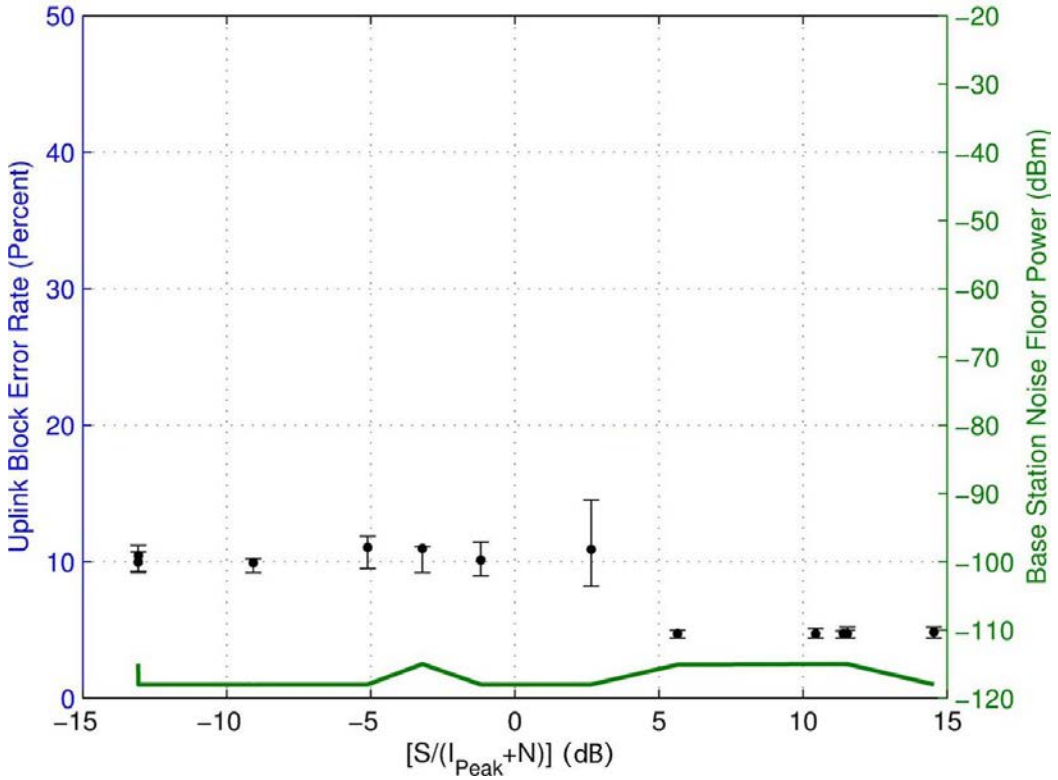

Figure 36. BLER for ECC-2/WFM-2 (PW = 100 µs, PRR = 300/sec, DC = 3%) interference.

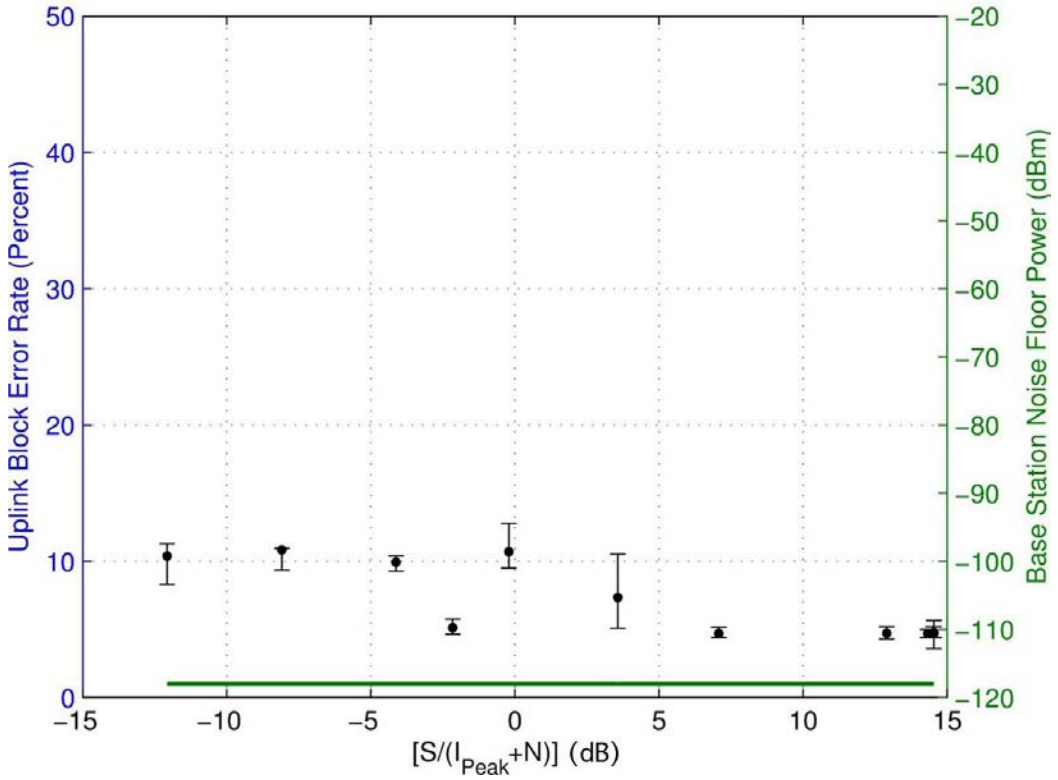

Figure 37. BLER for P0N-1 (PW = 1 µs, PRR = 1000/sec, DC = 0.1%) interference.

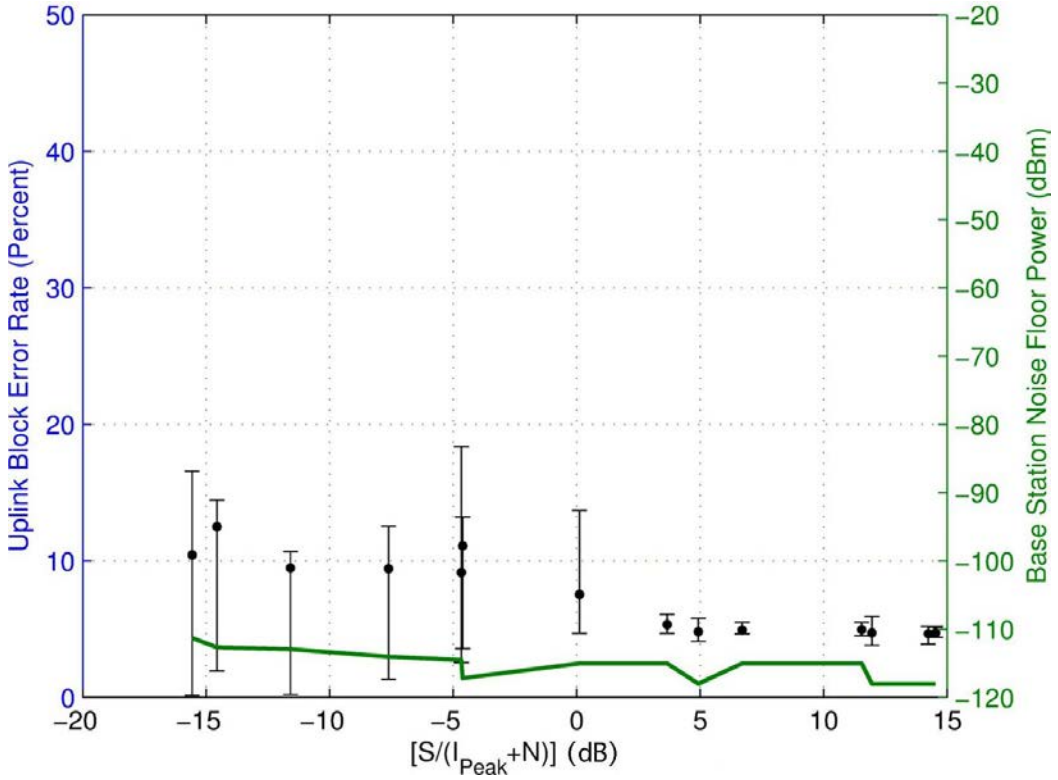

Figure 38. BLER for P0N-2 (PW = 0.33 µs, PRR = 3000/sec, DC = 0.1%) interference.

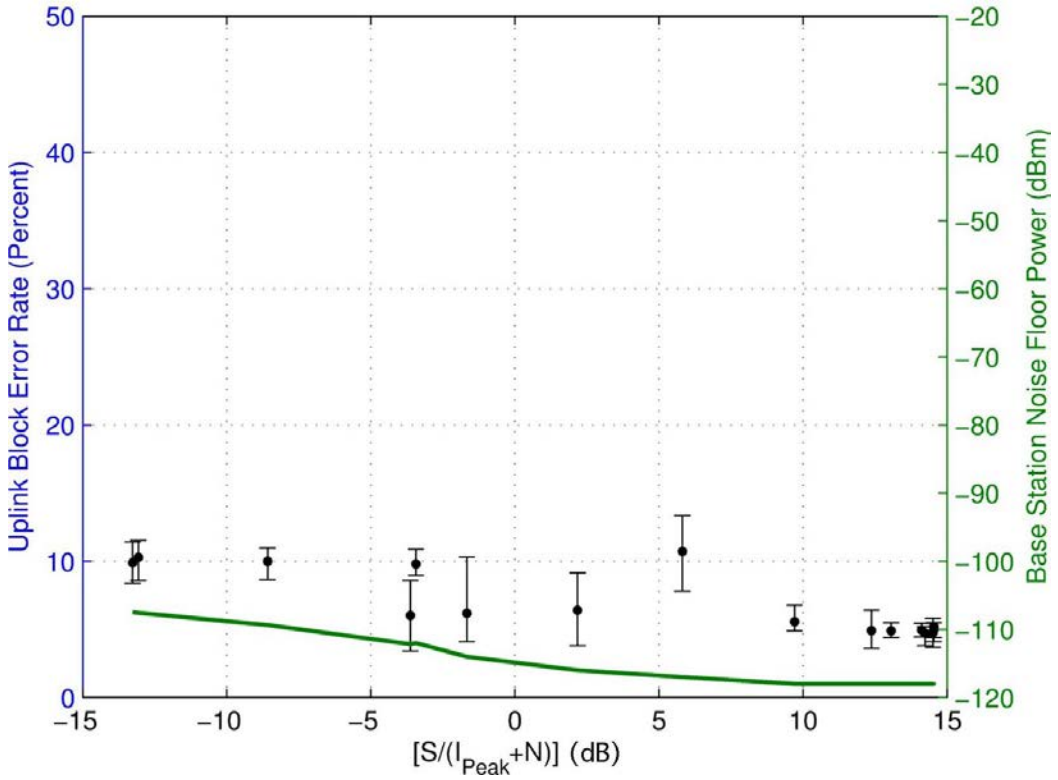

Figure 39. BLER for P0N-3 (PW = 0.1 µs, PRR = 10,000/sec, DC = 0.1%) interference.

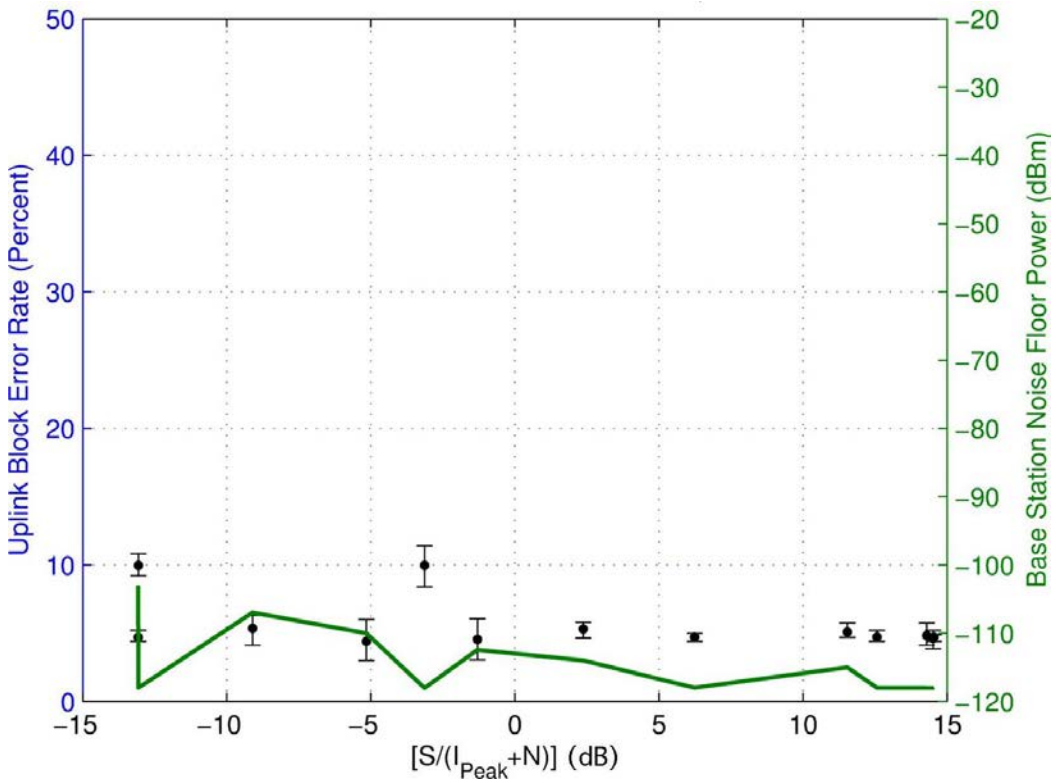

Figure 40. BLER for P0N-4 (PW = 10 µs, PRR = 1,000/sec, DC = 1%) interference.

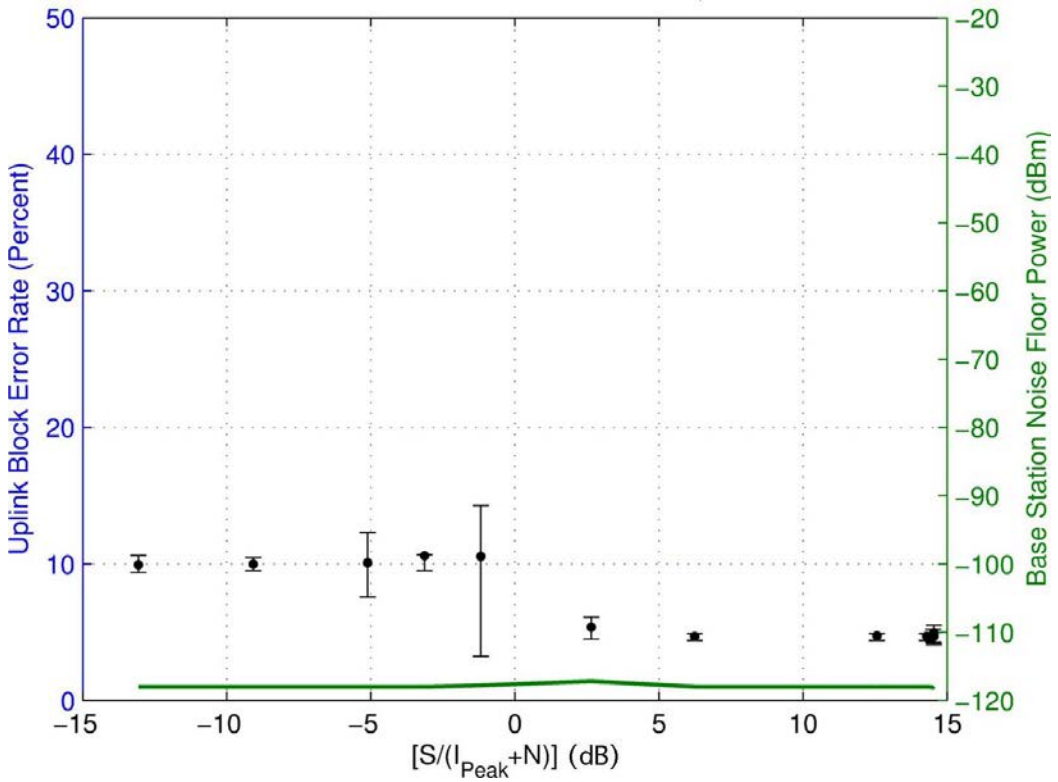

Figure 41. BLER for P0N-5 (PW = 3.33 µs, PRR = 3,000/sec, DC = 1%) interference.

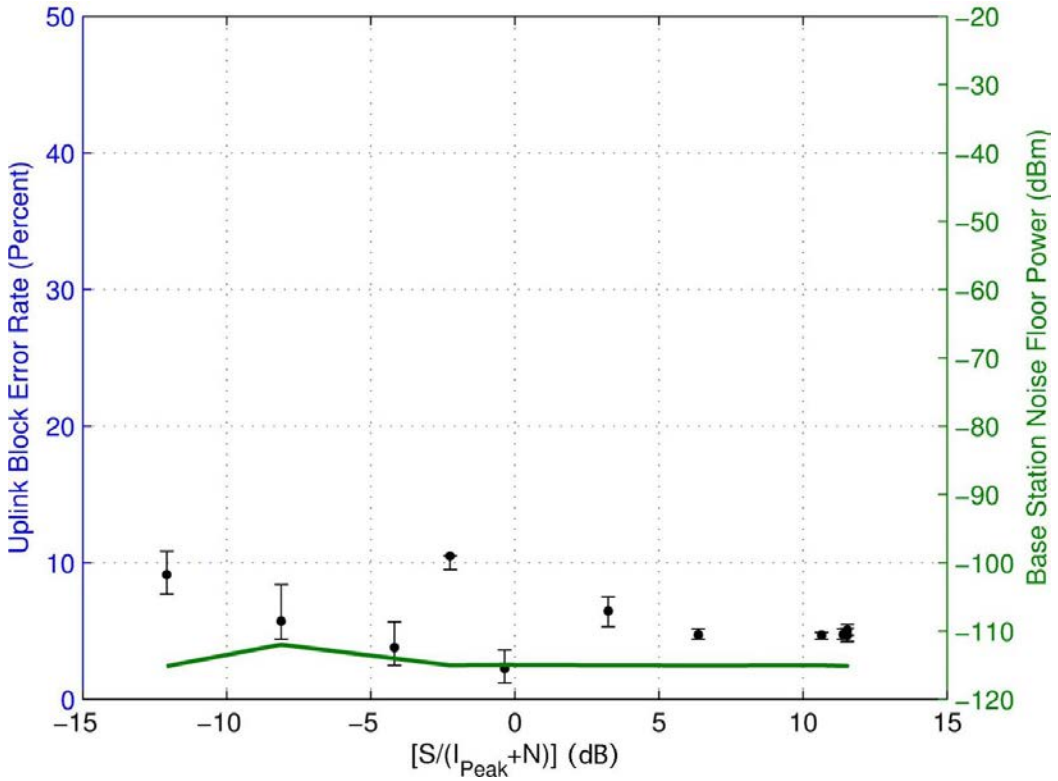

Figure 42. BLER for P0N-6 (PW = 1 µs, PRR = 10,000/sec, DC = 1%) interference.

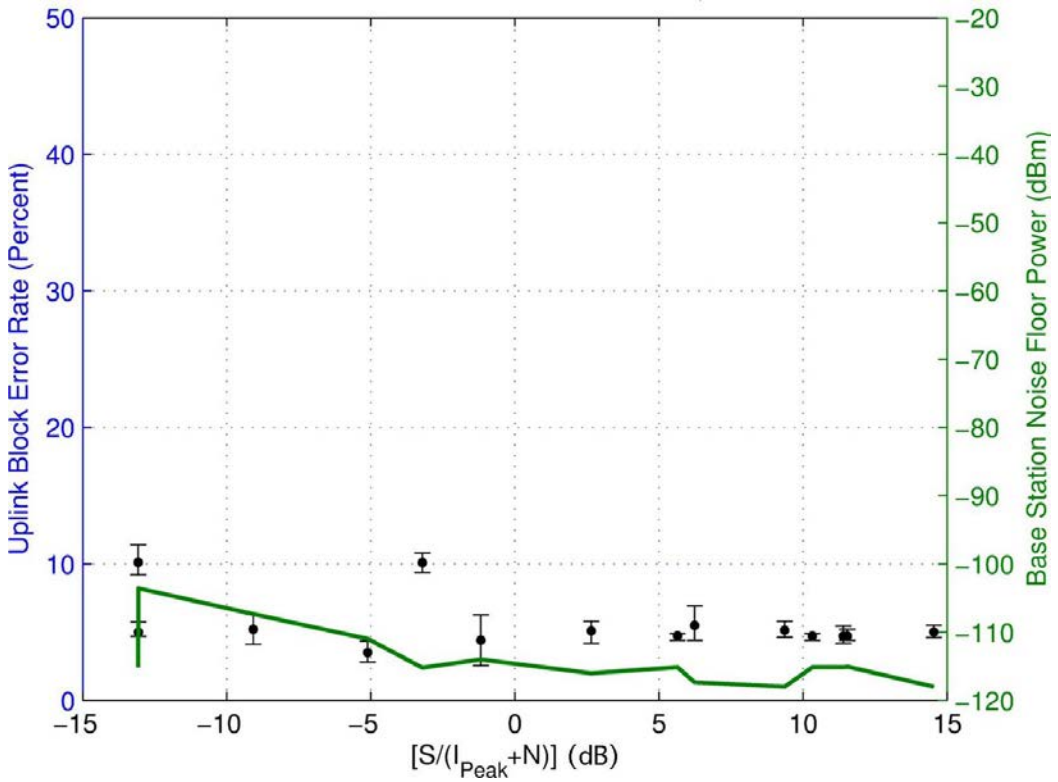

Figure 43. BLER for P0N-7 (PW = 30 µs, PRR = 1,000/sec, DC = 3%) interference.

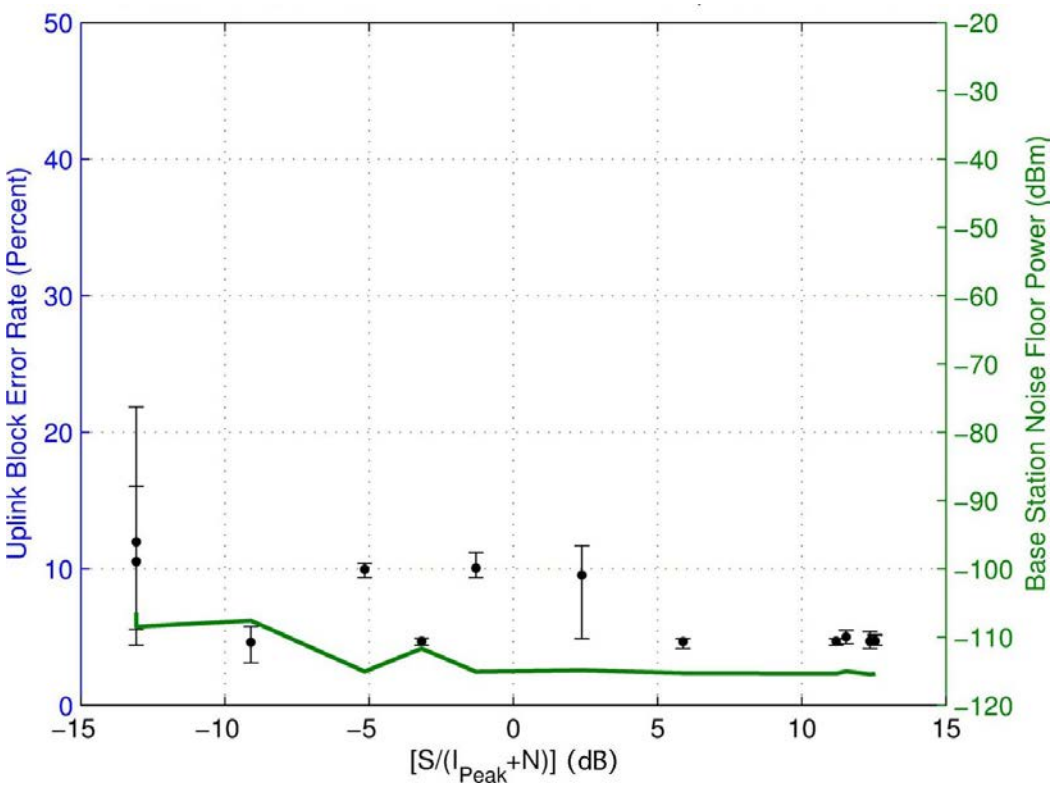

Figure 44. BLER for P0N-8 (PW = 10 µs, PRR = 3,000/sec, DC = 3%) interference.

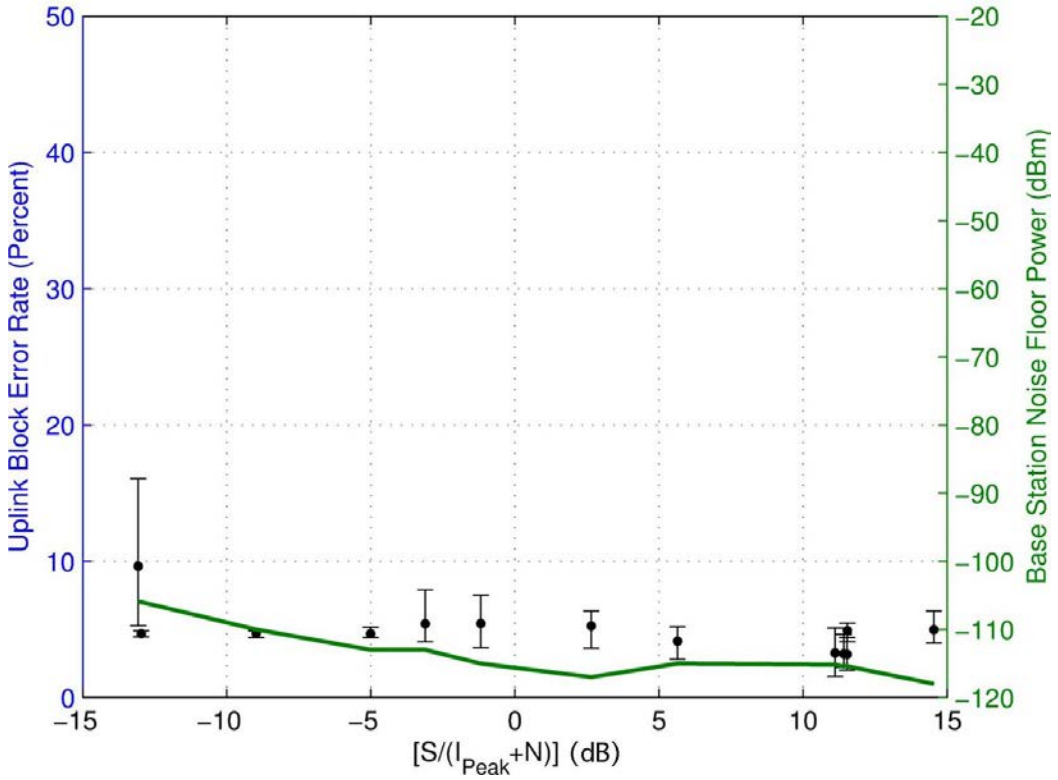

Figure 45. BLER for P0N-9 (PW = 3 µs, PRR = 10,000/sec, DC = 3%) interference.

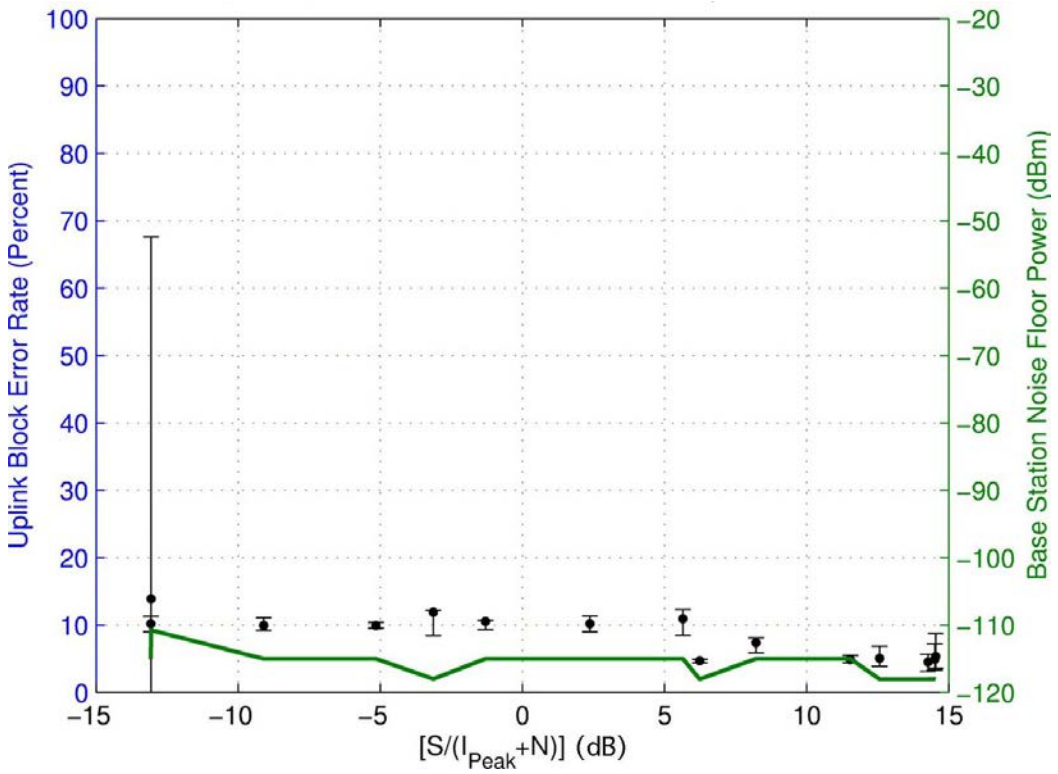

Figure 46. BLER for P0N-10 (PW = 100 µs, PRR = 1,000/sec, DC = 10%) interference.

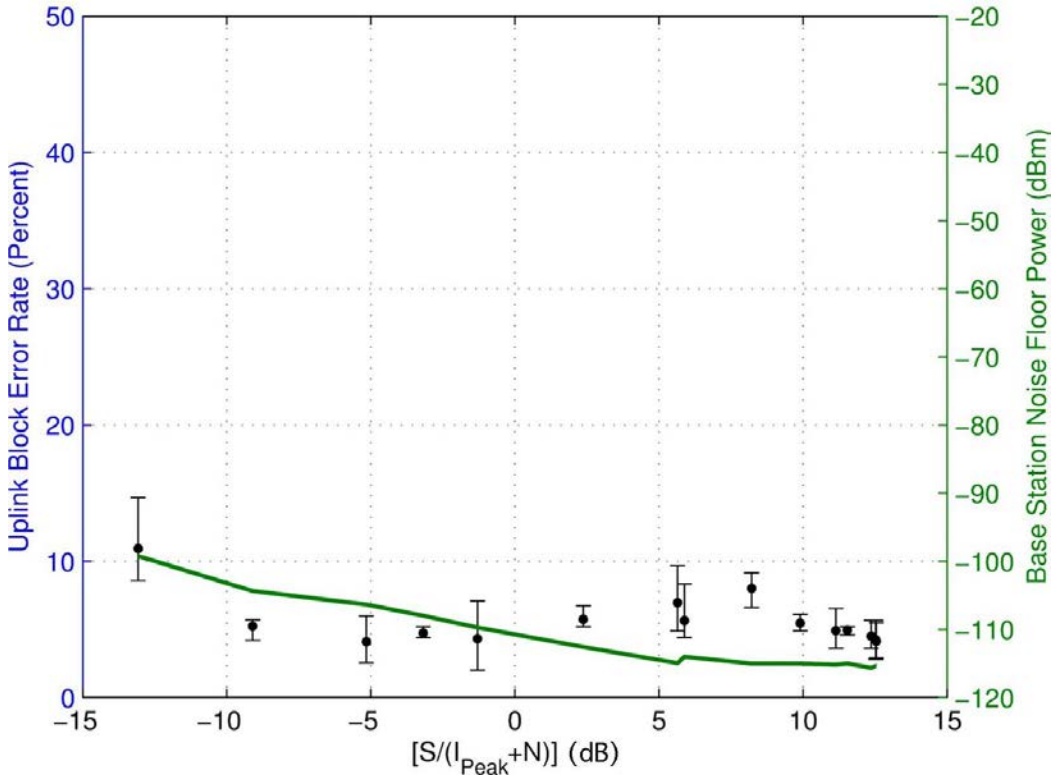

Figure 47. BLER for P0N-11 (PW = 33.3 µs, PRR = 3,000/sec, DC = 10%) interference.

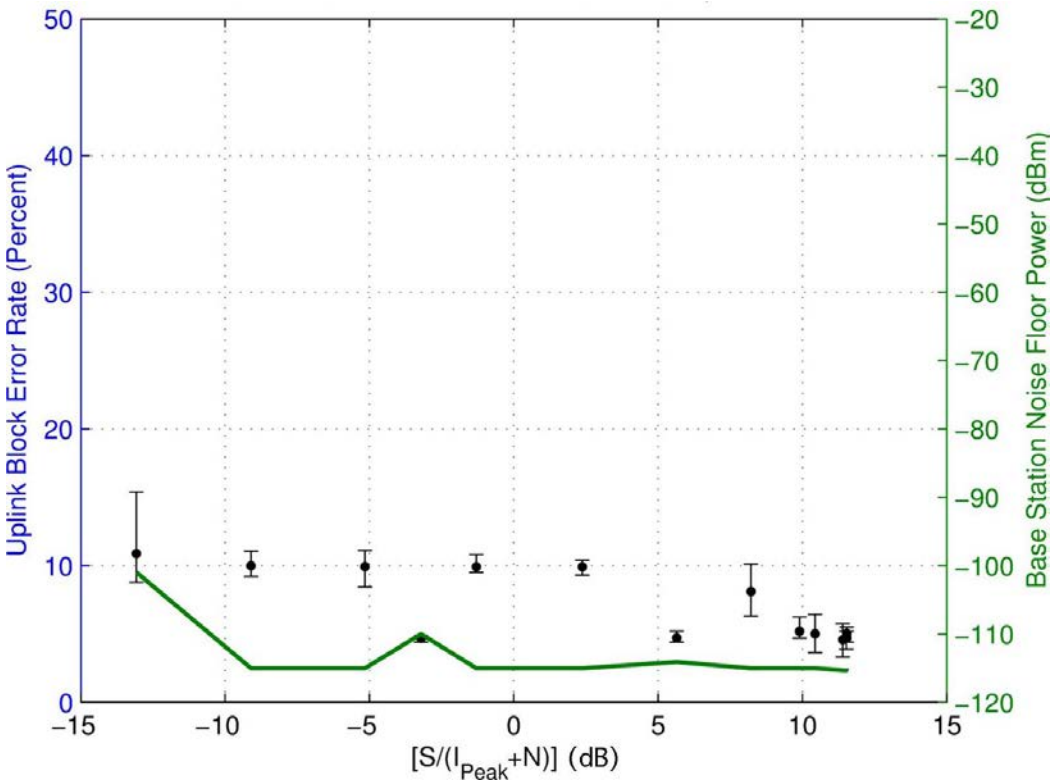

Figure 48. BLER for P0N-12 (PW = 10 µs, PRR = 10,000/sec, DC = 10%) interference.

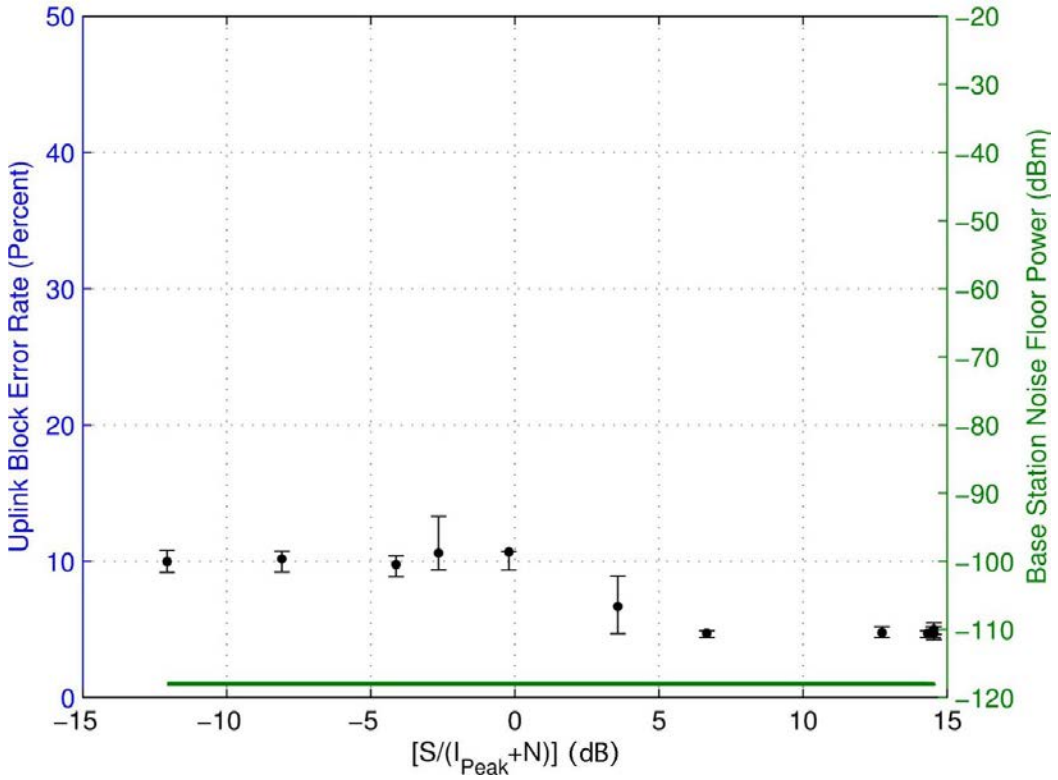

Figure 49. BLER for P0N-13/TDWR (PW = 1 µs, PRR = 500/sec, DC = 0.05%) interference.

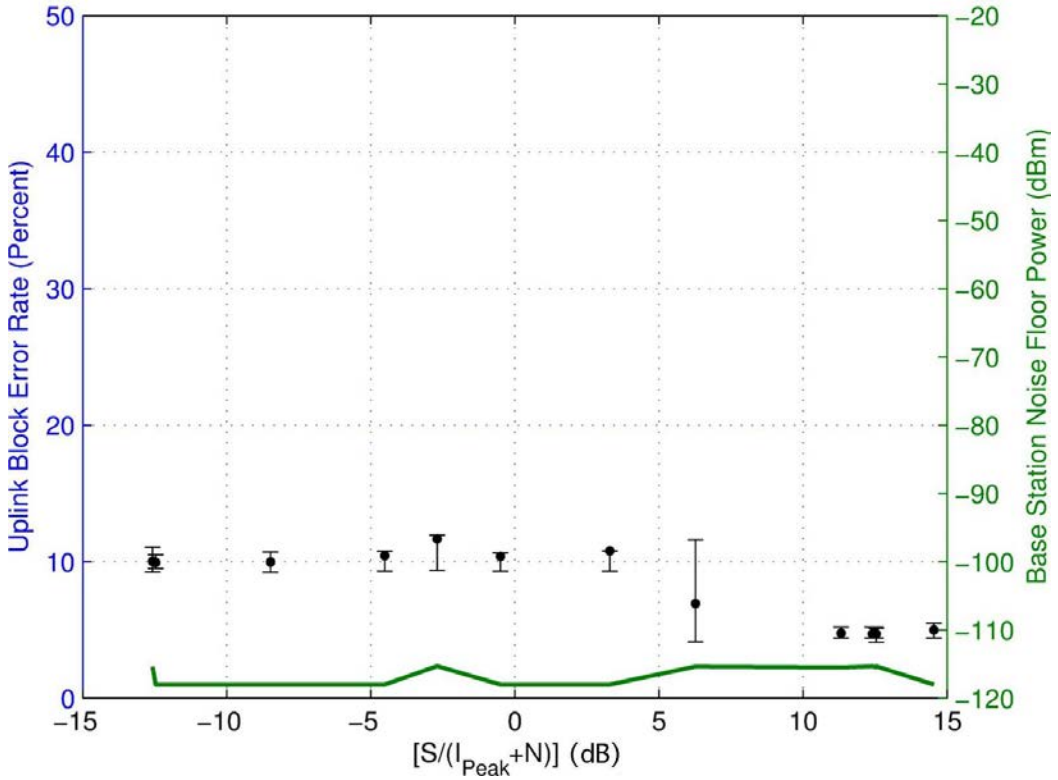

Figure 50. BLER for Q3N-1 (PW = 10 µs, PRR = 1,000/sec, DC = 1%) interference.

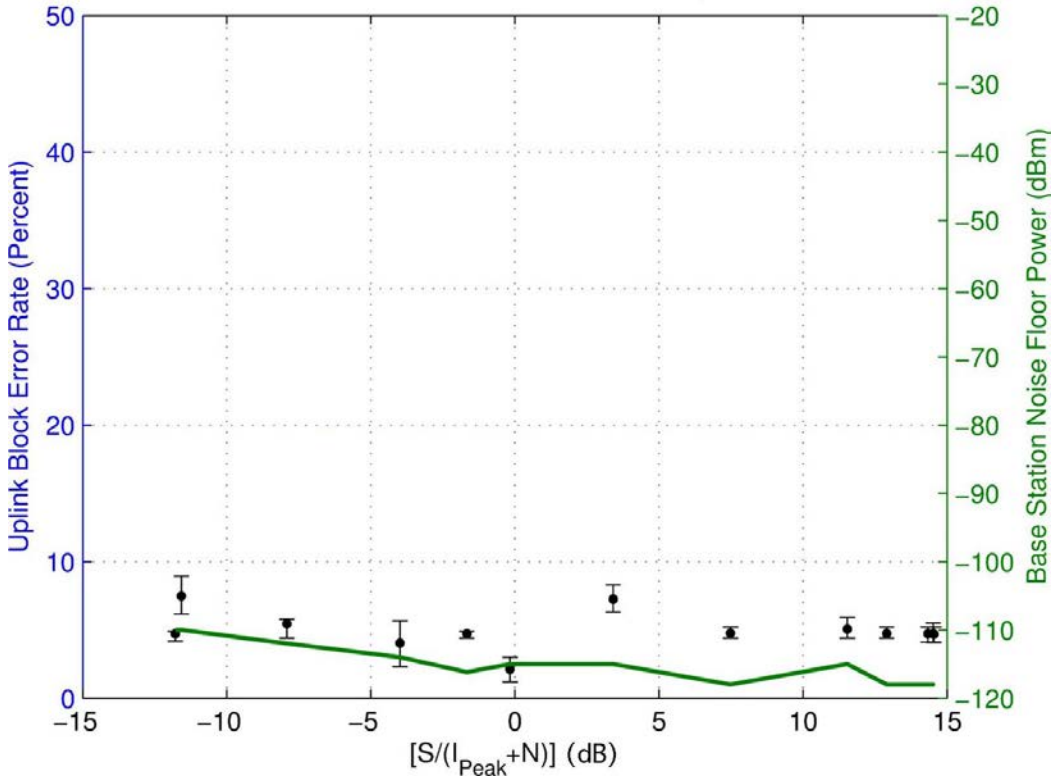

Figure 51. BLER for Q3N-2 (PW = 1 µs, PRR = 10,000/sec, DC = 1%) interference.

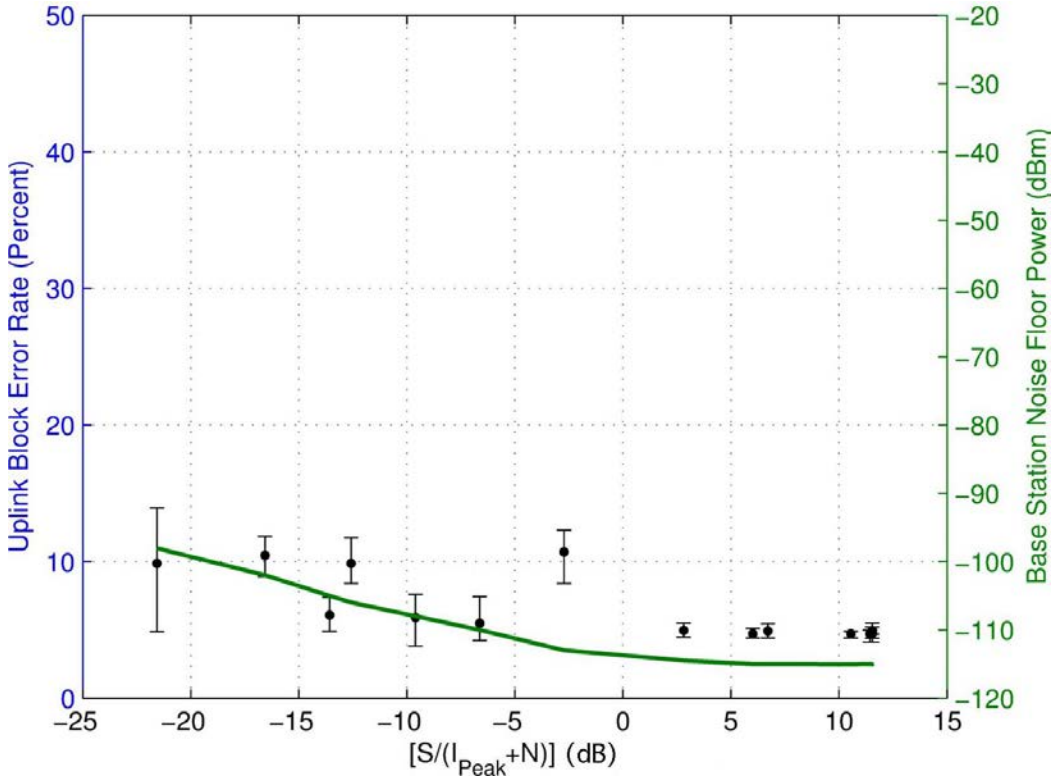

Figure 52. BLER for Q3N-3 (PW = 0.33 µs, PRR = 30,000/sec, DC = 1%) interference.

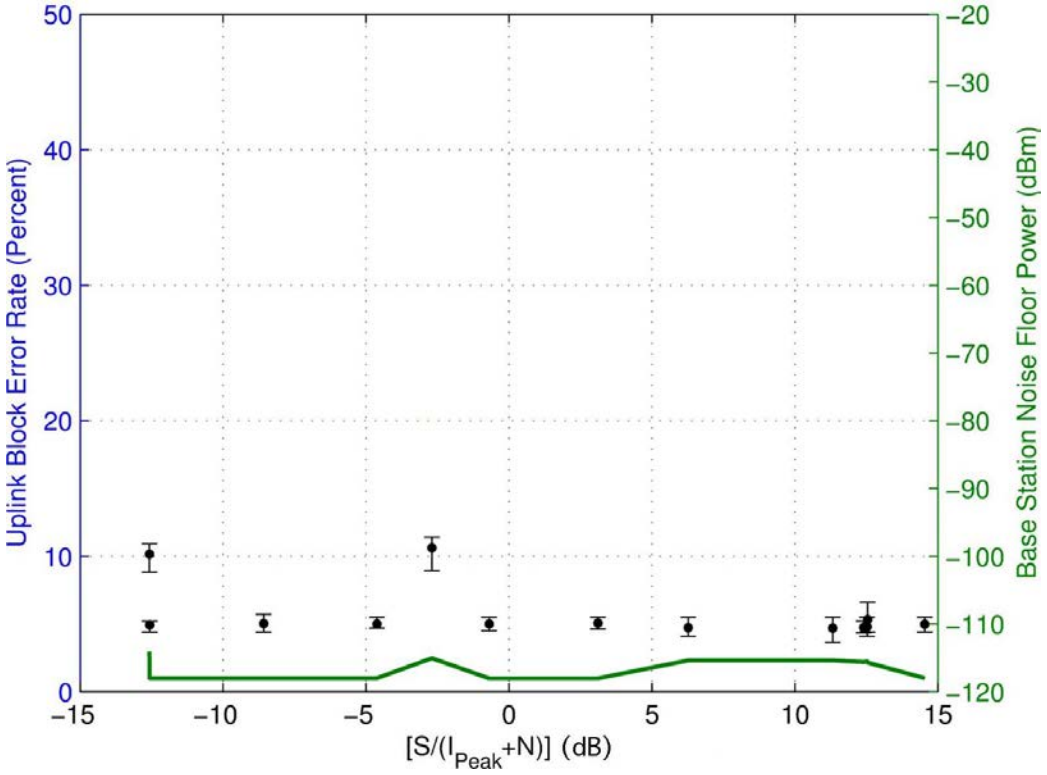

Figure 53. BLER for Q3N-4 (PW = 20 µs, PRR = 200/sec (equivalent to PW = 100 µs, PRR = 1,000/sec), DC = 0.4%) interference.

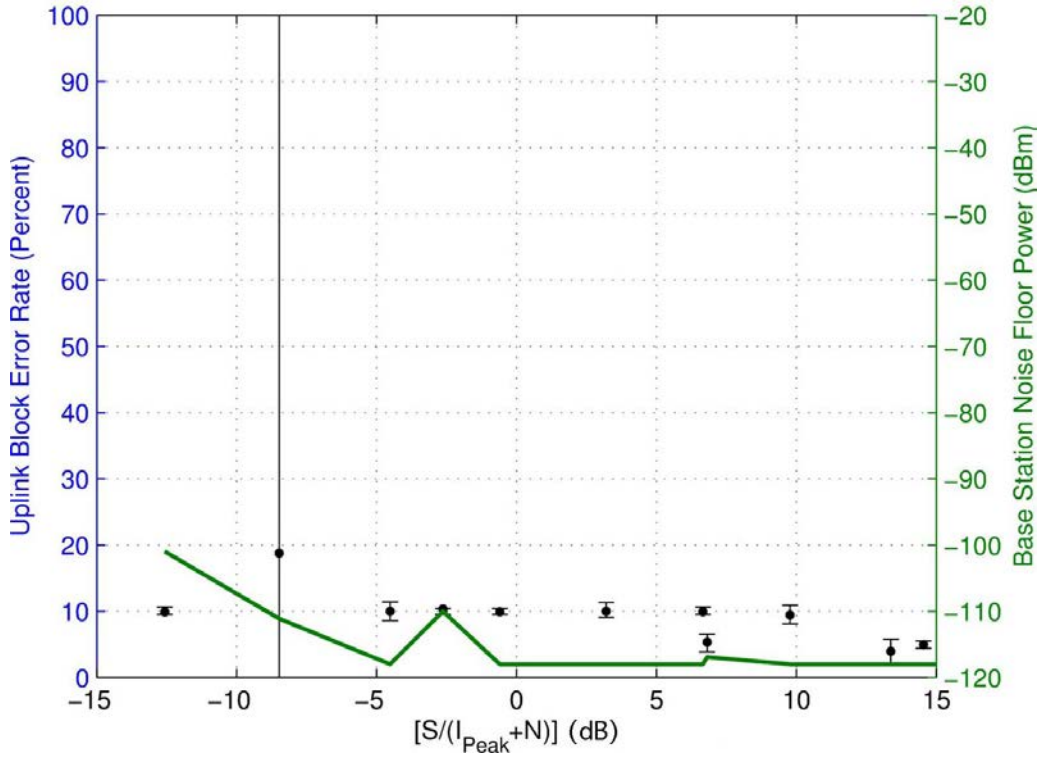

Figure 54. BLER for Q3N-5 (PW = 10 µs, PRR = 10,000/sec, DC = 10%) interference.

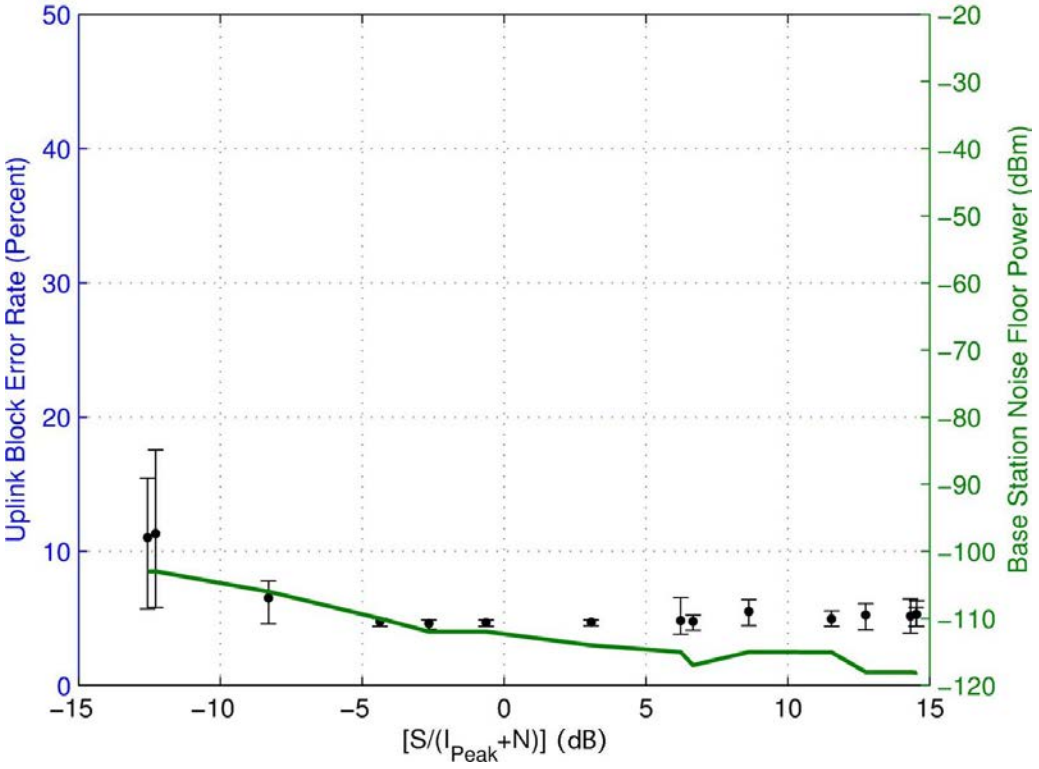

Figure 55. BLER for Q3N-6 (PW = 3.3 µs, PRR = 30,000/sec, DC = 10%) interference.

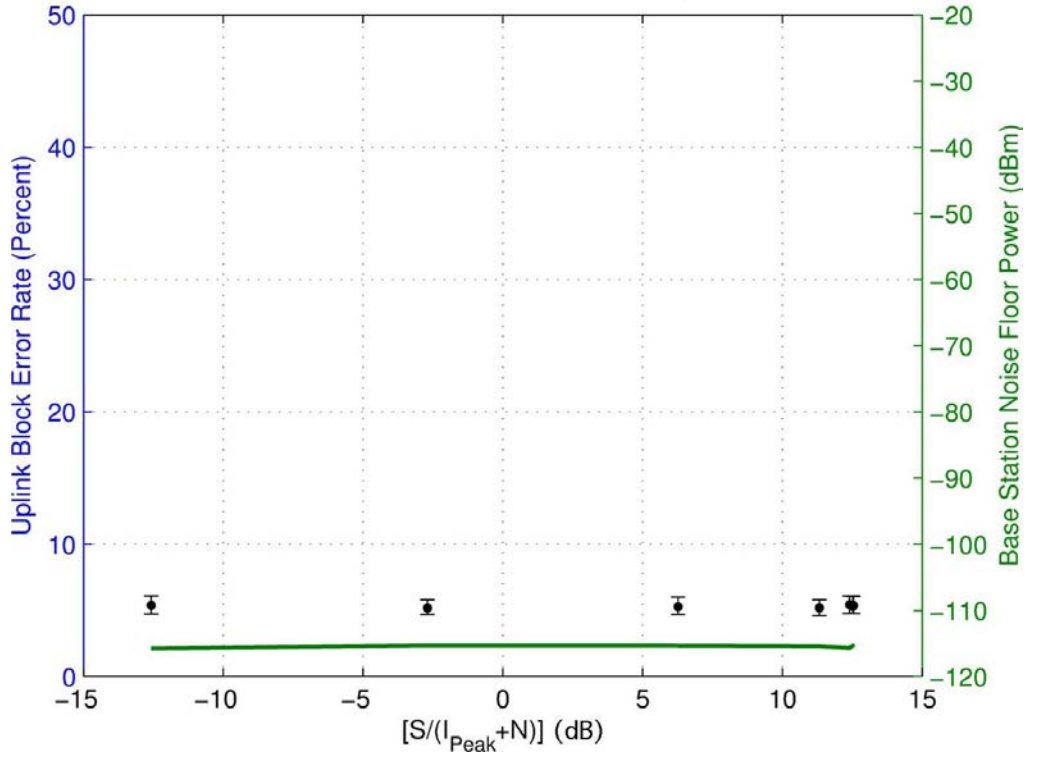

Figure 56. BLER for Q3N-7 (PW = 20 µs, PRR = 100/sec (equivalent to PW = 200 µs, PRR = 1,000/sec), DC = 0.2%) interference.

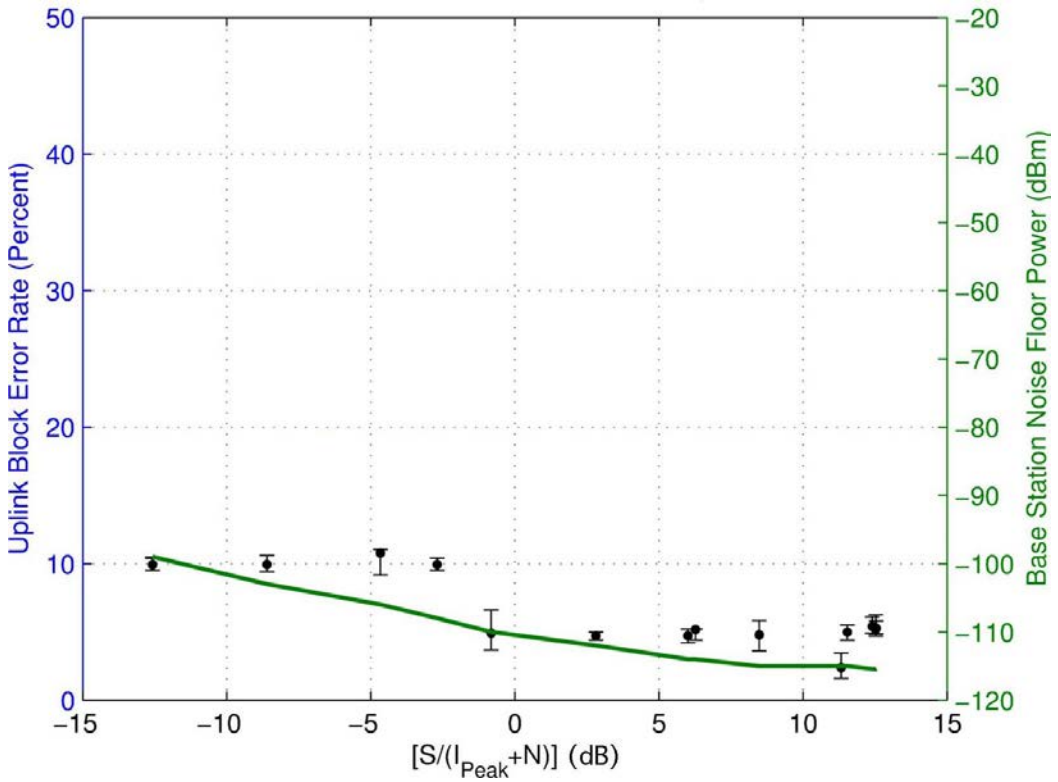

Figure 57. BLER for Q3N-8 (PW = 20 µs, PRR = 10,000/sec, DC = 20%) interference.

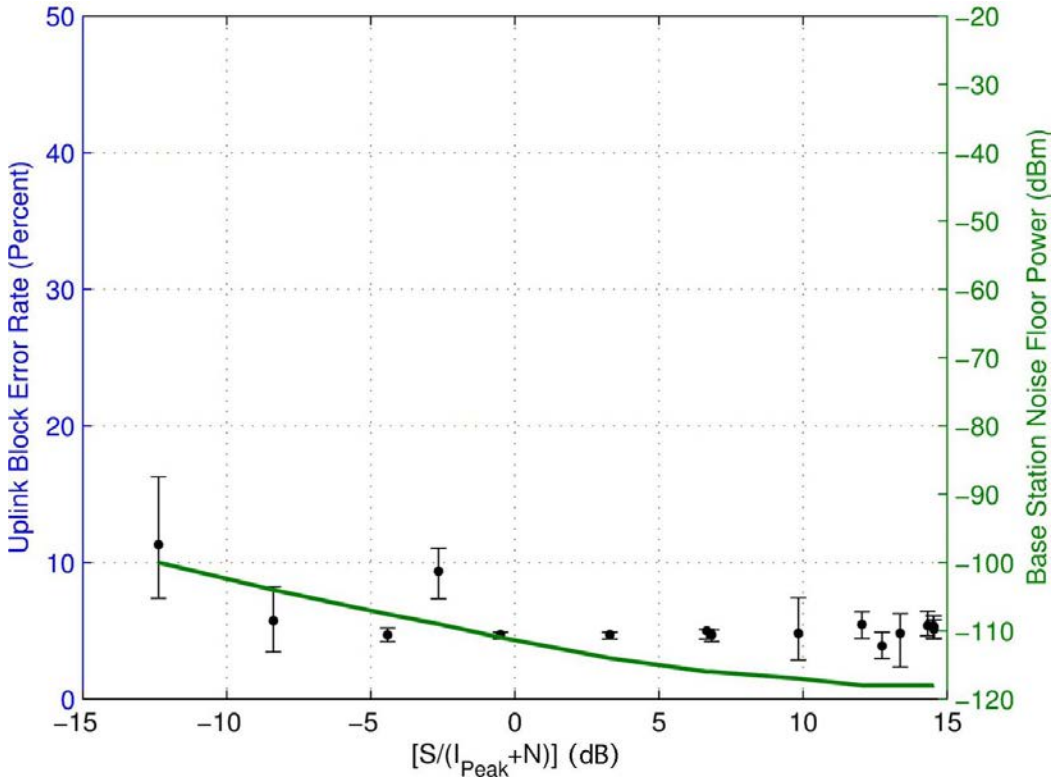

Figure 58. BLER for Q3N-9 (PW = 6.6 µs, PRR = 30,000/sec, DC = 20%) interference.

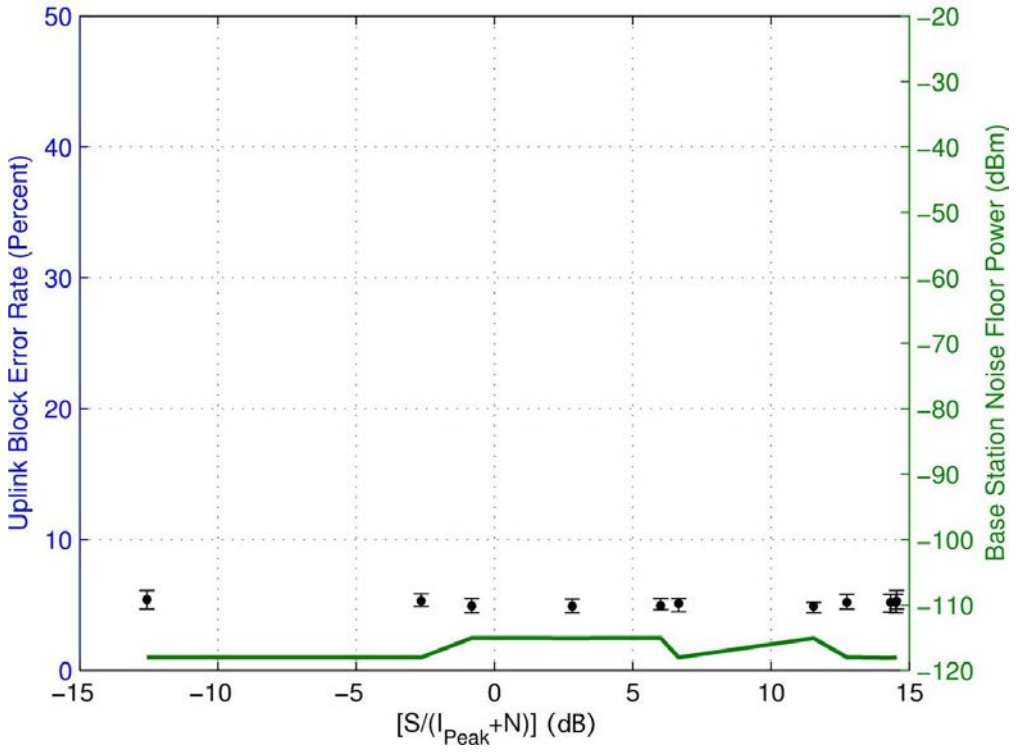

Figure 59. BLER for Q3N-10 (PW = 20 µs, PRR = 67/sec (equivalent to PW = 300 µs, PRR = 1,000/sec), DC = 0.13%) interference.

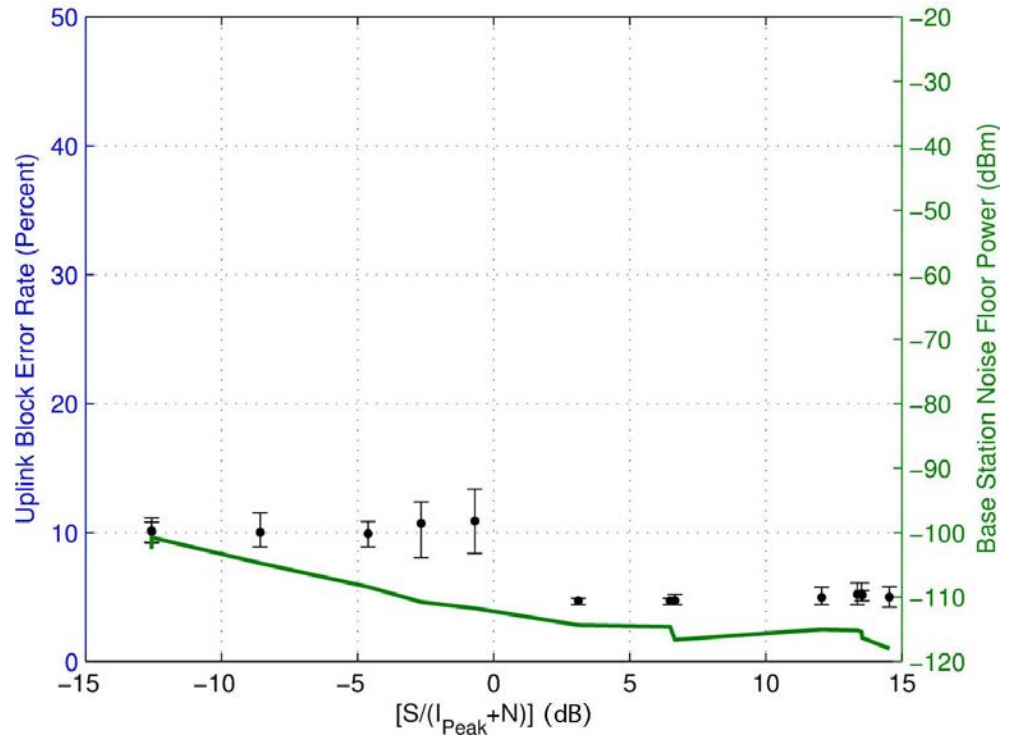

Figure 60. BLER for Q3N-11 (PW = 20 µs, PRR = 6,667/sec (equivalent to PW = 30 µs, PRR = 10,000/sec), DC = 13%) interference.

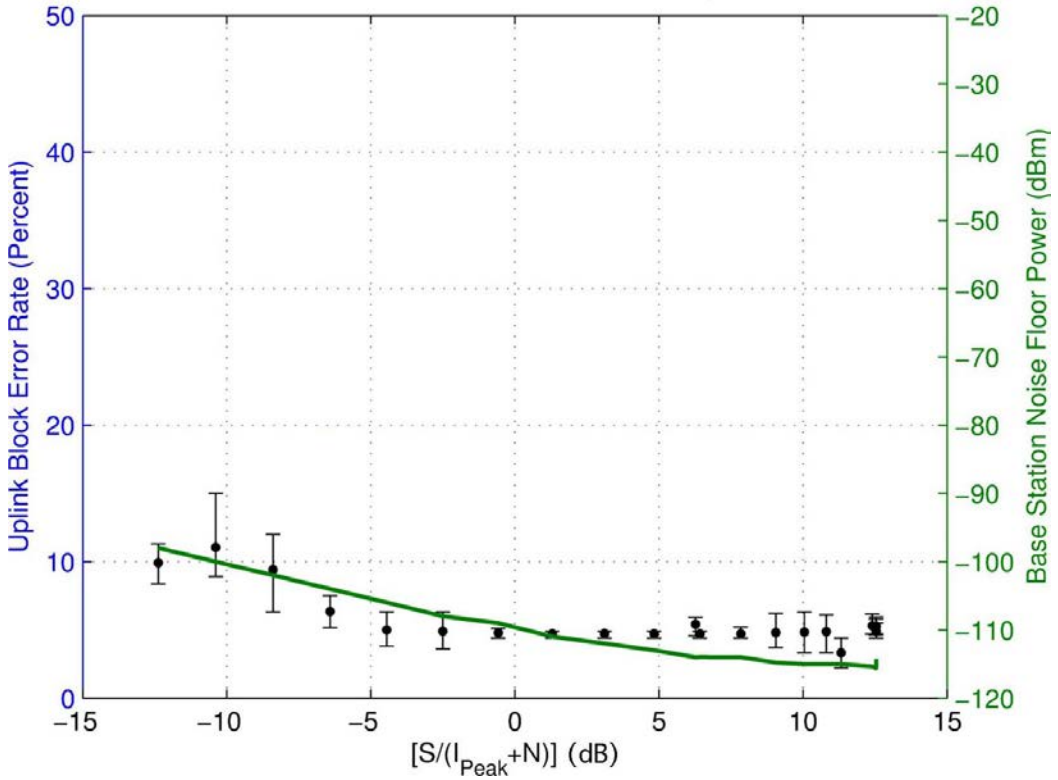

Figure 61. BLER for Q3N-12 (PW = 10 µs, PRR = 30,000/sec, DC = 30%) interference.

4 LTE BASE STATION EMISSION SPECTRUM MEASUREMENT

4.1 Notes on LTE Base Station Emission Spectrum Measurement Data Collection

While the authors had access to the emissions of an LTE (TDD) base station during the course of the interference-effects measurements, they measured the emission spectrum of an unfiltered LTE base station transmitter. The measurements were performed, with a slight variation, in accord with the procedures of [5], with both peak detection and average detection. The measurement set-up is shown in Figure 62. The spectra were measured with 100 dB of dynamic range; the results are shown in Figure 63.

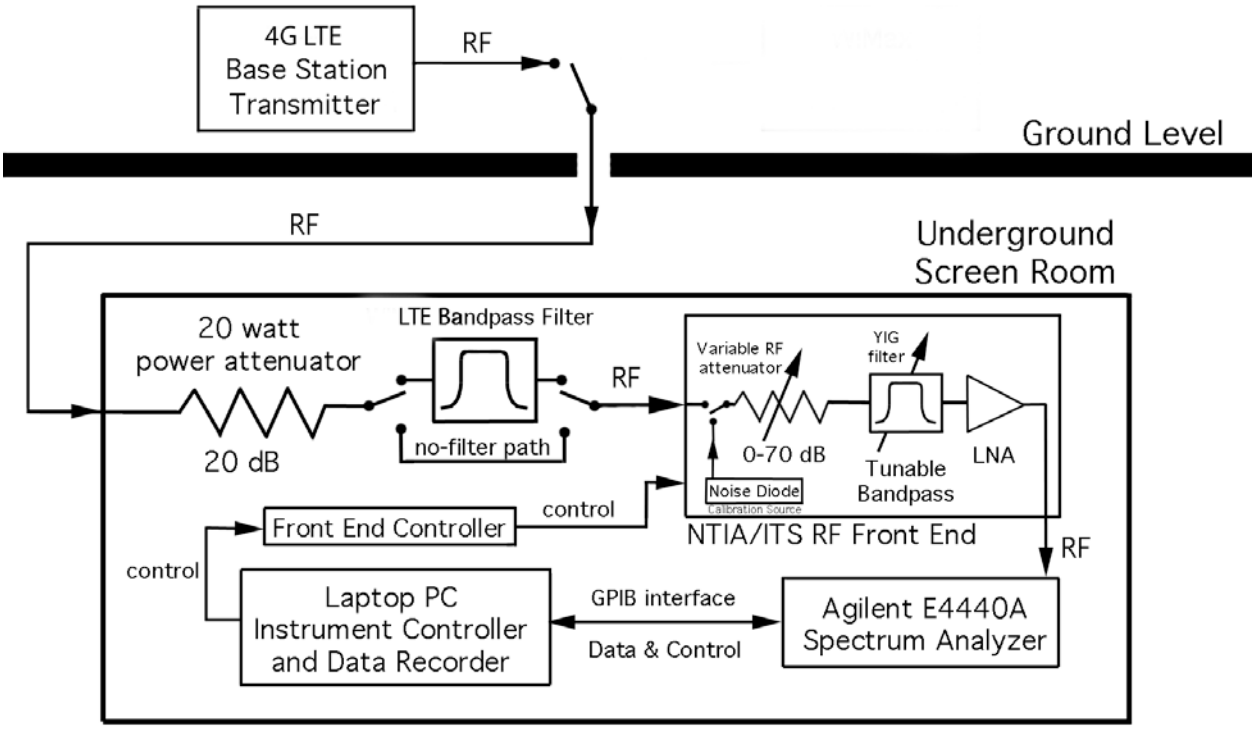

Figure 62. System set-up for the LTE base station emission spectrum measurement.

The standard wide-dynamic range measurement procedure of [5] was followed exactly for the peak-detected spectrum measurement, the key aspect of this procedure being that the measurement progressed as a stepped-frequency rather than a swept-frequency process, allowing for control of dynamic range during the measurement. For the average spectrum, however, the procedure was varied slightly. To obtain the average spectrum data points, the spectrum analyzer collected 8,000 sample-detected points at each measured frequency in the spectrum. Then the linear power average of those 8,000 points was computed as the *average* emission spectrum power level at each frequency. Both the peak and average spectra were measured with a dwell interval of 300 ms per frequency data point. The measurement bandwidth of 30 kHz was selected to ensure that it was within the range in which the fundamental-frequency and out-of-band and

spurious emissions all varied as 10log of the measurement bandwidth, as per the measurement-bandwidth discussion presented in [5].

4.2 LTE Base Station Emission Spectra

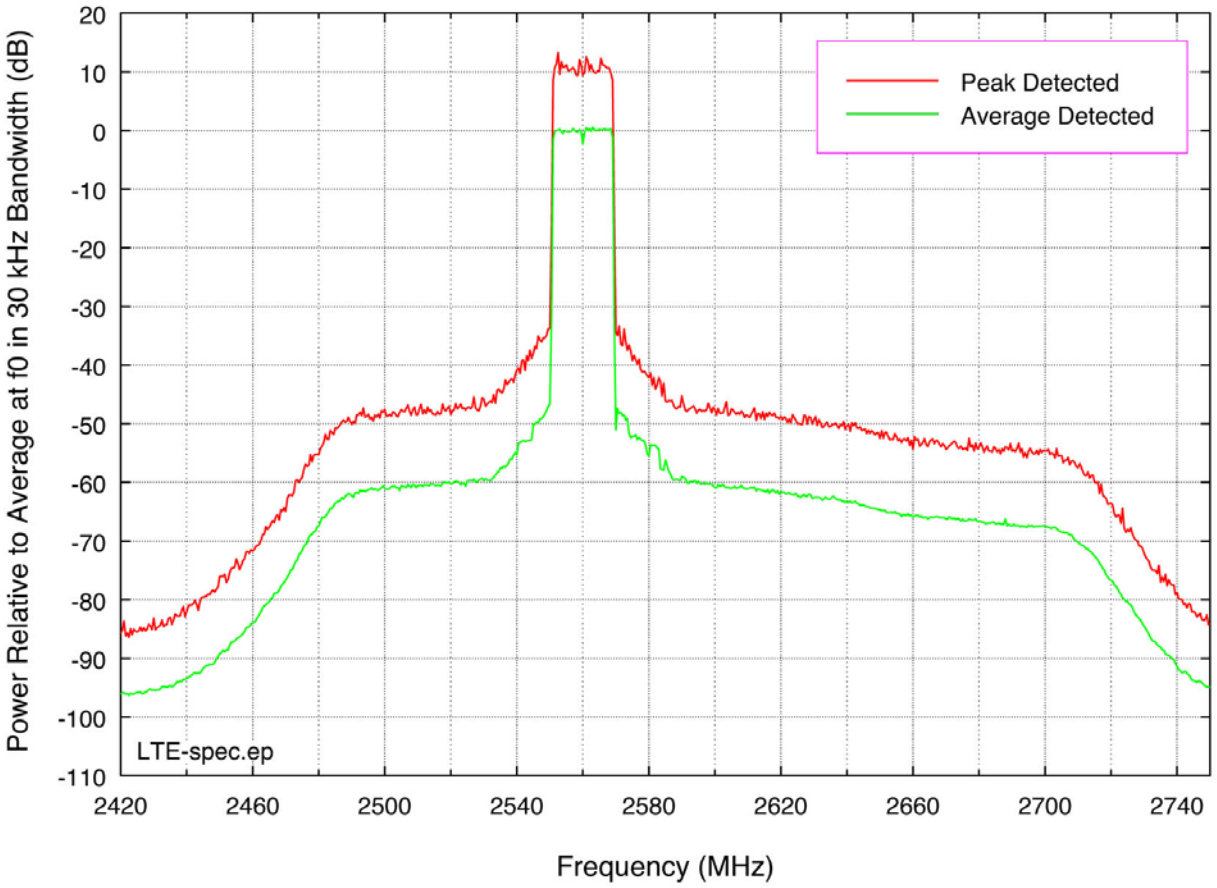

Figure 63. Peak-detected and average-detected LTE base station emission spectra.

The authors believe that the emission spectrum of a 3.5 GHz LTE station would be nearly identical to the 2.6 GHz spectrum of Figure 63. This is because identical RF technology is used for 2.6 and 3.5 GHz stations while LTE modulation is independent of transmitted frequency. Moreover, the spectrum structure of the LTE transmitter in Figure 63 is similar to WiMAX emission spectra presented in a recent NTIA Report [6]. In Figure 63, the LTE emission spectrum exhibits a flat porch on each side of the fundamental emission. The power levels in these two regions are 60–70 dB below the fundamental. At 75 MHz below the fundamental frequency and 145 MHz above the fundamental frequency, the porch emissions roll off. The roll-off continues until the emissions finally drop into the measurement system noise floor at about 100 dB below the fundamental-frequency power. NTIA believes this device has FCC certification, and that it meets all FCC rules regarding its emissions.

WiMAX base station emission spectrum characteristics can be modified via installation of RF filtering of base station transmitter outputs, as documented by NTIA [6]. Strong similarities

between LTE and WiMAX stations indicate that LTE emissions can be similarly modified. While filter installation on transmitters can produce faster spectrum roll-off rates, filters are not always installed on base stations and the FCC does not require them to meet any existing regulations; they might not be installed unless interference with other systems develops and needs to be mitigated.

The spectra of other LTE base station stations manufactured by other companies may be assumed to generally look similar to Figure 63, unless supplemental RF filtering is installed. This is due to the fact that various existing manufacturers use similar transmitter designs and they obtain their transmitter power amplifiers from a limited number of suppliers who are all working from the same current technology base.

5 SUMMARY AND CONCLUSIONS

5.1 Summary of Work and Results

The effects of radar interference on the performance of an LTE (TDD) base station have been assessed with a hardware test bed for a wide variety of radar waveforms. The parameters of the waveforms that have been tested span the range of existing and likely future radar systems at 3.5 GHz. The LTE base station that was tested is designed to be used in macro-cells, but the test results are believed to likely be valid for future micro-cell systems. This is because LTE protocols should not depend on the size of cell coverage. As a sanity check on the radar interference results, 10 MHz-wide and 20 MHz-wide Gaussian noise was also injected into the base station receiver.

5.2 Radar Interference Impacts on LTE Base Station (TDD) Performance

The impacts of the waveforms on the data throughput rate, BLER, and internal noise level of the base station receiver are shown in Figures 4–61. Most waveforms produced appreciable effects at *S/(I+N)* levels below 0 dB, and many of the waveforms degraded LTE performance at *S/(I+N)* levels somewhat above 0 dB. The figures show that as the interference power level was increased, the waveforms' impact gradually increased from slight to moderate to severe. Sudden impacts as a function of interference level, what might be called cliffs, are not observed in the graphs. Some waveforms seemed to have no impact. The figures also show that at times the LTE system was able to mitigate the interference.

Regarding results for specific waveforms and trends, the simple pulsed waveforms that caused the most loss of data throughput were ECC-1 and -2 and P0N-1, -5, -10 and -12. All of the P0N waveforms caused some data throughput loss, with the least effects being from P0N-9 and -11.

For the chirped-pulsed waveforms, Q3N-1, -5 and -11 caused the most data throughput loss. Q3N-2 and -4 caused small data throughput loss. Waveform Q3N-7 caused no loss in data throughput, probably due to its low duty cycle of 0.4%. It is beyond the scope of this report to determine *why* particular waveforms had the most or least effects. NTIA welcomes LTE operators and other technical readers to review these data and share their views on these test results.

5.3 On-Tuned Versus Off-Tuned Interference

In this study, radar interference was on-tuned (co-channel) with the frequency of the LTE base station receiver. This begs the obvious question of what would be the effects of off-tuned interference.

The answer is that the on-tuned interference-effects data in this report can be used to approximately determine off-tuned interference effects. This is because, putting aside the so-called rabbit ears effect for off-tuned radar pulses (as described in [7]) off-tuned radar pulses have the same characteristics (pulse width and pulse repetition rate) as on-tuned pulses.

Therefore, variation in *S/(I+N)* levels in the victim receiver is equivalent to changing the tuned frequency of the interfering source relative to the frequency of the victim receiver. For example, a change of 10 dB in the level of *S/(I+N)* in the victim receiver is equivalent to having changed the tuned frequency of the interferer enough to cause a corresponding 10 dB change in interference level in the victim receiver. Put another way, the X-axis in the interference-effects data graphs in this report can be interpreted as showing the varying tuned frequency of a radar transmitter relative to the center frequency of a victim LTE base station receiver. The off-tuned interpretation is imperfect because off-tuned radar waveforms are not identical to on-tuned radar emissions. But this interpretation nevertheless provides some guidance regarding the effects of off-tuned interference if no better data are available.

But how *much* of a change would be required in the relative tuning of a radar transmitter and an LTE base station receiver to cause any given amount of change in *S/(I+N)* (of, for example, 10 dB)? That question can only be answered if two additional pieces of information are gathered. These are the emission spectrum of the radar transmitter and the frequency-domain shape, or frequency-dependent rejection (FDR) curve, of the victim receiver's intermediate frequency (IF) stage. The radar spectrum shows the amount of transmitted radar spectrum roll-off, and resulting spectrum power density, in the out-of-band (OOB) and spurious regions as a function of frequency. The receiver IF stage shape measurement allows precise calculation of the total amount of power coupled from the radar's OOB or spurious emissions into the receiver's tuned channel.

5.4 Recommendations for Future Work

- Although the authors believe that testing on a micro-cell LTE system will yield results similar to those presented in this report for a macro-cell LTE receiver, they seek to confirm this hypothesis by performing a similar set of tests on a micro-cell LTE base station.

- Theoretical analysis is recommended to better understand *why* various radar interference waveforms have the particular effects that have been published in this report. LTE signal detection needs to be understood to perform such analyses.

- Based on results of previous NTIA investigations of radar-to-earth station interference [8], LTE receivers may be expected to experience RF front end saturation and power overload in littoral zones. Therefore, LTE receivers need be tested to determine the non-linear effects of saturation and front-end overload from radar signals.

- Emission spectra of 3.5 GHz radars need to be collected and published so that coupling levels between radar transmitters and LTE receivers can be determined based on the amount of frequency separation between the systems.

- Similarly, more emission spectra of LTE base station transmitters need to be measured.

- The frequency domain responses of the IF stages of 3.5 GHz radar receivers and LTE stations need to be measured or acquired in order to perform FDR calculations.

- The interference effects of off-tuned radar pulses showing the so-called rabbit ears effect [7] should be measured for LTE base station receivers.

- The effects of a variety of radar beam-dwell periods need to be determined for LTE base station receivers.

- Using data from this report and from the tasking described above, frequency-distance separation curves need to be developed for spectrum sharing between 3.5 GHz radars and LTE systems.

The final step in all of this work will be a comparison of the frequency-distance separation curves (including 3.5 GHz propagation characteristics) for radar-to-LTE interference and LTE-to-radar interference. That comparison will determine which scenario (which interference direction) is the limiting factor for future band sharing.

6 REFERENCES

[1] "*Proposal to Create a Citizen's Broadband Service in the 3550-3650 MHz Band*," FCC Docket No. 12-354. http://www.fcc.gov/document/enabling-innovative-small-cell-use-35-ghz-band-nprm-order

[2] "An Assessment of the Near-Term Viability of Accommodating Wireless Broadband Systems in the 1675-1710 MHz, 1755-1780 MHz, 3500-3650 MHz, 4200-4220 MHz and 4380-4400 MHz Bands (President's Spectrum Plan Report)," NTIA, U.S. Dept. of Commerce, Nov. 2010. http://www.ntia.doc.gov/report/2010/assessment-near-term-viability-accommodating-wireless-broadband-systems-1675-1710-mhz-17

[3] CEPT ECC Report 174, "Compatibility Between the Mobile Service in the Band 2500-2690 MHz and the radiodetermination service in the band 2700-2900 MHz," CEPT Electronic Communications Committee, Mar. 2012. http://www.erodocdb.dk/docs/doc98/official/Pdf/ECCRep174.pdf

[4] "LTE radio link budgeting and RF planning," Section 2.1 (Typical parameter values). https://sites.google.com/site/lteencyclopedia/lte-radio-link-budgeting-and-rf-planning

[5] Sanders, F. H., R. L. Hinkle and B. J. Ramsey, "Measurement Procedures for the Radar Spectrum Engineering Criteria (RSEC)," NTIA Technical Report TR-05-420, U.S. Dept. of Commerce, Mar. 2005. http://www.its.bldrdoc.gov/publications/2450.aspx

[6] Sanders, F. H., R. L. Sole, J. E. Carroll, G. S. Secrest and T. Lynn Allmon, "Analysis and Resolution of RF Interference to Radars Operating in the Band 2700-2900 MHz from Broadband Communication Transmitters," NTIA Technical Report TR-13-490, U.S. Dept. of Commerce, Oct. 2012. http://www.its.bldrdoc.gov/publications/2684.aspx

[7] Sanders, F. H., "The Rabbit Ears Pulse Envelope Phenomenon in Off-Fundamental Detection of Pulsed Signals," NTIA Technical Report TR-12-487, U.S. Dept. of Commerce, Jul. 2012. http://www.its.bldrdoc.gov/publications/2678.aspx

[8] Sanders, F. H., R. L. Hinkle and B. J. Ramsey, "Analysis of Electromagnetic Compatibility Between Radar Stations and 4 GHz Earth Stations," NTIA Technical Report TR-94-313, U.S. Dept. of Commerce, Jul. 1994. http://www.its.bldrdoc.gov/publications/2340.aspx

APPENDIX A: CALCULATION OF S/(I+N) LEVELS IN THE LTE RECEIVER

A.1 Signal and Interference Power Levels in the LTE Base Station Receiver

The LTE base station receiver provided diagnostic monitoring of both its internal noise level and the power level of the desired, UE signal. However, neither the radar interference power levels nor the *S/(I+N)* levels could be monitored or measured directly inside the receiver. The radar power and *S/(I+N)* level had to be inferred (calculated) based on power monitored at the spectrum analyzer, as shown in Figure A-1 (derived from Figure 3 of this report).

Figures A-1 and A-2 demonstrate graphically, through examples, the relationships between Gaussian and radar power outputs, respectively, at the VSG and interference power levels per resource block on each MIMO channel (RMS and peak detected, respectively) in the base station receiver. The power offset between Test Points 1 and 2 (TP-1 and TP-2 in the figures) was 24.5 dB, and the total offset between the VSG output and the base station receiver was 65.8 dB. The losses between hardware components shown in the figures were measured, not calculated.[15]

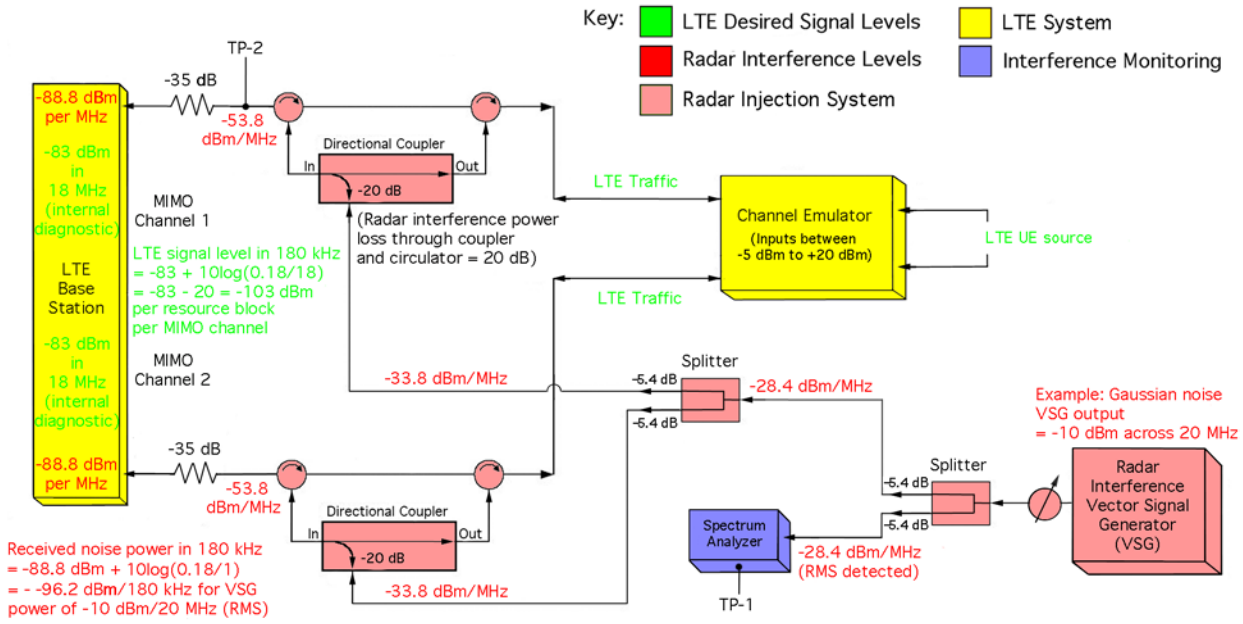

Figure A-1. Graphical example of relationships among VSG output power, RMS power measured at the spectrum analyzer, and RMS interference power in the LTE base station receiver per LTE resource block, for Gaussian noise interference injection.

[15] All losses were measured by ITS personnel except the final 35 dB of loss at the base station receiver inputs, which was measured by the carrier's personnel. For operational simplicity during the measurements, the spectrum analyzer outputs were programmed with a -24.5 dB offset, allowing the authors to use the spectrum analyzer to read (virtually) and record the radar interference power at the circulator output, TP-2.

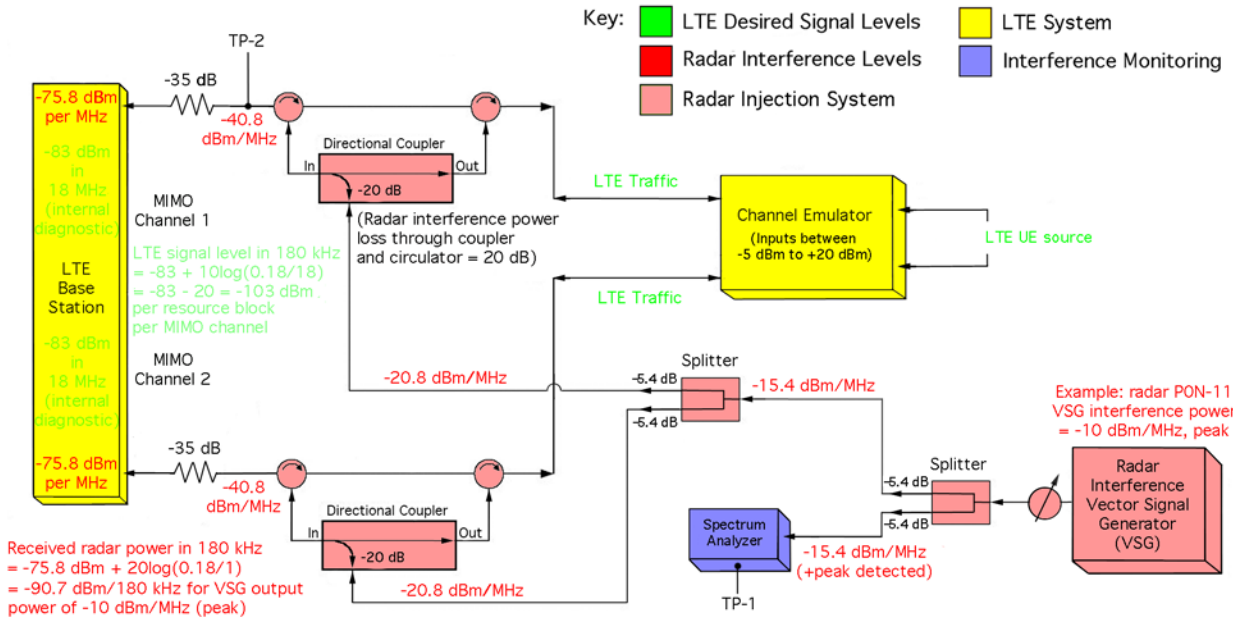

Figure A-2. Graphical example of relationships among VSG output power, peak power measured at the spectrum analyzer, and peak interference power in the LTE base station receiver per LTE resource block, for radar interference waveform P0N-11 injection.

The authors did not have access to the LTE base station radio input and so were not able to directly measure the power of the desired LTE UE signal at that point. The LTE UE desired signal level measured at TP-2 (see figures) was -63.6 dBm/MHz RMS = -51.0 dBm/18 MHz. Subtracting 35 dB of attenuation at the receiver input (see figures) yields -85.6 dBm/18 MHz RMS for the desired UE signal level at the receiver input.

However, the base station receiver power diagnostic indicated -83 dBm/18 MHz for the desired signal level. This differed from the measured power because the LTE receiver's signal-sensing diagnostics reported the *average level of the desired signal when the signal was on,* which is nearly the same as the peak power level of the signal, whereas the authors measured RMS power across multiple LTE duty cycles, each cycle consisting of a 3 ms RF burst and a 2 ms inter-burst quiet interval.[16] The theoretical difference between the authors' measured RMS power and the average level of the desired signal as reported by the receiver's diagnostic software should have been -2.2 dB.[17] The difference between the calculated offset of -2.2 dB and the measured offset of -2.6 dB was within the uncertainty of the authors' RMS power measurement. In this report, the desired signal level, *S*, is taken to be that of the receiver's diagnostic-reporting level of -83 dBm/18 MHz, the average power of the LTE signal within each LTE 3 ms data burst.

[16] This is the same signal structure as used by WiMAX systems [A-1].

[17] The LTE signal was measured by the authors as running in bursts that each lasted 3 ms, with a 2 ms interval between each burst. The periodicity of the entire LTE signal was (3 ms + 2 ms) = 5 ms. The signal duty cycle was therefore about 3/5, and the ratio between maximum, or peak, desired signal level and RMS signal level was approximately 10log(3/5) = -2.2 dB.

A.2 Determination of *S/(I+N)* Levels in the LTE Base Station Receiver

The effects of interference need to be determined as a function of *S/(I+N)* levels in the LTE base station receiver. Obviously this term can only be computed when the levels of *N*, *S*, and *I* are determined in a uniform bandwidth. However, the three parameters were measured in three distinct bandwidths. These were 180 kHz (the resource block bandwidth) for internal noise, 18 MHz (the MIMO channel bandwidth) for the level of the desired UE signal, and 1 MHz (a standard reference bandwidth for radar systems) in the spectrum analyzer for interference waveforms. For purposes of data analysis, the LTE resource block bandwidth of 180 kHz was selected as the bandwidth in which all three parameters would be determined. Although in principle any bandwidth could have been used for analysis, 180 kHz was selected because it is the effective operational bandwidth for LTE resource block traffic processing.

Once every second during the measurements, the LTE base station provided an internal, diagnostic output showing the level of average-detected, inherent receiver noise, *N*, in the resource block bandwidth of 180 kHz. When measured under baseline (non-interference) conditions, this power level was -118 dBm throughout the measurement series. Since *kTB* thermal noise at room temperature is -121.4 dBm, this indicated that the receiver's noise figure was 3.4 dB.[18]

In each MIMO channel (see Figure A-1), desired signal from the UE, *S*, was indicated by the receiver's internal diagnostic software to be -83 dBm/18 MHz (see above). In the resource block bandwidth this level was reduced by a factor of 10log(0.18/18) = -20 dB. So, *S* = -103 dBm/resource block. Like the value of *N*, the value of *S* was constant throughout the measurements. The signal-to-noise ratio, *S/N*, throughout the measurements was held constant at -103 dBm – (-118 dBm) = +15 dB in the LTE base station receiver.

Interference power was measured with the monitoring spectrum analyzer (Figures A-1 and A-2) in a bandwidth of 1 MHz. Peak detection was used to measure radar interference power and average detection was used for Gaussian noise interference. Since peak-detected power measurements of pulsed waveforms vary as 20log of measurement bandwidth (see Figure 3 of [A-2] and associated equations), the correction between the spectrum analyzer's 1 MHz measurement bandwidth and the 180 kHz of an LTE resource block bandwidth is 20log(0.18/1) = -14.9 dB. The correction for average-detected Gaussian interference is the conventional (direct proportionality) of 10log(0.18/1) = -7.4 dB.

The three parameters were combined, in the uniform resource block bandwidth of 180 kHz, to yield *S/(I+N)*. For example (see Figure A-2), consider the case in which pulsed radar interference (P0N-11 waveform) was peak-detected at a value of -10 dBm/MHz at the spectrum analyzer. This level (which was -10 dBm/MHz, peak, at the VSG output) was -75.8 dBm/MHz at the LTE base station receiver, as shown in Figure A-2. Corrected to the LTE resource block bandwidth,

[18] *kTB* noise at room temperature is -174 dBm/Hz. In 180 kHz the theoretical limit is -174 dBm/Hz + 10log (180,000) = -174 dBm/Hz + 52.6 dB = -121.4 dBm/180 kHz. Since the receiver's inherent noise level in each resource block was -118 dBm, the LTE base station receiver noise figure was -118 dBm – (-121.4 dBm) = 3.4 dB.

this radar interference level was -90.7 dBm/180 kHz. To compute *S/(I+N)*, the analysis software first linearized all of the three parameters (dividing by 10 and taking the antilog of the result):

$$S = 10\text{^}(-103 \text{ dBm}/10) = 5.012\text{E-}11 \text{ mW};$$

$$N = 10\text{^}(-118 \text{ dBm}/10) = 1.585\text{E-}12 \text{ mW};$$

$$I = 10\text{^}(-90.7 \text{ dBm}/10) = 8.511\text{E-}10 \text{ mW}.$$

Then the expression was first computed in the linear terms and then converted into decibels:

$10\log(S/(I+N)) = 10\log((5.012\text{E-}11/(8.511\text{E-}10 + 1.585\text{E-}12))) = 10\log(0.0588) = -12.3$ dB.

Of course, in cases such as this in which $I >> N$, the quantity *S/(I+N)* reduces to approximately *S/I*; at high interference levels (at the left-hand sides of the data graphs in this report, the values of *S/(I+N)* are essentially just *S/I*.

Because the interference was peak-detected when the waveform was pulsed, and was average-detected when the waveform was Gaussian interference, the *S/(I+N)* term was computed (and is displayed in interference-effects Figures 4–61) as $S/(I_{peak} + N)$, *dB* for pulsed radar interference and as $S/(I_{average} + N)$, *dB* for Gaussian interference.

The values of the testing parameters for all work described in this report are summarized in Table A-1.

Table A-1. Summary of test parameters for all work described in this report.

Test Parameter	Test Parameter Value
LTE base station receiver inherent noise per 180 kHz resource block per MIMO channel	-118 dBm
LTE base station receiver noise figure	3.4 dB
LTE base station signal power received from UE per 180 kHz resource block per MIMO channel	-105.6 dBm (measured RMS) across multiple 5 ms RF cycles;
	-103 dBm (reported average by LTE diagnostics) during single 3 ms RF bursts
S/N of UE signals in LTE base station	*S/N* = -103 dBm – (-118 dBm) = +15 dB
Range of *S/(I+N)* levels tested	From +15 dB to -13 dB

A.3 References

[A-1] Sanders, F. H., Sole, R. L., J. E. Carroll, G. S. Secrest and T. L. Allmon, "Analysis and Resolution of RF Interference to Radars Operating in the Band 2700-2900 MHz from Broadband Communication Transmitters," NTIA Technical Report TR-13-490, Oct. 2012. Available: http://www.its.bldrdoc.gov/publications/2684.aspx

[A-2] Sanders, F. and R. Dalke, "Relationships Between Measured Power and Measurement Bandwidth for Frequency-Modulated (Chirped) Pulses," NTIA Technical Report TR-12-488, Aug. 2012. Available: http://www.its.bldrdoc.gov/publications/2680.aspx

APPENDIX B: Emission Spectra OF Interference Waveforms

B.1 Notes on Measured Emission Spectra of Interference Waveforms

The emission spectra of all of the interference waveforms were measured in 120 kHz, an approximation of the bandwidth of the LTE base station receiver resource blocks.

B.2 Measured Emission Spectra of Interference Waveforms

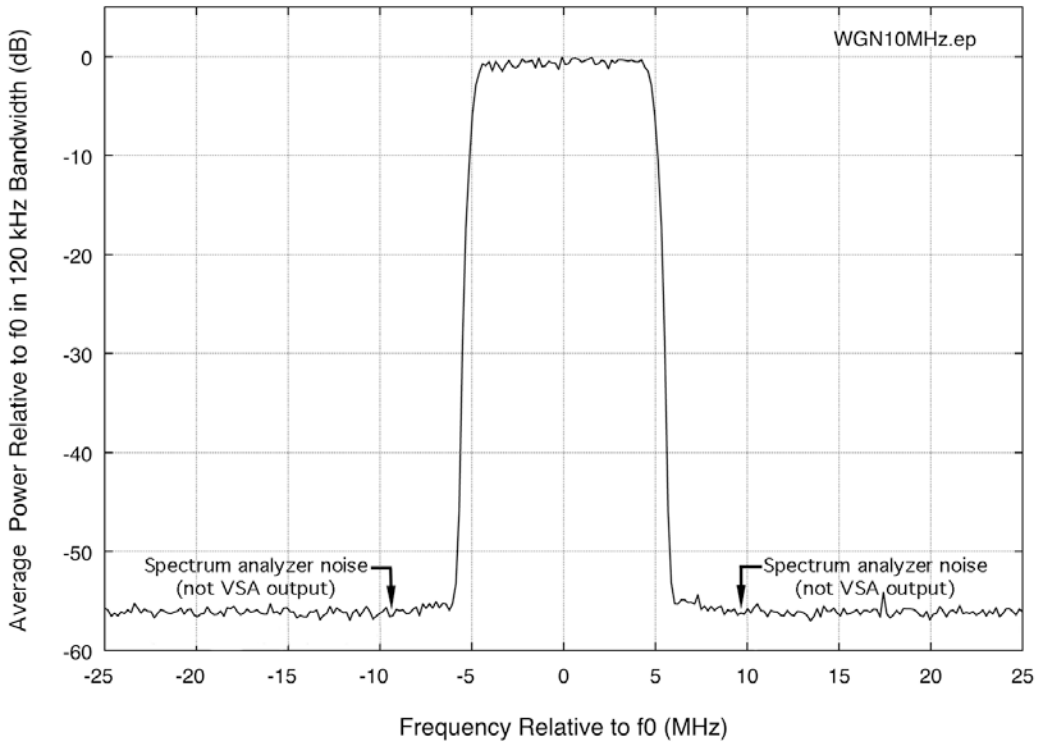

Figure B-1. Spectrum of 10 MHz-wide Gaussian noise interference.

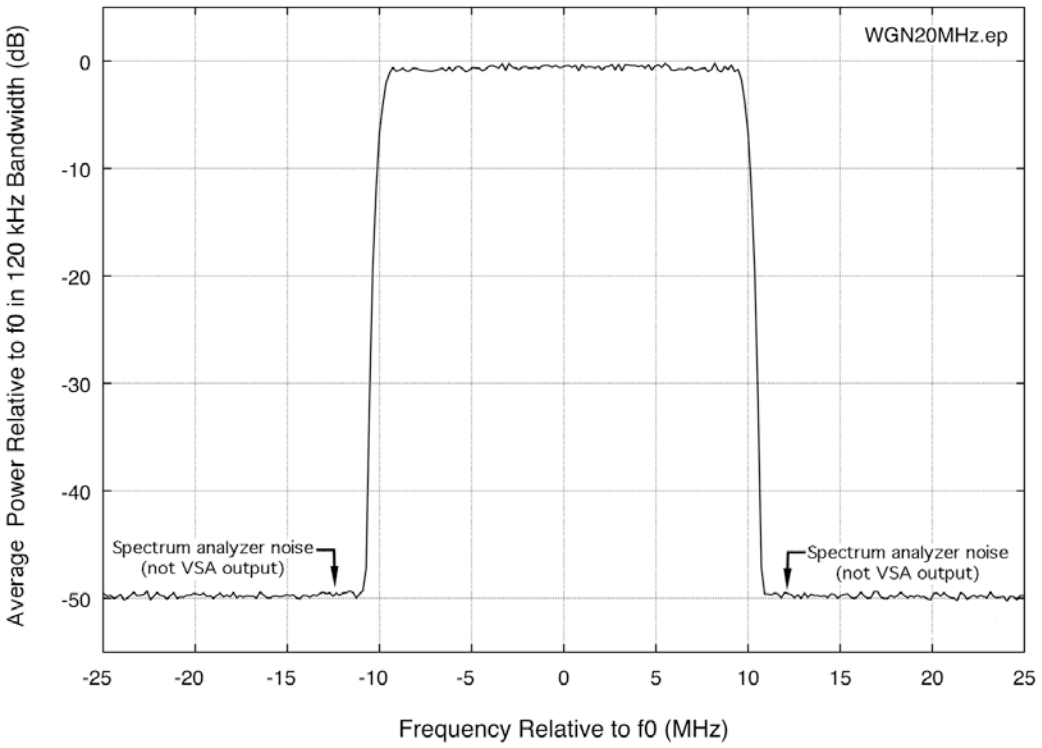

Figure B-2. Spectrum of 20 MHz-wide Gaussian noise interference.

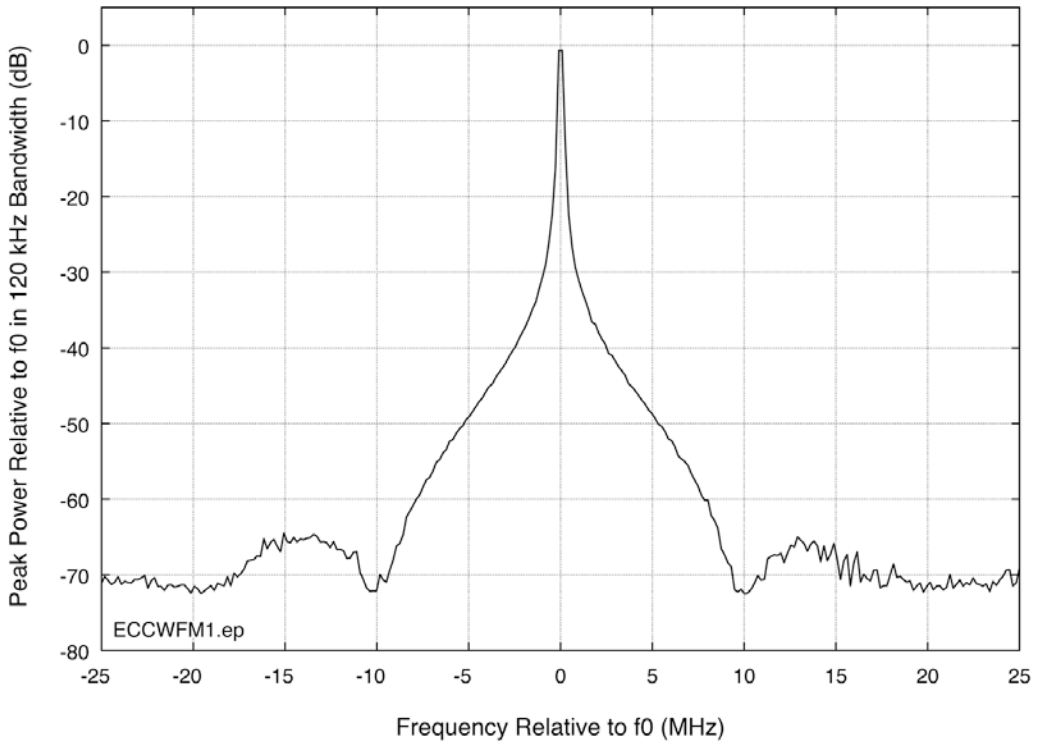

Figure B-3. Spectrum of ECC-1/WFM-1 (PW = 4 μs, PRR =1000/sec) interference.

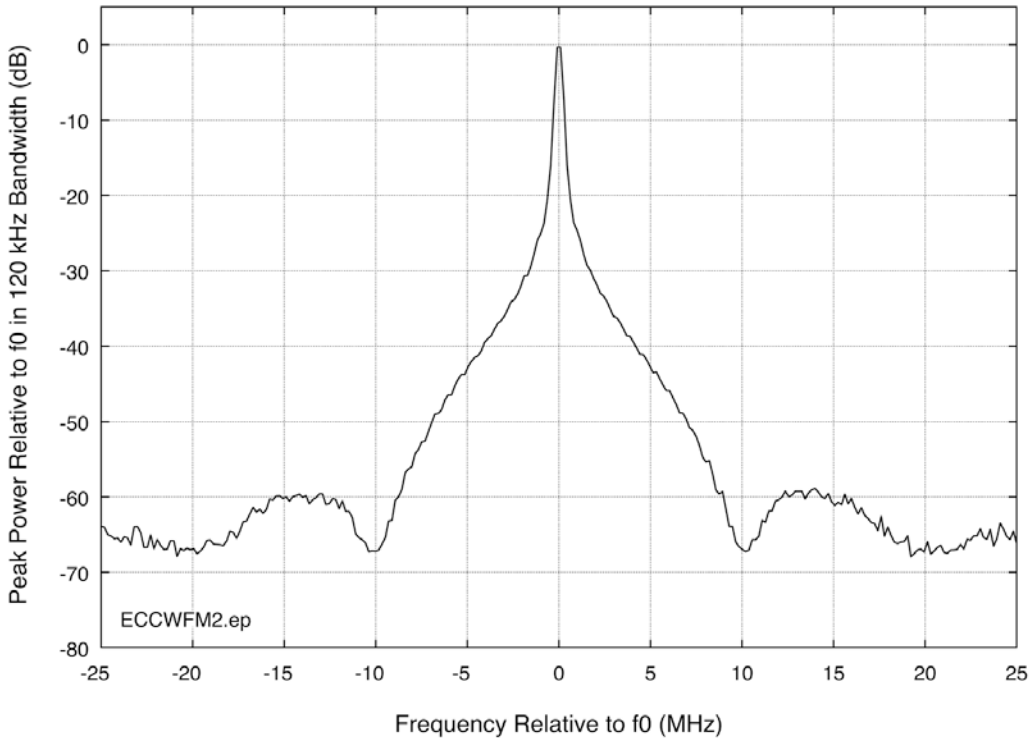

Figure B–4. Spectrum of ECC-2/WFM-2 (PW = 100 µs, PRR = 300/sec) interference.

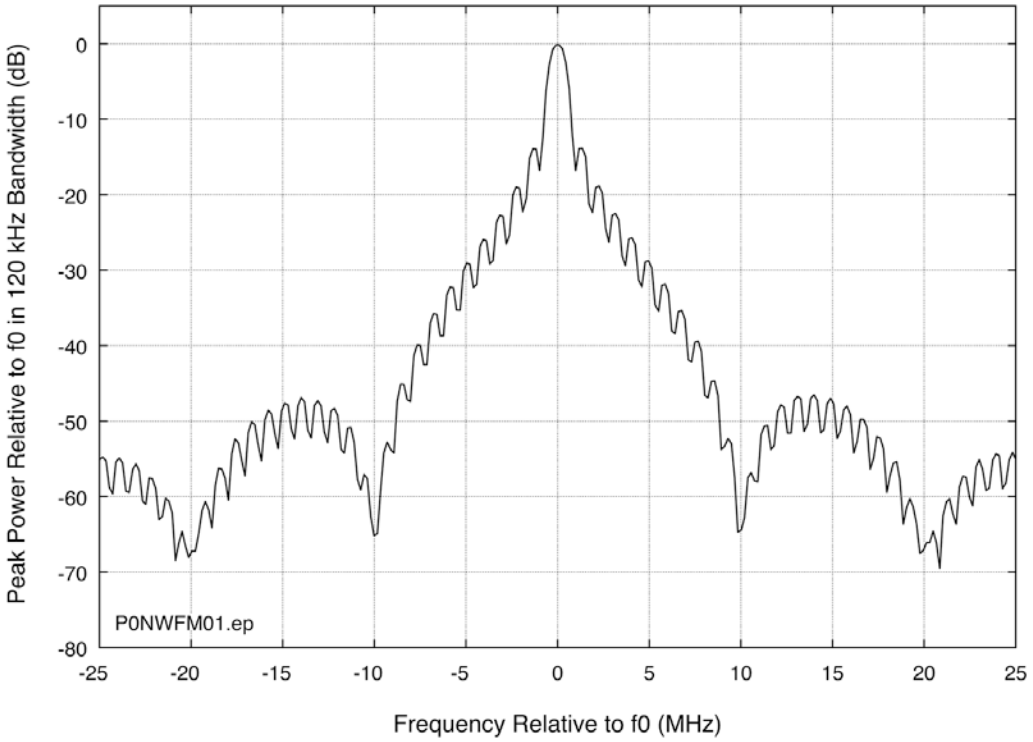

Figure B-4. Spectrum of P0N-1 (PW = 1 µs, PRR = 1000/sec, DC = 0.1%) interference.

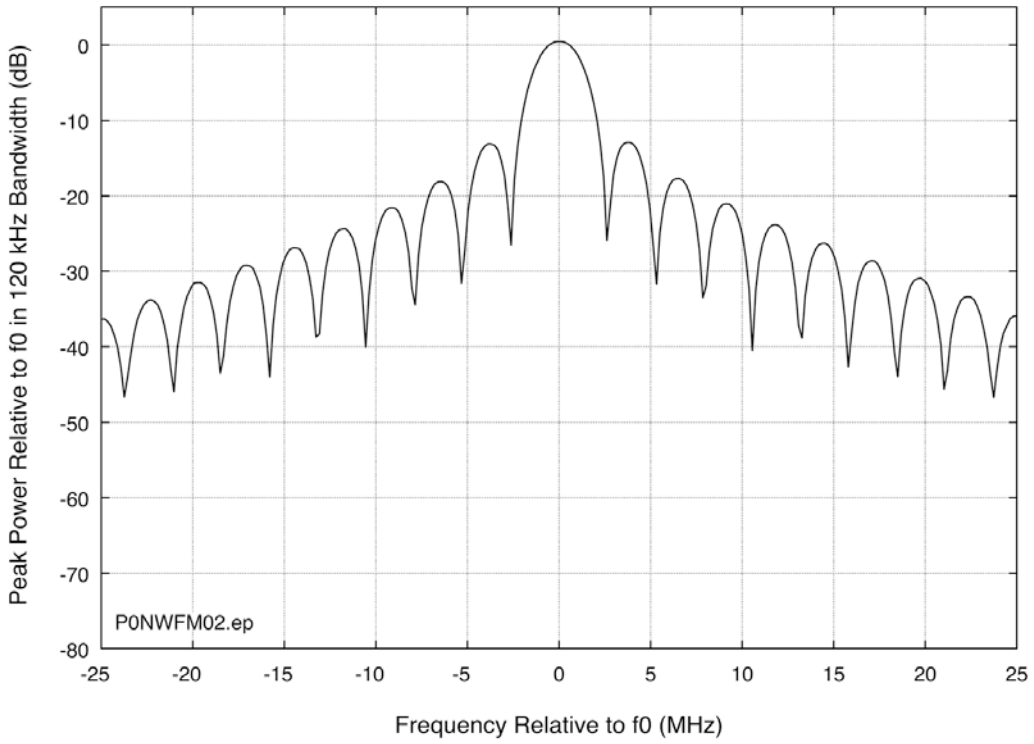

Figure B-5. Spectrum of P0N-2 (PW = 0.33 µs, PRR = 3000/sec, DC = 0.1%) interference.

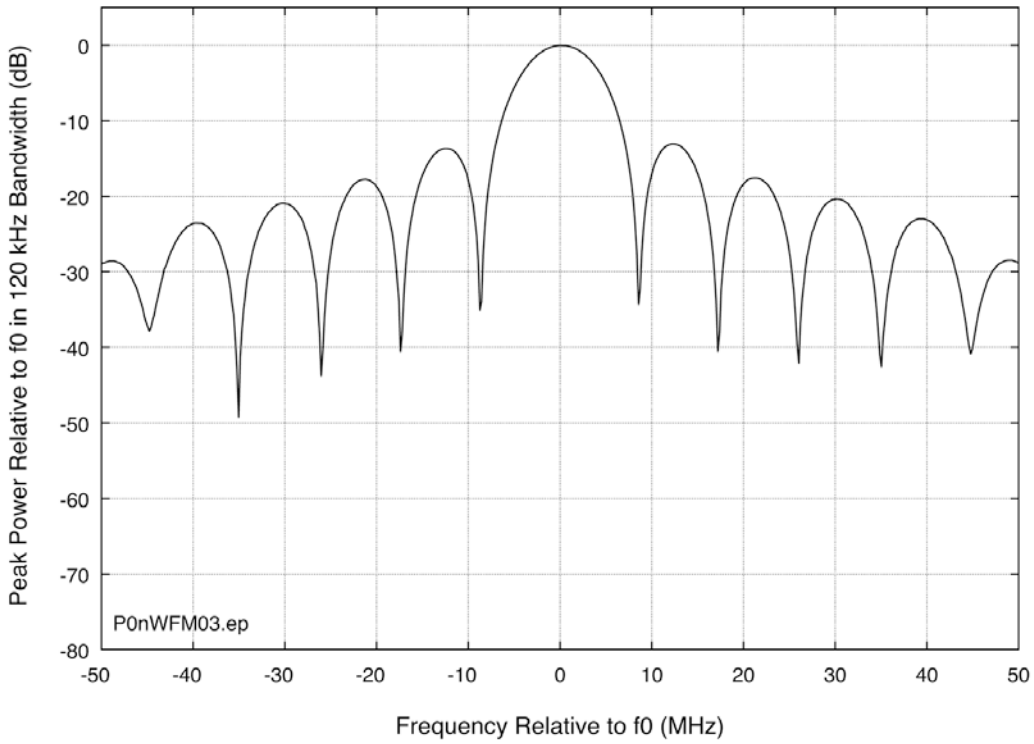

Figure B-6. Spectrum of P0N-3 (PW = 0.1 µs, PRR = 10,000/sec, DC = 0.1%) interference.

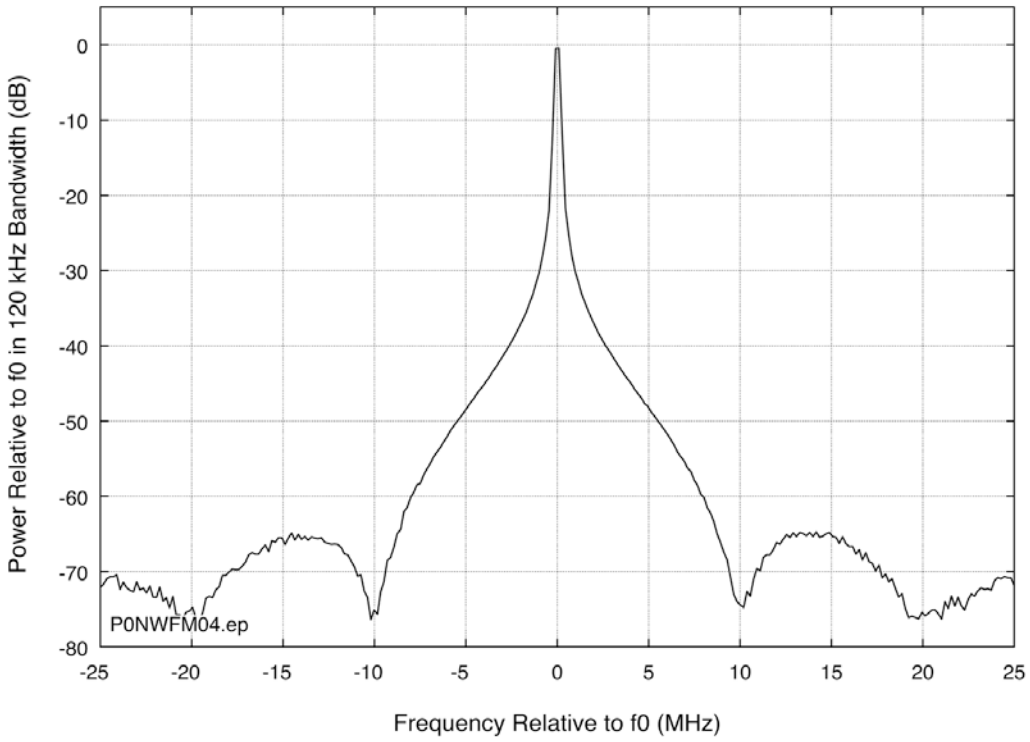

Figure B-7. Spectrum of P0N-4 (PW = 10 µs, PRR = 1,000/sec, DC = 1%) interference.

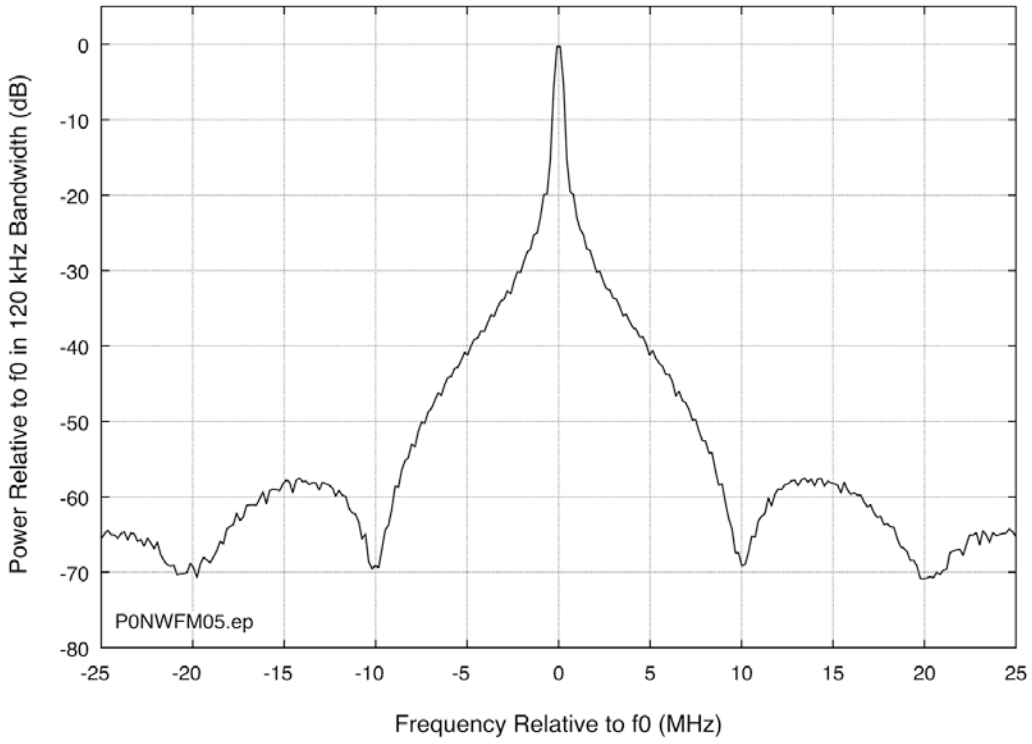

Figure B-8. Spectrum of P0N-5 (PW = 3.33 µs, PRR = 3,000/sec, DC = 1%) interference.

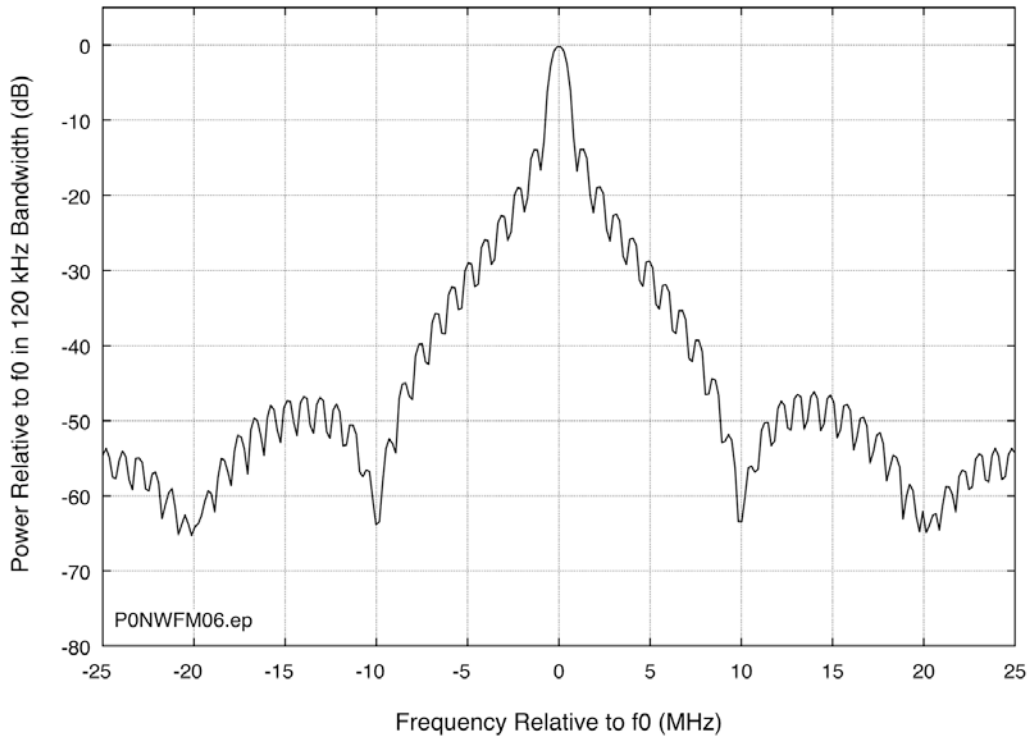

Figure B-9. Spectrum of P0N-6 (PW = 1 μs, PRR = 10,000/sec, DC = 1%) interference.

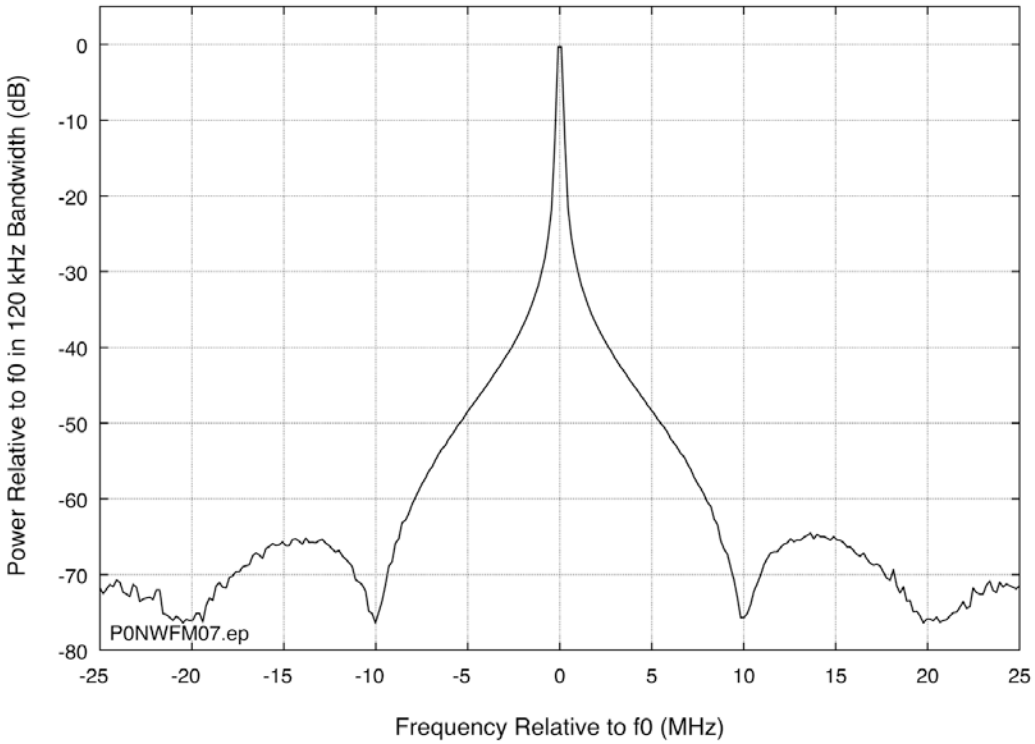

Figure B-10. Spectrum of P0N-7 (PW = 30 μs, PRR = 1,000/sec, DC = 3%) interference.

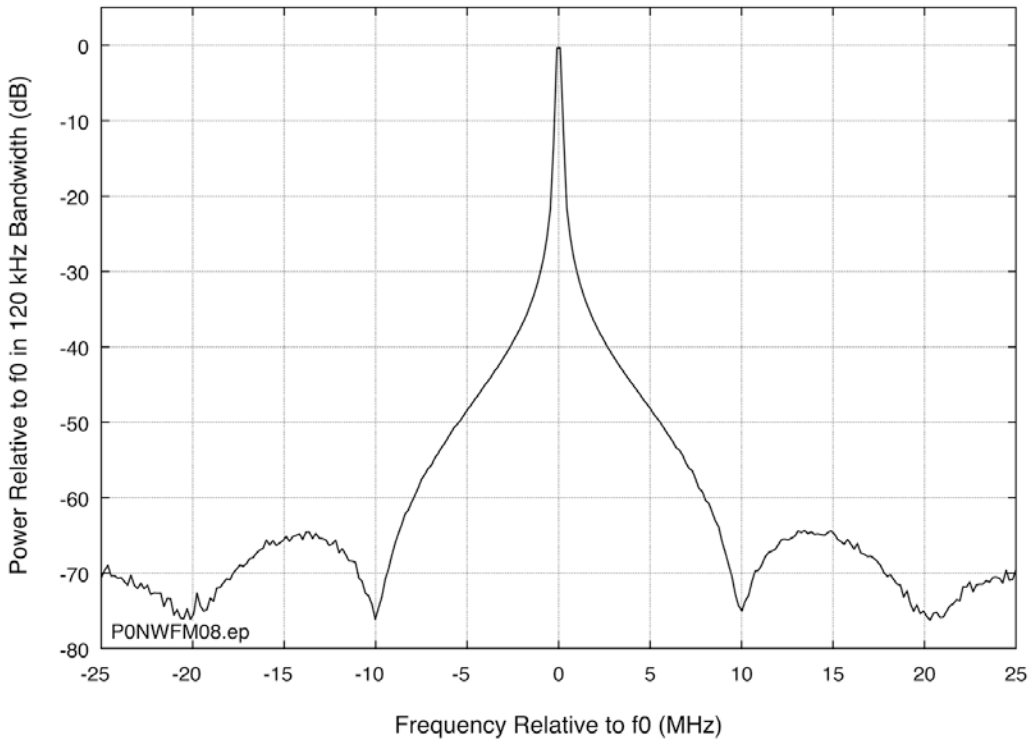

Figure B-11. Spectrum of P0N-8 (PW = 10 µs, PRR = 3,000/sec, DC = 3%) interference.

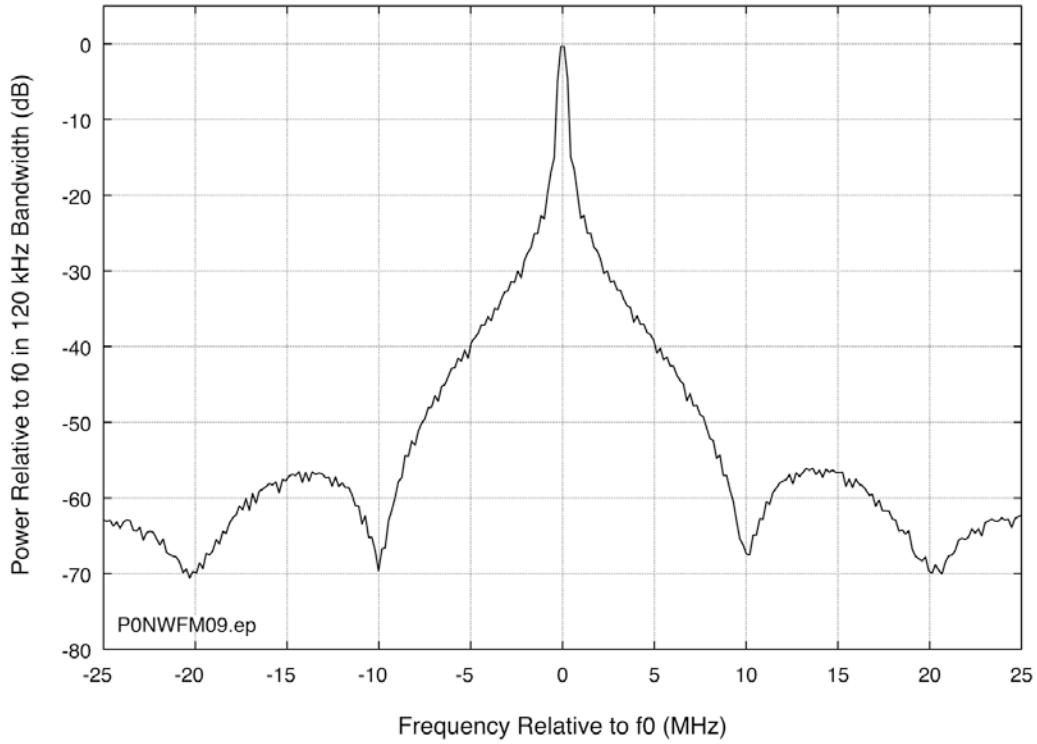

Figure B-12. Spectrum of P0N-9 (PW = 3 µs, PRR = 10,000/sec, DC = 3%) interference.

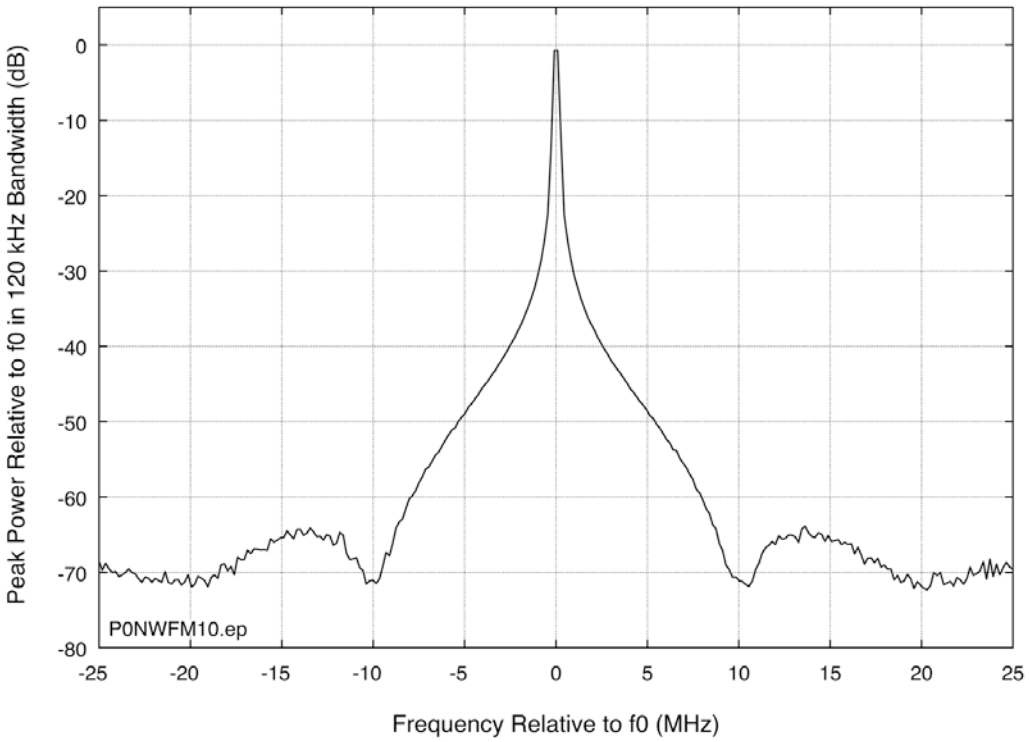

Figure B-13. Spectrum of P0N-10 (PW = 100 µs, PRR = 1,000/sec, DC = 10%) interference.

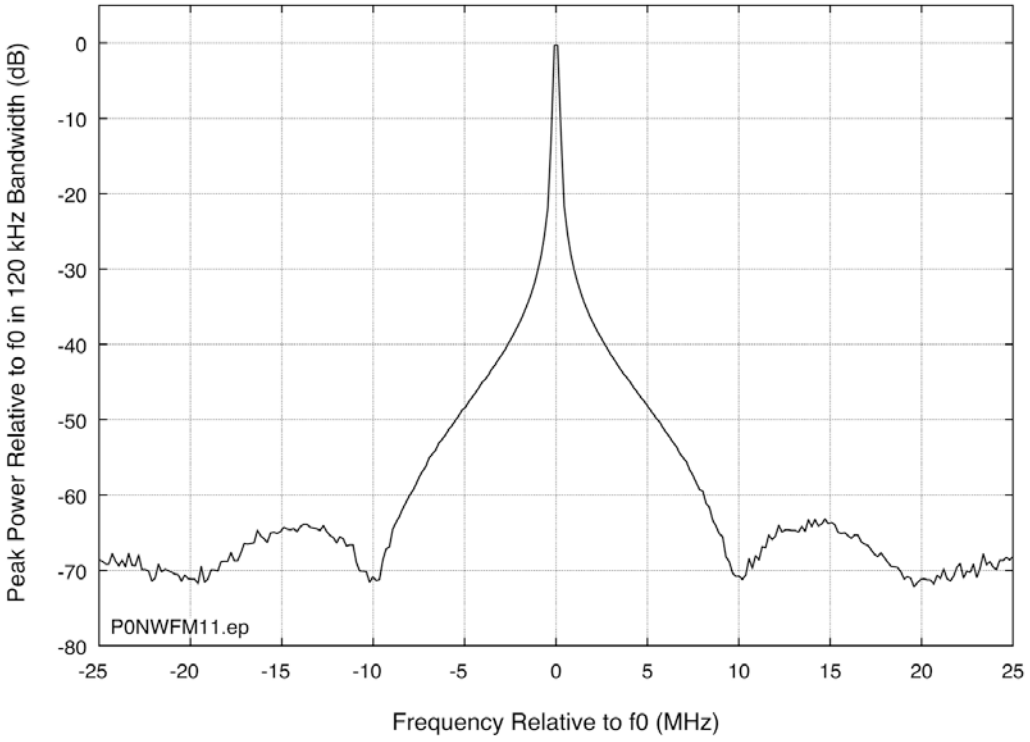

Figure B-14. Spectrum of P0N-11 (PW = 33.3 µs, PRR = 3,000/sec, DC = 10%) interference.

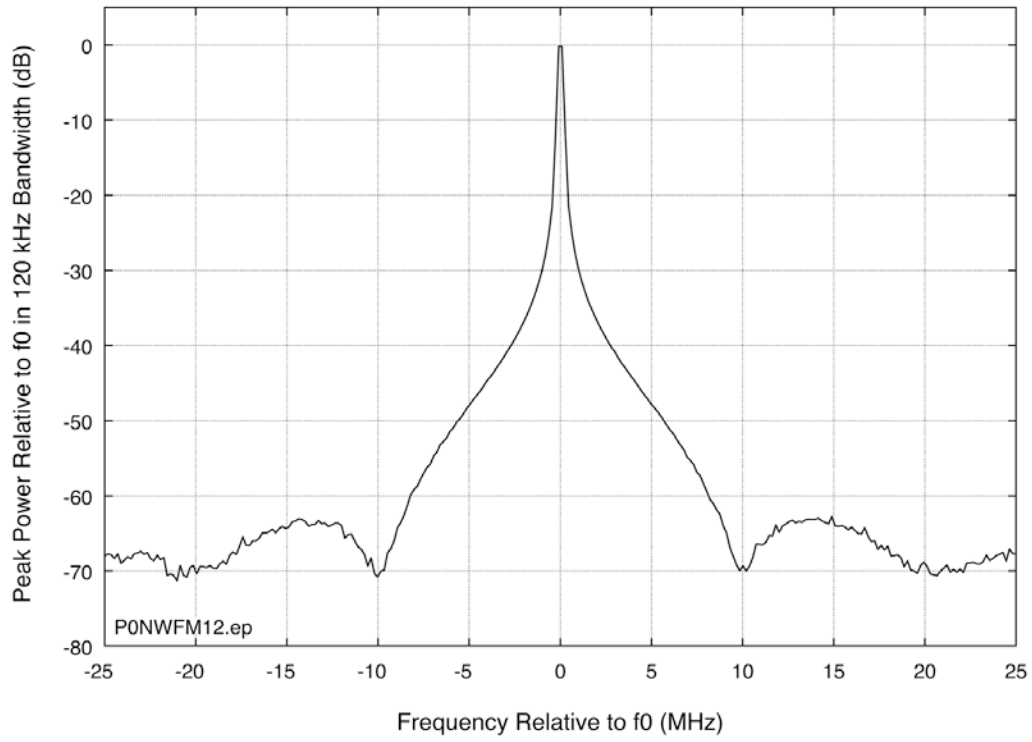

Figure B-15. Spectrum of P0N-12 (PW = 10 µs, PRR = 10,000/sec, DC = 10%) interference.

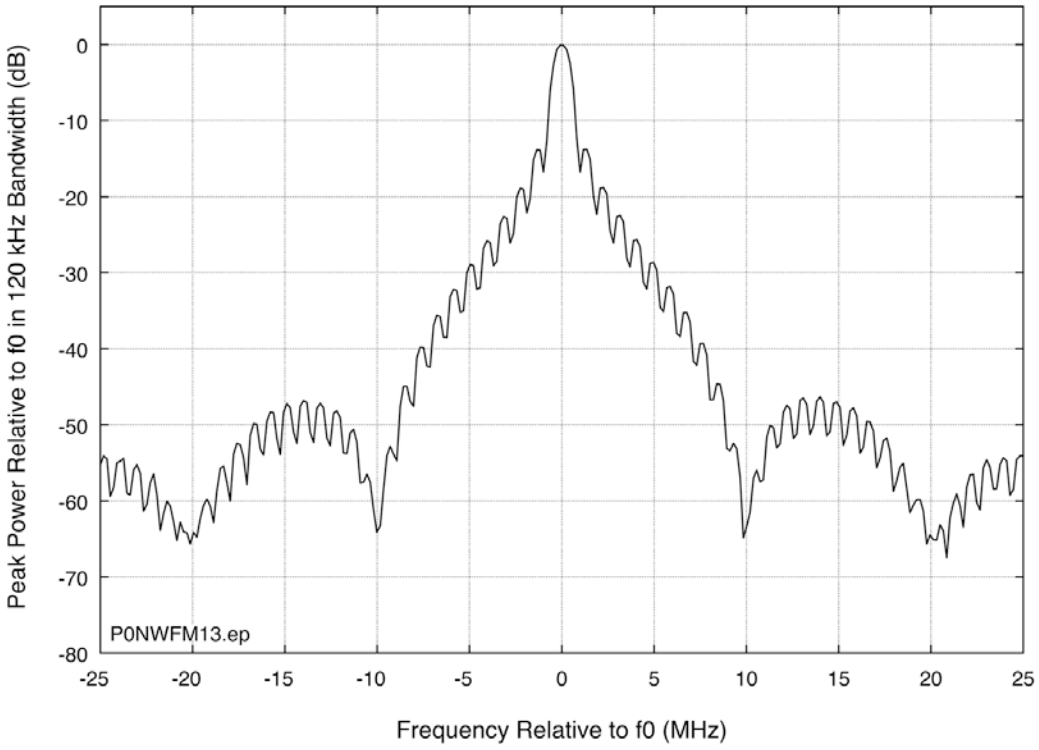

Figure B-16. Spectrum of P0N-13/TDWR (PW = 1 µs, PRR = 500/sec, DC = 0.05%) interference.

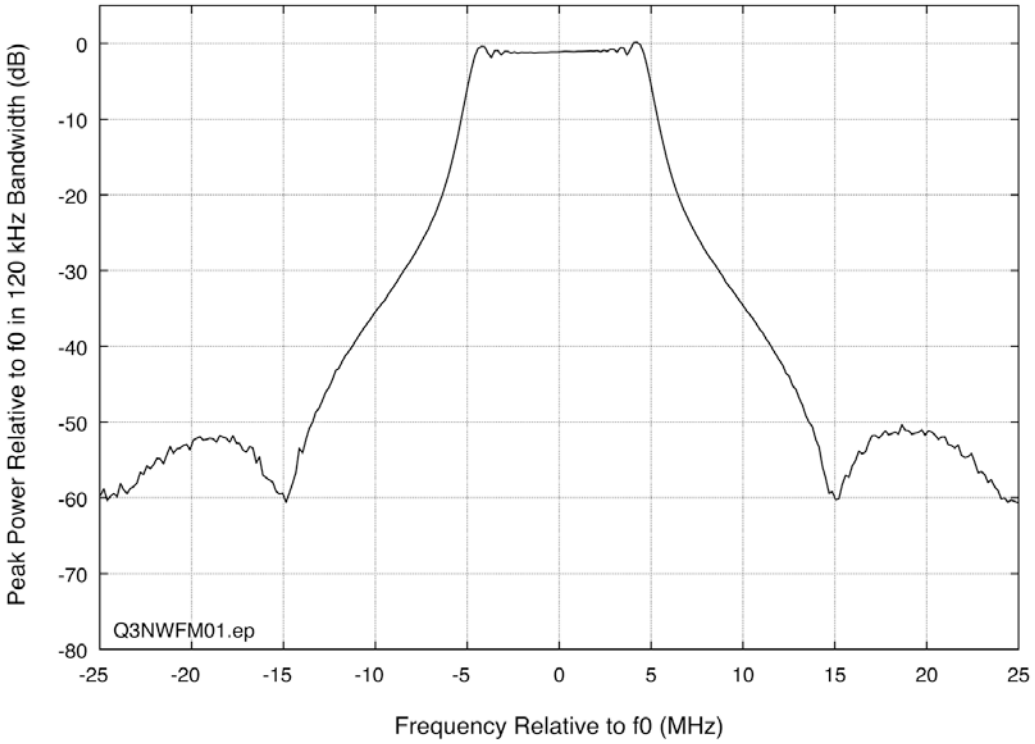

Figure B-17. Spectrum of Q3N-1 (PW = 10 µs, PRR = 1,000/sec, DC = 1%) interference.

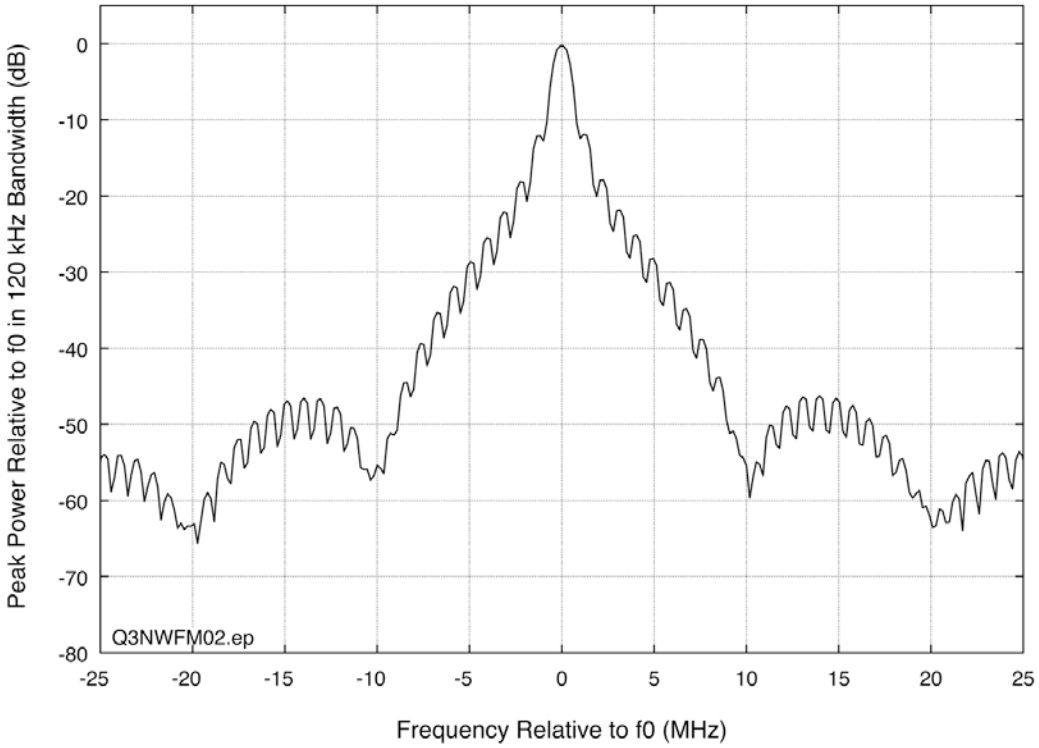

Figure B-18. Spectrum of Q3N-2 (PW = 1 µs, PRR = 10,000/sec, DC = 1%) interference.

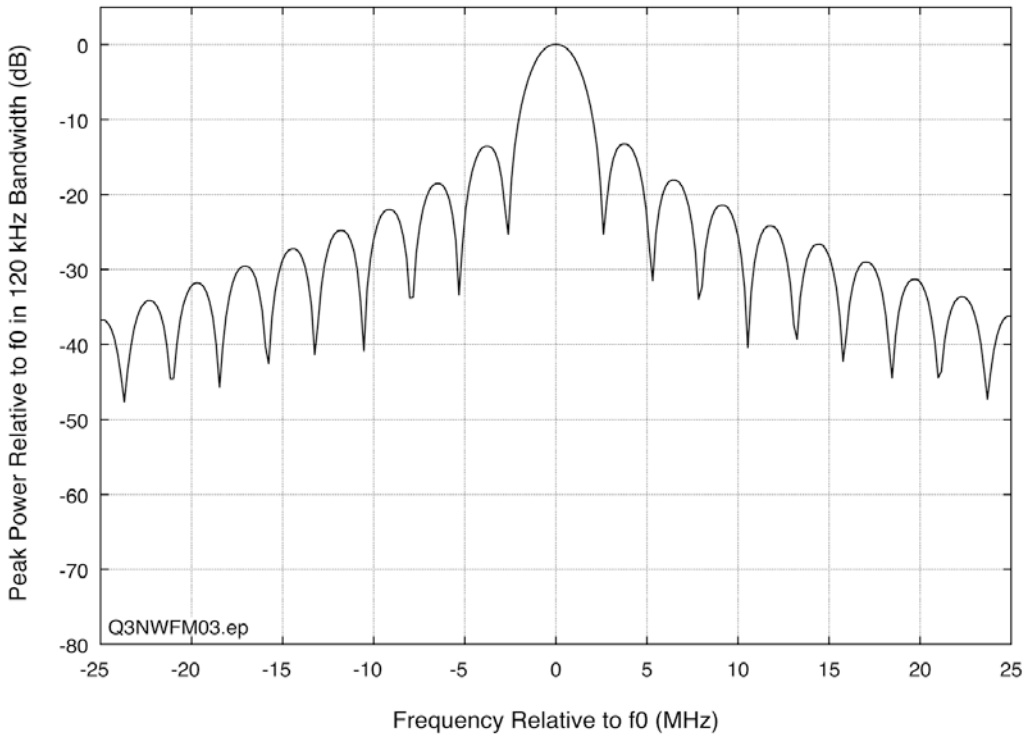

Figure B-19. Spectrum of Q3N-3 (PW = 0.33 µs, PRR = 30,000/sec, DC = 1%) interference.

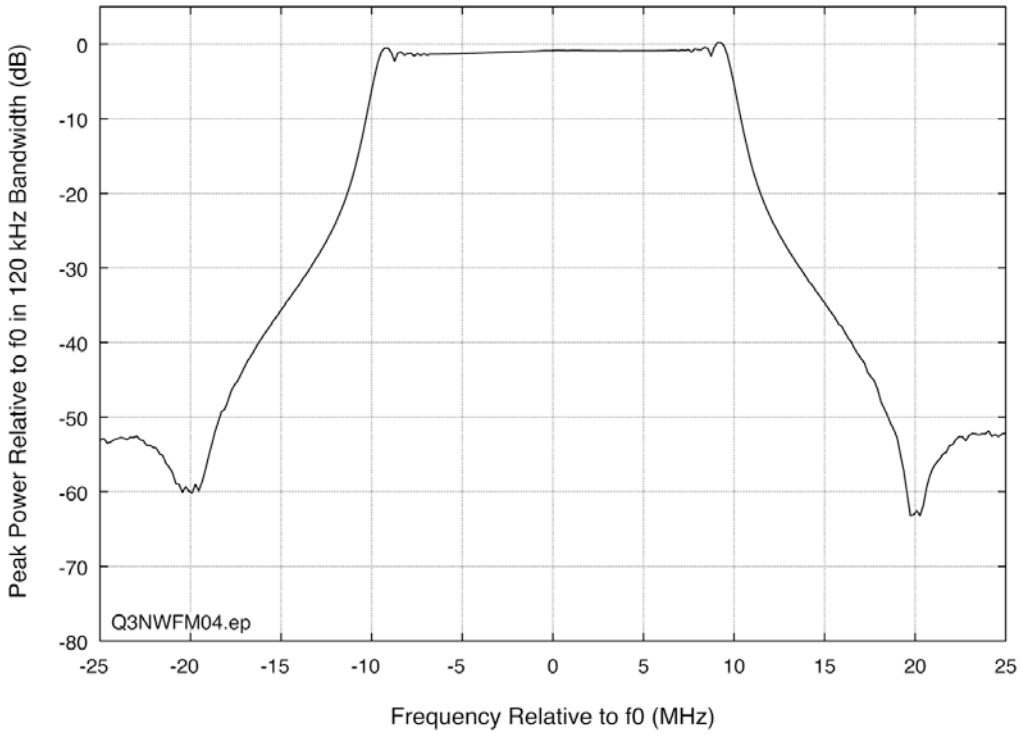

Figure B-20. Spectrum of Q3N-4 (PW = 20 µs, PRR = 200/sec (equivalent to PW = 100 µs, PRR = 1,000/sec), DC = 0.4%) interference.

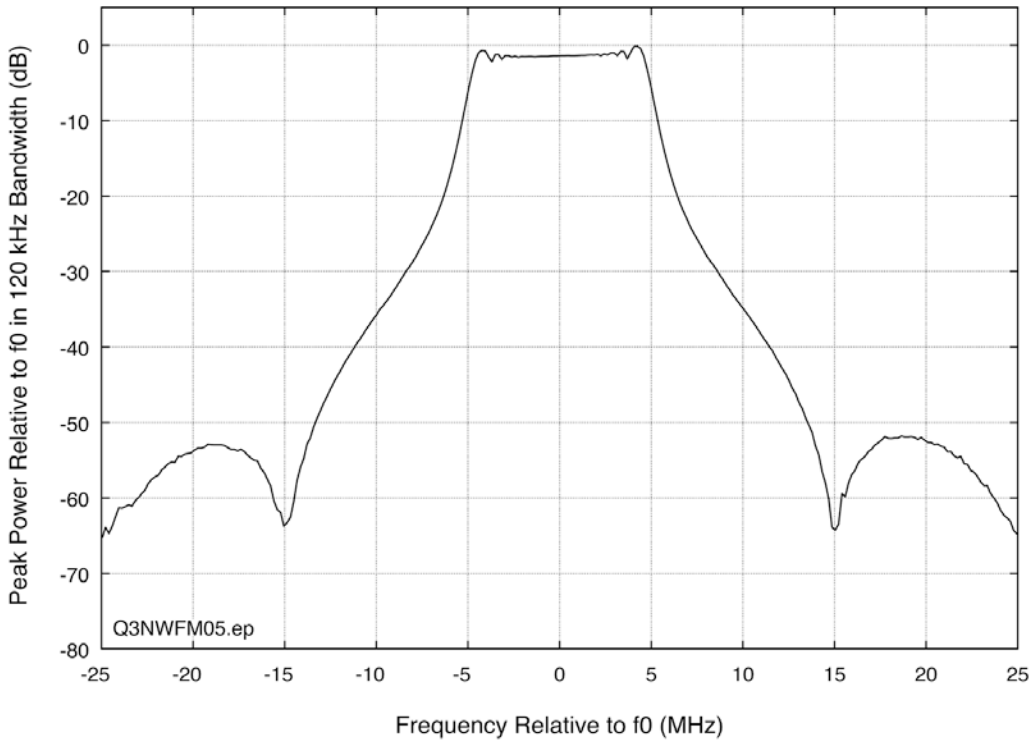

Figure B-21. Spectrum of Q3N-5 (PW = 10 µs, PRR = 10,000/sec, DC = 10%) interference.

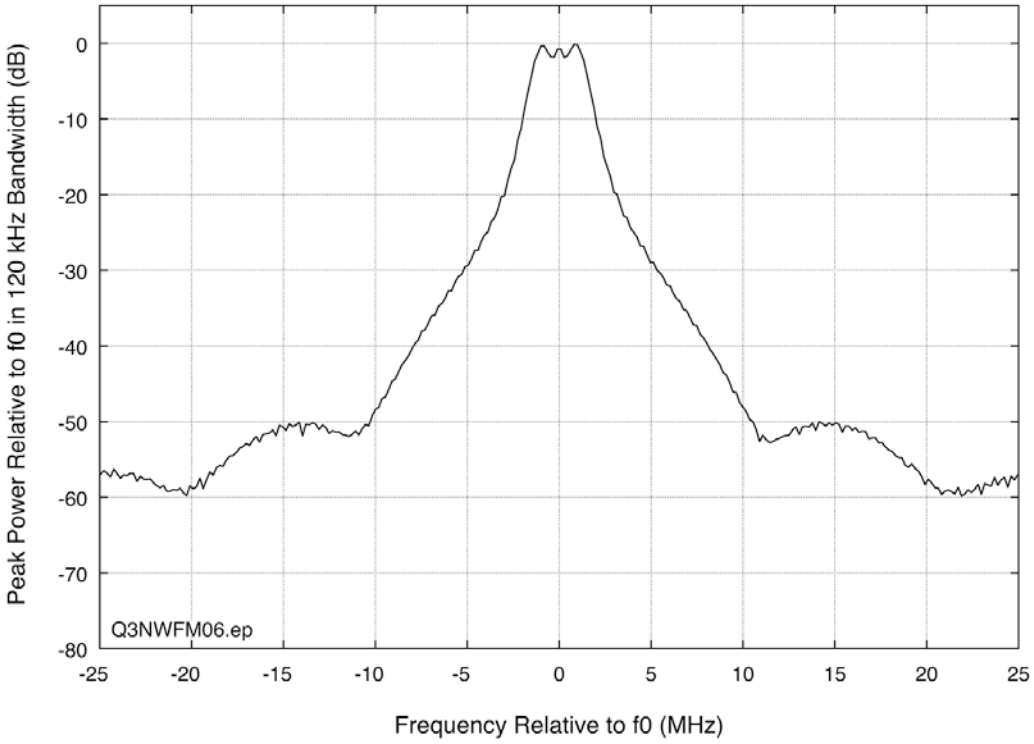

Figure B-22. Spectrum of Q3N-6 (PW = 3.3 µs, PRR = 30,000/sec, DC = 10%) interference.

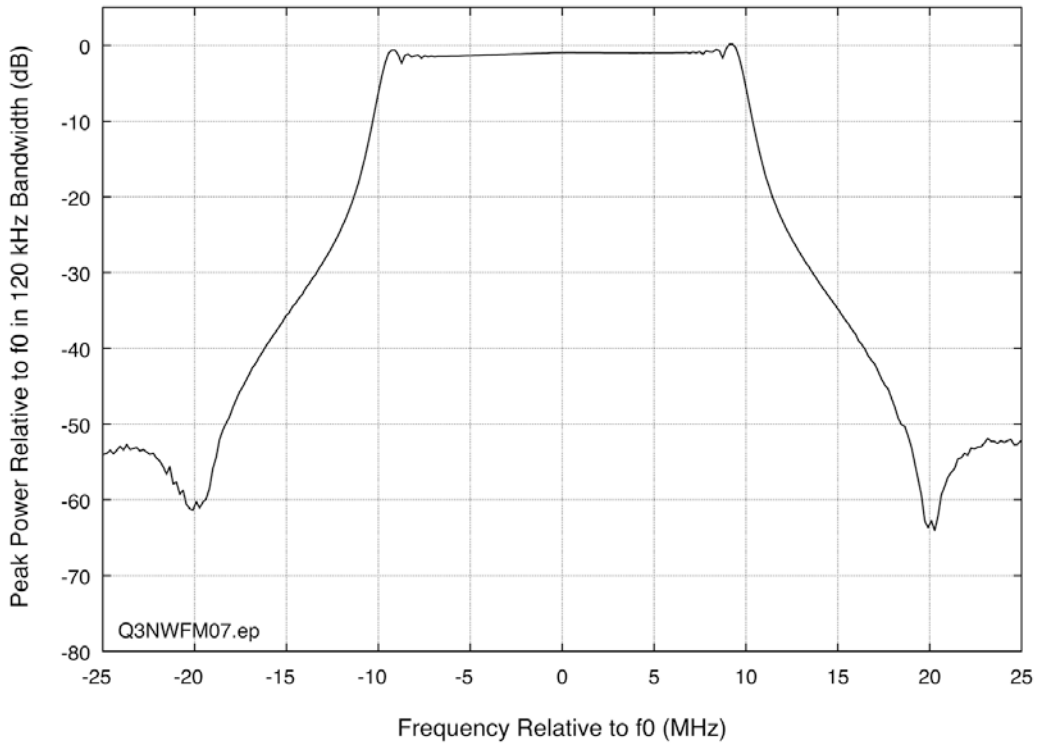

Figure B-23. Spectrum of Q3N-7 (PW = 20 µs, PRR = 100/sec (equivalent to PW = 200 µs, PRR = 1,000/sec), DC = 0.2%) interference.

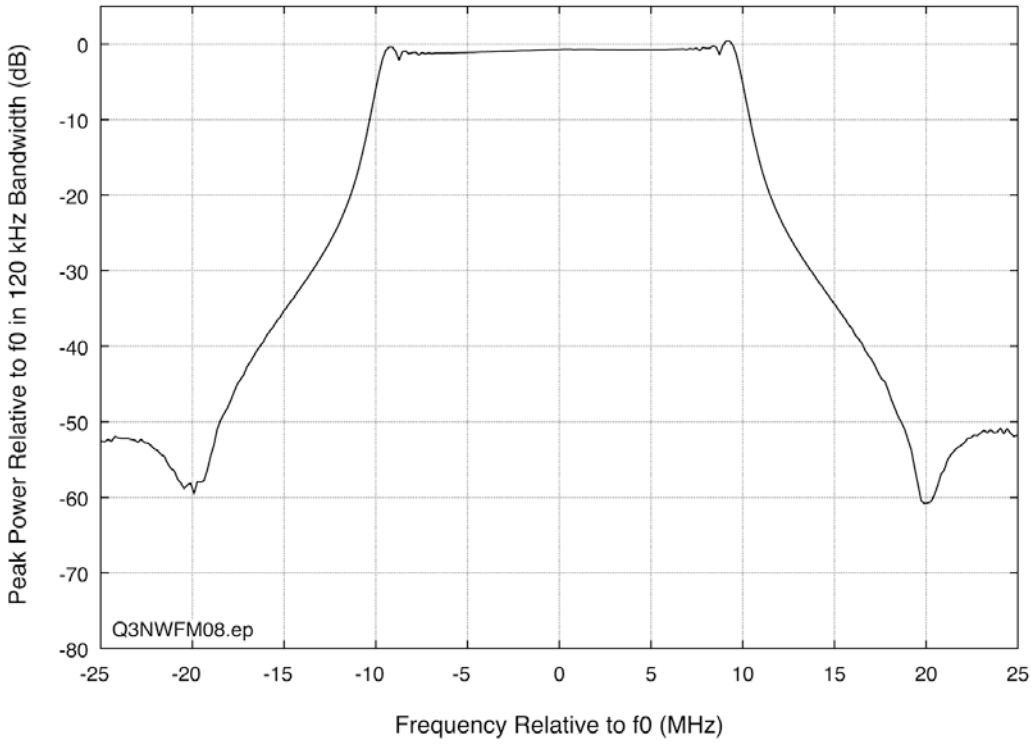

Figure B-24. Spectrum of Q3N-8 (PW = 20 µs, PRR = 10,000/sec, DC = 20%) interference.

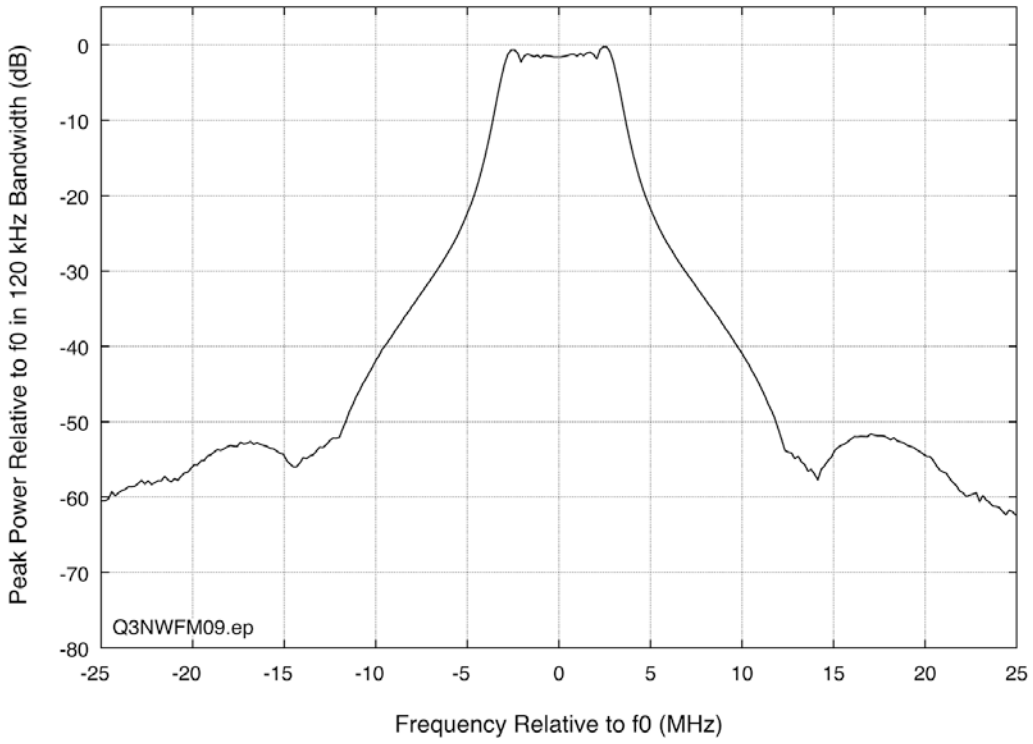

Figure B-25. Spectrum of Q3N-9 (PW = 6.6 µs, PRR = 30,000/sec, DC = 20%) interference.

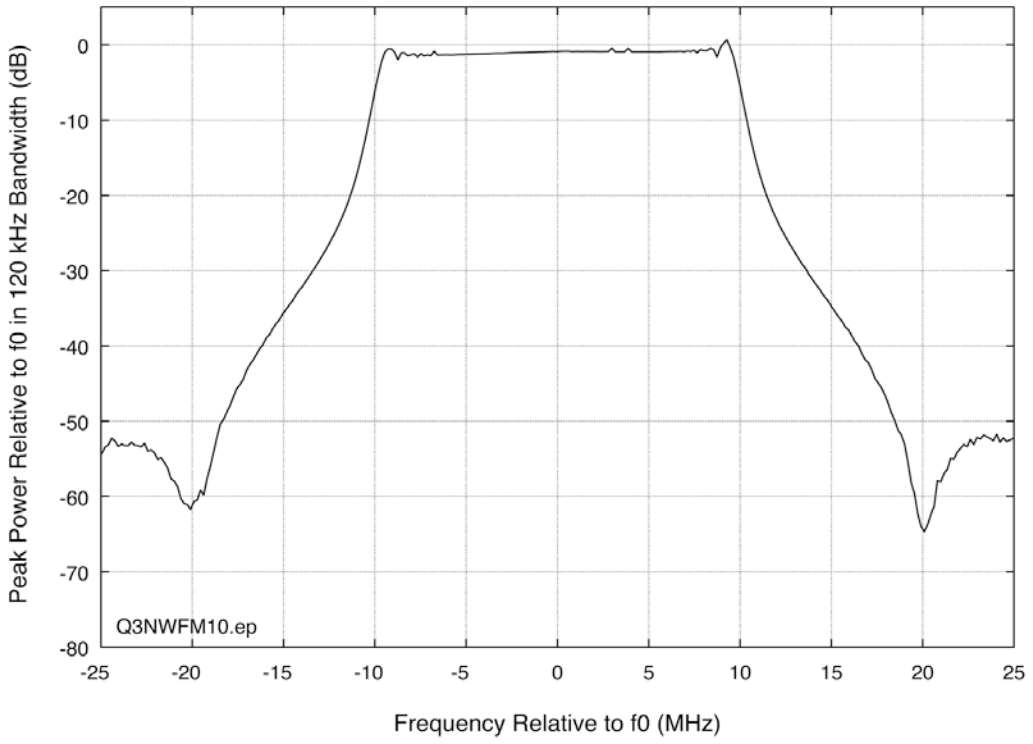

Figure B-26. Spectrum of Q3N-10 (PW = 20 µs, PRR = 67/sec (equivalent to PW = 300 µs, PRR = 1,000/sec), DC = 0.13%) interference.

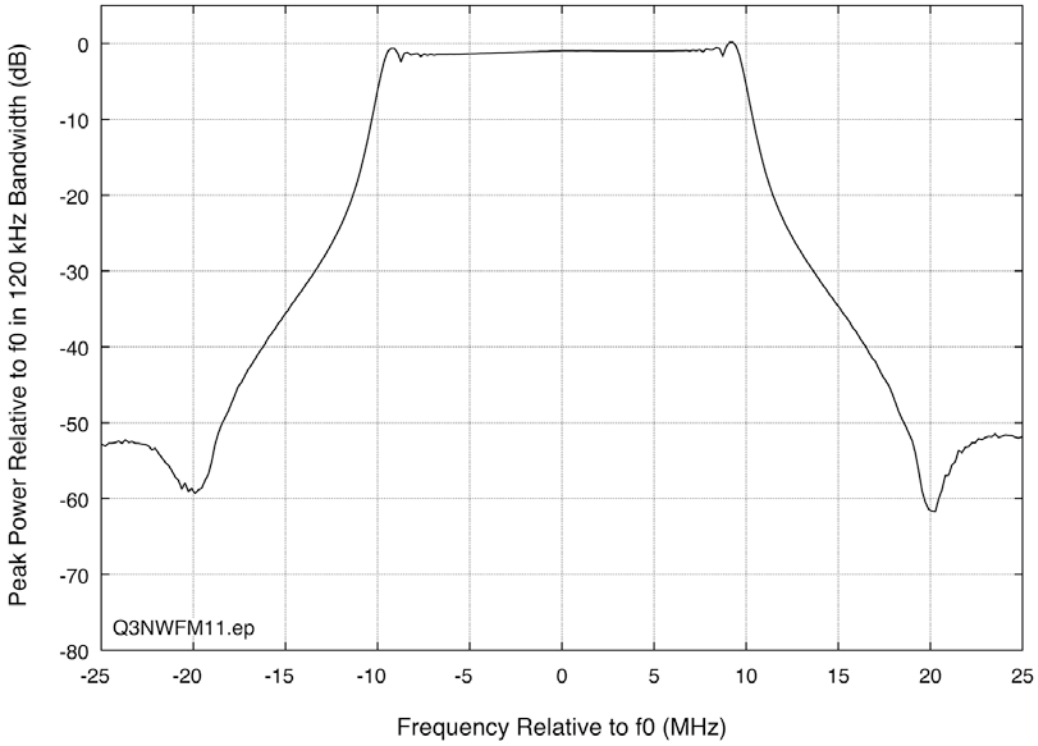

Figure B-27. Spectrum of Q3N-11 (PW = 20 µs, PRR = 6,667/sec (equivalent to PW = 30 µs, PRR = 10,000/sec), DC = 13%) interference.

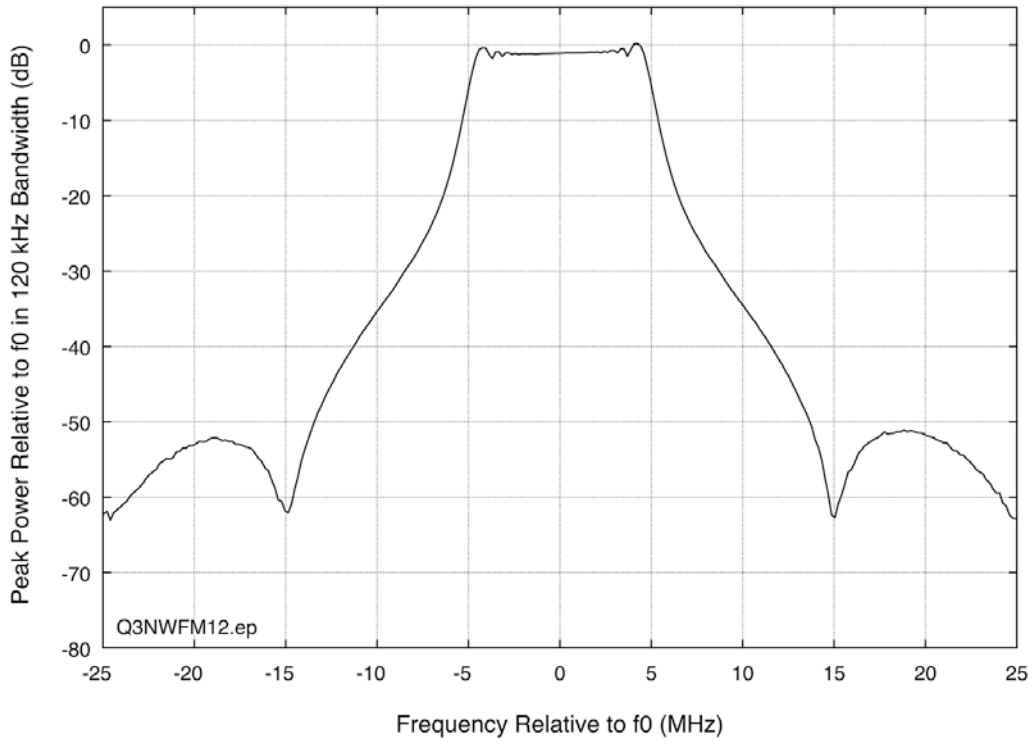

Figure B-28. BLER for Q3N-12 (PW = 10 µs, PRR = 30,000/sec, DC = 30%) interference.

FORM **NTIA-29**
(4-80)

U.S. DEPARTMENT OF COMMERCE
NAT'L. TELECOMMUNICATIONS AND INFORMATION ADMINISTRATION

BIBLIOGRAPHIC DATA SHEET

1. PUBLICATION NO.	2. Government Accession No.	3. Recipient's Accession No.
TR-14-499		

4. TITLE AND SUBTITLE	5. Publication Date
Effects of Radar Interference on LTE Base Station Receiver Performance	December 2013 Reissued May 2014
	6. Performing Organization Code NTIA ITS.T/NTIA OSM

7. AUTHOR(S)	9. Project/Task/Work Unit No.
Frank H. Sanders, John E. Carroll, Geoffrey A. Sanders, Robert L. Sole	6469000-200

8. PERFORMING ORGANIZATION NAME AND ADDRESS	10. Contract/Grant Number.
Institute for Telecommunication Sciences National Telecommunications & Information Administration U.S. Department of Commerce 325 Broadway Boulder, CO 80305	

11. Sponsoring Organization Name and Address	12. Type of Report and Period Covered
National Telecommunications & Information Administration Herbert C. Hoover Building 14th & Constitution Ave., NW Washington, DC 20230	

14. SUPPLEMENTARY NOTES

15. ABSTRACT (A 200-word or less factual summary of most significant information. If document includes a significant bibliography or literature survey, mention it here.)

In response to proposals to introduce new radio systems into 3550–3650 MHz radio spectrum in the United States, the authors have performed measurements and analysis on effects of interference from a variety of radar waveforms to the performance of a Long Term Evolution (LTE) base station receiver. This work has been prompted by the possibility that LTE base station receivers may eventually share spectrum with radar operations in this spectrum range. The base station receiver that was tested used time division duplex (TDD) modulation. Radar pulse parameters used in this testing spanned the range of both existing and anticipated future radar systems in the 3100–3650 MHz spectrum range. LTE base station receiver data throughput rates, block error rates (BLER), and internal noise levels have been measured as a function of radar pulse parameters and the incident power level of radar pulses in the base station receiver. The authors do not determine the acceptability of radar interference effects on LTE base station performance. Rather, these data are presented for the use of spectrum managers and engineers who can use this information as a building block in the construction of frequency-and-distance separation curves for radar transmitters and LTE base station receivers, supporting possible future spectrum sharing at 3.5 GHz.

16. Key Words (Alphabetical order, separated by semicolons)

Block error rate (BLER); chirped pulses; Long Term Evolution (LTE); P0N pulses; radar; spectrum sharing; time division duplexing (TDD)

17. AVAILABILITY STATEMENT	18. Security Class. (This report)	20. Number of pages
☒ UNLIMITED.	Unclassified	87
☐ FOR OFFICIAL DISTRIBUTION.	19. Security Class. (This page) Unclassified	21. Price: n/a

NTIA FORMAL PUBLICATION SERIES

NTIA MONOGRAPH (MG)

A scholarly, professionally oriented publication dealing with state-of-the-art research or an authoritative treatment of a broad area. Expected to have long-lasting value.

NTIA SPECIAL PUBLICATION (SP)

Conference proceedings, bibliographies, selected speeches, course and instructional materials, directories, and major studies mandated by Congress.

NTIA REPORT (TR)

Important contributions to existing knowledge of less breadth than a monograph, such as results of completed projects and major activities. Subsets of this series include:

NTIA RESTRICTED REPORT (RR)

Contributions that are limited in distribution because of national security classification or Departmental constraints.

NTIA CONTRACTOR REPORT (CR)

Information generated under an NTIA contract or grant, written by the contractor, and considered an important contribution to existing knowledge.

JOINT NTIA/OTHER-AGENCY REPORT (JR)

This report receives both local NTIA and other agency review. Both agencies' logos and report series numbering appear on the cover.

NTIA SOFTWARE & DATA PRODUCTS (SD)

Software such as programs, test data, and sound/video files. This series can be used to transfer technology to U.S. industry.

NTIA HANDBOOK (HB)

Information pertaining to technical procedures, reference and data guides, and formal user's manuals that are expected to be pertinent for a long time.

NTIA TECHNICAL MEMORANDUM (TM)

Technical information typically of less breadth than an NTIA Report. The series includes data, preliminary project results, and information for a specific, limited audience.

For information about NTIA publications, contact the NTIA/ITS Technical Publications Office at 325 Broadway, Boulder, CO, 80305 Tel. (303) 497-3572 or e-mail info@its.bldrdoc.gov.